INVESTIGATIONS OF FOUR-COORDINATE AND FIVE-COORDINATE NICKEL(I) MACROCYCLIC LIGAND COMPLEXES

Thesis by

David Michael Ingle

In Partial Fulfillment of the Requirements

for the Degree of

Doctor of Philosophy

California Institute of Technology

Pasadena, California

1980

(Submitted October 25, 1979)

Acknowledgements

First, to Bob Gagné I owe thanks - beyond numeration. His amiable guidance and leadership have been greatly appreciated. His friendship is one of the most valued experiences I have found at Caltech.

Early in my studies I was fortunate in having friends like Ron Hodges, Carol Jones, Bill Hinsberg, Frances Houle, Amy Abe, and others. During an era of transition and uncertainties, Dave (Flipper) Erwin, our eldest "son," helped to keep it all in perspective with a song and a great deal of cherished insanity: 'Hurrah for Hollywood."

My friends in the Gagné group have made the past two years most enjoyable; their work and problems have been as important to me as my own. Nearly.

My wife, Jean, has held it all together. She has been my link to reality. Our relationship, not based on success or good times, continues through the adversities because we love each other and have a mutual faith.

Abstract

The affinity for the binding of carbon monoxide as a fifth ligand to several formally-nickel(I) complexes of tetraazamacrocyclic ligands has been studied; CO binding constants measured in DMF range from zero to 10^5. Reduced nickel complexes, which may occur either as four-coordinate nickel(I) species or, for those ligands having conjugated α-diimine moieties, as four-coordinate nickel(II)-stabilized ligand radicals, have been found to bind carbon monoxide as a fifth ligand, forming paramagnetic, presumably five-coordinate nickel(I) carbonyl complexes. Intramolecular electron transfer appears to occur upon the binding of CO to several of the four-coordinate nickel(II)-stabilized ligand radicals to give five-coordinate nickel(I) carbonyl complexes. Intramolecular electron transfer within a four-coordinate framework appears to occur for one complex, [1,1,-difluoro-4,5,12,13-tetramethyl-1-bora-3,6,11,14-tetraaz a-2,15-dioxacyclopentadeca-3,5,11,-13,-tetraenato]nickel(I), for which the nickel(I) form appears to lie 0.75±0.15 kcal/mole higher in energy than the nickel(II) ligand radical form.

These nickel complexes have been characterized by elemental analysis, bulk magnetic susceptibility, carbon monoxide binding constants, electron paramagnetic resonance spectroscopy, electronic

absorption spectroscopy, infrared spectroscopy, and electrochemical analysis. These nickel complexes appear to be quite analogous to their copper counterparts. On the basis of chemical and physical similarities to the nickel complexes, particularly with respect to their infrared spectra, four-coordinate copper complexes may be formally described as either copper(I) or copper(III)-stabilized ligand dianion species, depending on the ligand system, although both copper species have very similar chemical properties.

A discussion of EHMO calculations on the system is included. In the four-coordinate Ni(II) ligand radical the HOMO is a ligand π^* orbital having some metal character; in the five-coordinate Ni(I) carbonyl complexes, the HOMO is the $d_{x^2-y^2}$ orbital.

An approach to the synthesis of cofacial dimethylglyoxime dimer complexes using 1,4-bis(difluoroboro)butane is included in Appendix II.

Table of Contents

Introduction

Among the myriad of areas of research in inorganic chemistry, the chemistry of copper complexes as exploited in biological systems is certainly one of the more active. Attempts to model active sites of copper-containing proteins, for which there is little information, have led to a rapid proliferation of copper complexes. Because of the kinetic lability of both copper(II) and copper(I) complexes, polydentate ligands and macrocyclic ligands have been employed by many to provide a more static environment for the metal ion. As much of the usage of copper in biochemical systems relies either directly or indirectly on the redox properties of the metal center, the ligand must provide the metal surroundings conducive to complexes stable in either the reduced copper(I) state or the oxidized copper(II) state. Approaches to this problem are progressively becoming more complex, employing more diverse varieties of synthetic ligands.

One of the simplest approaches to the study of copper complexes involves the coordination compounds of tetraazamacrocyclic ligands. Early work by Endicott and coworkers[1] and by Olson and Vasilevskis[2] have demonstrated that trivalent, divalent, and univalent copper complexes may be formed in such complexes. The

copper(I) species are highly air sensitive and, as such, provide a starting point for the investigation of basic research into the chemistry between dioxygen and copper(I). In the course of these preliminary investigations, a most unusual copper complex was synthesized.

Gagné and coworkers[3,4] have shown that $Cu(II)(DOBF_2)\cdot ClO_4$ (Figure 1) undergoes one-electron reduction in non-aqueous media. The isolated, deep blue, neutral product is diamagnetic and, by crystallographic analysis,[5] appears to be a tetrahedrally-distorted square-planar copper(I) complex — an unusual geometry for copper(I). The complex is also unusual in that it forms a novel, five-coordinate, twenty electron copper-carbonyl complex upon exposure to carbon monoxide in solution. This complex, $Cu(I)(DOBF_2)CO$ (Figure 1), has been shown by crystallography[4] to be a square-pyramidal species. A combination of physical techniques strongly suggests that the complex be regarded as a twenty electron, copper(I)-carbonyl complex. At the point of discovery of $Cu(I)(DOBF_2)CO$, the only other carbonyl complex known to violate the "18 electron rule" was $W(CO)(C_6H_5C{\equiv}CC_6H_5)_3$, for which there is a simple explanation.[6] Those factors that determine the ability of $Cu(DOBF_2)$ to form $Cu(I)(DOBF_2)CO$ are a central topic of this thesis.

The four-coordinate and five-coordinate copper(I) complexes

Figure 1

Skeletal Representations of $Cu(II)(DOBF_2)\cdot ClO_4$ and $Cu(I)(DOBF_2)CO$

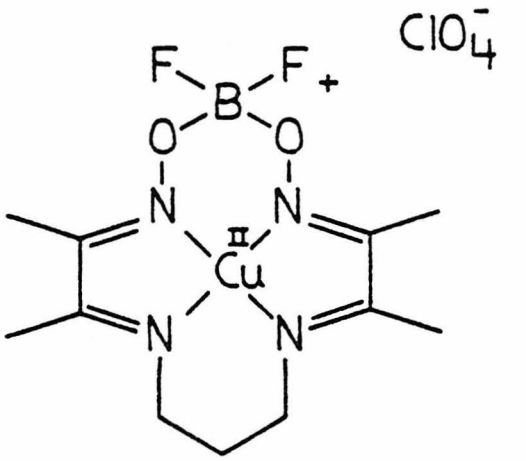

Cu(II)(DOBF$_2$)·ClO$_4$

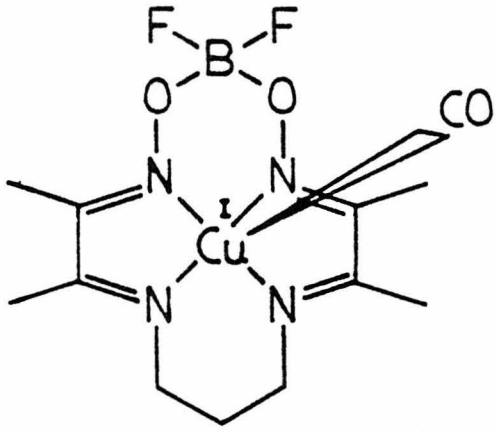

Cu(I)(DOBF$_2$)CO

Figure 1

had already been made and characterized when this present work described within this thesis was begun. One approach to the problem of five-coordinate, twenty electron, copper-carbonyls was to establish the generality of this class of compounds, and to determine a hierarchy of ligands, L, capable of binding as a fifth ligand in $Cu(I)(DOBF_2)L$; the results,[7] obtained in collaboration with J. L. Allison, are the basis of Appendix I. An electrochemical technique was used to monitor ligand binding; although some problems were encountered with this method, the approach permitted convenient, facile determinations of ligand binding constants using the relatively available copper(II) complexes. The results indicated that many four-coordinate complexes of polydentate and macrocyclic ligands can accommodate carbon monoxide as a fifth ligand. Ligands other than CO can bind as fifth ligands to $Cu(DOBF_2)$; typically, π-acid ligands, i.e., isonitriles, phosphites, and phosphines, are seen to bind stronger than σ-bases, i.e., N-methylimidazole and pyridine. These results are consistent with an electron-rich copper center in $Cu(I)(DOBF_2)L$, as expected.

Successful comparisons of iron and cobalt porphyrin-dioxygen complexes have led to a better understanding of the nature of the iron-dioxygen interactions in hemoglobin.[8] Through comparisons of nickel complexes to the copper complexes previously studied, much insight into the nature of the copper complexes may be gained. This

is the fundamental premise of the body of this thesis, which details the synthesis and reactivity of certain reduced nickel complexes analogous to copper complexes studied in Appendix I. The nickel analogues, being d^9 and therefore paramagnetic, provide the added bonus of investigation by EPR spectroscopy. Several nickel(II) mononuclear macrocyclic complexes have previously been studied electrochemically by Busch and coworkers[9] and have been shown by EPR methods to belong to two types: complexes which undergo one-electron metal reduction to give four-coordinate nickel(I) species and complexes which undergo one-electron reduction to give four-coordinate nickel(II)-stabilized ligand radicals. During the course of the work described in Chapters 1 and 2 of this thesis, both types of complexes were found to react cleanly with carbon monoxide to give paramagnetic, presumably five-coordinate nickel(I)-carbonyl complexes. Analysis of the EPR spectra indicates the nature of the reduced species. Nickel(I) complexes are characterized by their anisotropic g-values, with $g>2$. Ligand reduced complexes are indicated by their isotropic g-values near the free-electron value ($g = 2.00$). All of the nickel-carbonyl complexes studied here indicate that the nickel is in the +1 oxidation state. As a consequence of these investigations, it was found that, for those complexes which exist as nickel-stabilized ligand radicals, intramolecular electron transfer, ligand-to-metal, apparently occurs

upon binding of the carbon monoxide.

Moreover, this intramolecular electron transfer, which occurs upon going from four-coordinate to five-coordinate nickel, also appears, as is described in Chapter 1 and 2, to take place at the ambient temperature within a four-coordinate framework in Ni($DOBF_2$)Bn (Figure 2). Reasoning that since complexes exist in either the nickel(I) or nickel(II) ligand-radical form depending on the nature of the ligand, it might be possible by varying certain parameters to design a complex exhibiting a borderline nature. Ni($DOBF_2$) exists as a ligand radical stabilized by interaction with the metal center; reducing this interaction, it was thought, should lead to a relative destabilization of the ligand radical in favor of the nickel(I) form. Increasing the macrocycle's hole size is one way of accomplishing this. Thus, Ni($DOBF_2$)Bn, possessing a slightly larger ligand than Ni($DOBF_2$), does appear to favor the nickel(I) form sufficiently to cause the two reduced forms to exist in thermal equilibrium at ambient temperatures. The solution EPR spectrum shows two isotropic g-values (g=2.113 and g=2.048), whose ratio changes as a function of temperature. As the temperature is lowered, the radical signal increases and the high g-value signal decreases in intensity. This allows for a calculation of the energy separation between these two species; the nickel(I) species is found to be about 0.75 ± 0.15 kcal per mole higher

Figure 2

Skeletal Representation of $Ni(DOBF_2)Bn$

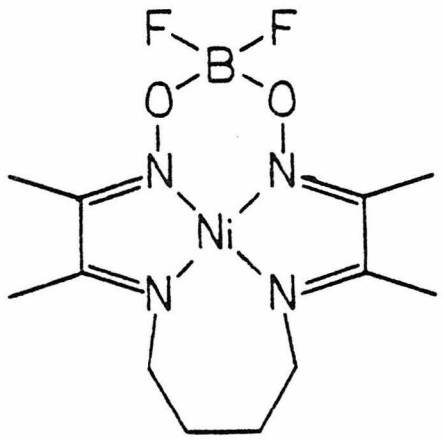

$Ni(DOBF_2)Bn$

Figure 2

in energy than the nickel(II) ligand radical.

Chapter 2, which describes the synthesis and reactivity of the reduced four-coordinate nickel species, shows that the binding constants of carbon monoxide to a number of four-coordinate nickel(I) complexes are very similar. Nickel(II)-stabilized ligand radical complexes show a much wider variation in binding constants, possibly due to the much larger variation in the ligand environment for these complexes, i.e., hole size, and charge, or perhaps the degree of stabilization of the nickel-ligand radical.

Infrared spectra, described in Chapter 3, also show indications of this electron transfer from ligand-to-metal upon change of coordination number. The four-coordinate nickel(I) complexes show C=N imine stretching frequencies in the 1600-1650 cm^{-1} range that change only slightly as a function of oxidation state or CO binding. Nickel(II)-stabilized ligand radical complexes show disappearance of the imine stretch (or very large displacement to lower energy due to partial reduction of the imine bond); these complexes with CO have normal region imine bands — consistent with the intramolecular electron transfer. Further support of this notion was provided by ^{15}N-labelled $Ni(DMGBF_2)_2$; the imine IR bands involved show dependence on the nitrogen isotope.

Finally, in Chapter 3, comparisons of these nickel complexes

to the analogous copper complexes has led to the formulation of $Cu(DOBF_2)$ as a "copper(III)-stabilized ligand dianion," which, upon coordination of carbon monoxide, undergoes a formal two-electron intramolecular electron transfer to give a five-coordinate copper(I)-carbonyl. The extended Hückel molecular orbital calculations of Burdett and Williams[10] also discussed in Chapter 3 suggest this description of $Cu(DOBF_2)$ and $Cu(DOBF_2)CO$ that has been proposed on the basis of experimental evidence. The designation of these complexes as copper(III)-stabilized ligand dianions must be tempered by the reminder that these complexes are actually covalent in nature — that copper(III) is probably one extreme, just as the copper(I) assignment for $Cu(DOBF_2)$ might represent another extreme.

Described in Appendix II is a short summary of an earlier project, which was terminated in order to pursue the work described in Chapters 1, 2 and 3. The project was a synthetic approach to the problem of cofacial dimers in the dimethylglyoxime system; preliminary results were included.

References and Notes

(1) Palmer, J.M.; Papaconstantinou, E.; Endicott, J.F. Inorg. Chem. 1969, 8, 1516.

(2) Olson, D.C.; Vasilevskis, J. Inorg. Chem. 1971, 10, 463.

(3) Gagné, R.R. J. Am. Chem. Soc. 1976, 98, 6709.

(4) Gagné, R.R.; Allison, J.L.; Gall, R.S.; Koval, C.A. J. Am. Chem. Soc. 1977, 99, 7170.

(5) Gagné, R.R.; Allison, J.L.; Lisensky, G.C. Inorg. Chem. 1978, 17, 3563.

(6) Tate, D.P.; Augl, J.M.; Ritchey, W.M.; Ross, B.L.; Grasselli, J.G. J. Am. Chem. Soc. 1964, 86, 3261.

(7) Gagné, R.R.; Allison, J.L.; Ingle, D.M. Inorg. Chem. 1979, 18, 2767.

(8) Buchler, J.W. Angew. Chem. Int. Ed. Eng. 1978, 17, 407.

(9) Lovecchio, V.F.; Gore, E.S.; Busch, D.H. J. Am. Chem. Soc. 1974, 96, 3109.

(10) Calculations were performed by J.K. Burdett and P.D. Williams (University of Chicago) to whom many thanks are owed.

Chapter 1

Intramolecular Electron Transfer in Mononuclear Nickel-Macrocyclic Ligand Complexes: Formation of Paramagnetic Nickel(I)-Carbonyl Complexes

Robert R. Gagné
D. Michael Ingle

Intramolecular Electron Transfer in Mononuclear Nickel-Macrocyclic Ligand Complexes: Formation of Paramagnetic Nickel(I)-Carbonyl Complexes

Robert R. Gagné and D. Michael Ingle

Abstract: Mononuclear nickel(II) complexes of tetraaza-macrocyclic ligands undergo one electron reduction to give either nickel(I) species or complexes containing nickel(II) complexed to a ligand radical anion. Both reduced species react with CO to give paramagnetic, five-coordinate, nickel(I)-carbonyl adducts.

A new complex was designed to promote equilibrium between both forms of the reduced nickel species. Condensation of 2, 3-butanedionemonoxime and 1, 4-diaminobutane followed by treatment with nickel(II) and then BF_3 gave the oxidized species. Reduction with cobaltocene gave the reduced complex, which, in propylene carbonate solution at 295 K, gives two EPR signals. One signal at g = 2.113 is attributable to a Ni(I) complex while the second, at g = 2.048, is likely due to a Ni(II)-ligand radical anion species. The relative intensities of the two signals are temperature dependent with the signal at g = 2.113 disappearing at lower temperatures with concomitant increase in the g = 2.048 signal. It is proposed that the two signals are due to two conformational forms of a single reduced nickel species, which are interconverting slowly on the EPR timescale. Double integration of

the first derivative signals gives an equilibrium constant, $K = 0.27 \pm 0.05$, with the Ni(I) form 0.75 ± 0.15 kcal/mole higher in energy than the Ni(II)-radical anion form.

Intramolecular Electron Transfer in Mononuclear Nickel-Macrocyclic Ligand Complexes: Formation of Paramagnetic Nickel(I)-Carbonyl Complexes

Sir:

Nickel(II) complexes of tetraaza macrocyclic ligands readily undergo one-electron reduction but various products are possible.[1-4] Ligands with at least one α-diimine moiety lead to formation of nickel(II)-ligand radical anion species, as indicated by EPR studies.[1] In contrast, non-conjugated systems are amenable to formation of nickel(I) complexes. We report here the design of a complex which exhibits an equilibrium between both extreme forms of the reduced species. In addition, we report that both classes of reduced complexes react with carbon monoxide to give paramagnetic, presumably five-coordinate, nickel(I) adducts.

Nickel(II) trans-diene, 1,[5] as the perchlorate salt, was reduced electrochemically (-1.24 V vs. nhe in DMF solution) to give the presumably four-coordinate complex, 2,[6]

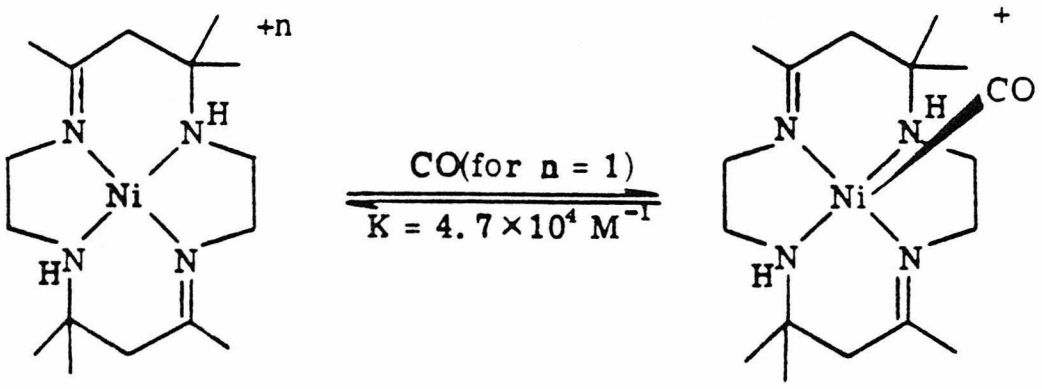

1, n = 2, Ni(II)

2, n = 1, Ni(I)

3, Ni(I)

which was confirmed to be a nickel(I) complex by its EPR spectrum ($g_{||} = 2.190$, $g_{\perp} = 2.056$).[1] Complex 2 binds carbon monoxide at ambient temperatures in DMF solution ($K = 4.7 \times 10^4\ M^{-1}$)[7] to give a bright green, air sensitive complex, 3, which was isolated under a CO atmosphere ($\nu_{CO} = 1961\ cm^{-1}$ (KBr)).[6] Complex 3, was found to be paramagnetic by magnetic susceptibility (2.27 B.M. at 293 K) and by its EPR spectrum ($g_1 = 2.238$, $g_2 = 2.159$, $g_3 = 2.066$), which is distinct from that of complex 2. Complex 3 is, apparently, a five-coordinate, Ni(I) adduct similar to five-coordinate Cu(I)-macrocyclic ligand adducts recently reported.[9-11]

Electrochemical reduction of bis(difluoroboroglyoximato)-nickel(II), 4,[12]

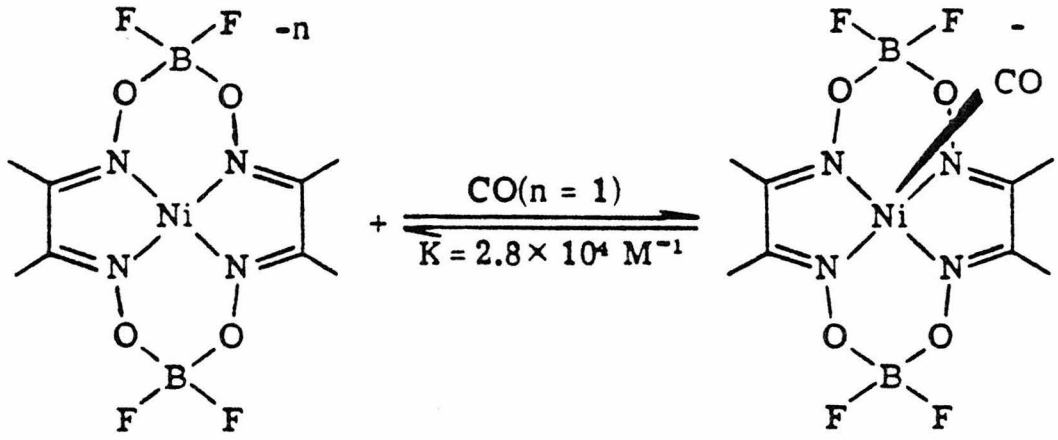

4, n = 0, Ni(II)

5, n = 1, Ni(II)

6, Ni(I)

(-0.79 V vs. nhe in DMF solution) apparently leads to a Ni(II) complex containing a one-electron-reduced ligand, 5, as demonstrated previously for analogous species.[1] Reduction with cobaltocene[13] permitted convenient isolation of the forest green complex, 5.[6] The EPR spectrum of 5 in propylene carbonate glass (100 K) shows a single isotropic line (g = 2.002), Figure 1, suggesting a metal-stabilized ligand radical.[1] At ambient temperatures 5 also binds CO (K = 2.8×10^5 M^{-1};[7] ν_{CO} = 2029 cm^{-1} (KBr)). The magnetic susceptibility of the carbonyl adduct, 6, (1.96 B.M. at 293 K) and its EPR spectrum in propylene carbonate glass ($g_{||}$ = 2.225, $g_{\perp}$ = 2.065 at 100 K) (Figure 1) indicate that the

Figure 1

Frozen Solution EPR Spectra in Propylene Carbonate at 100 K: a) $\underset{\frown}{5}$ under He atmosphere;

b) $\underset{\frown}{6}$ under CO atmosphere.

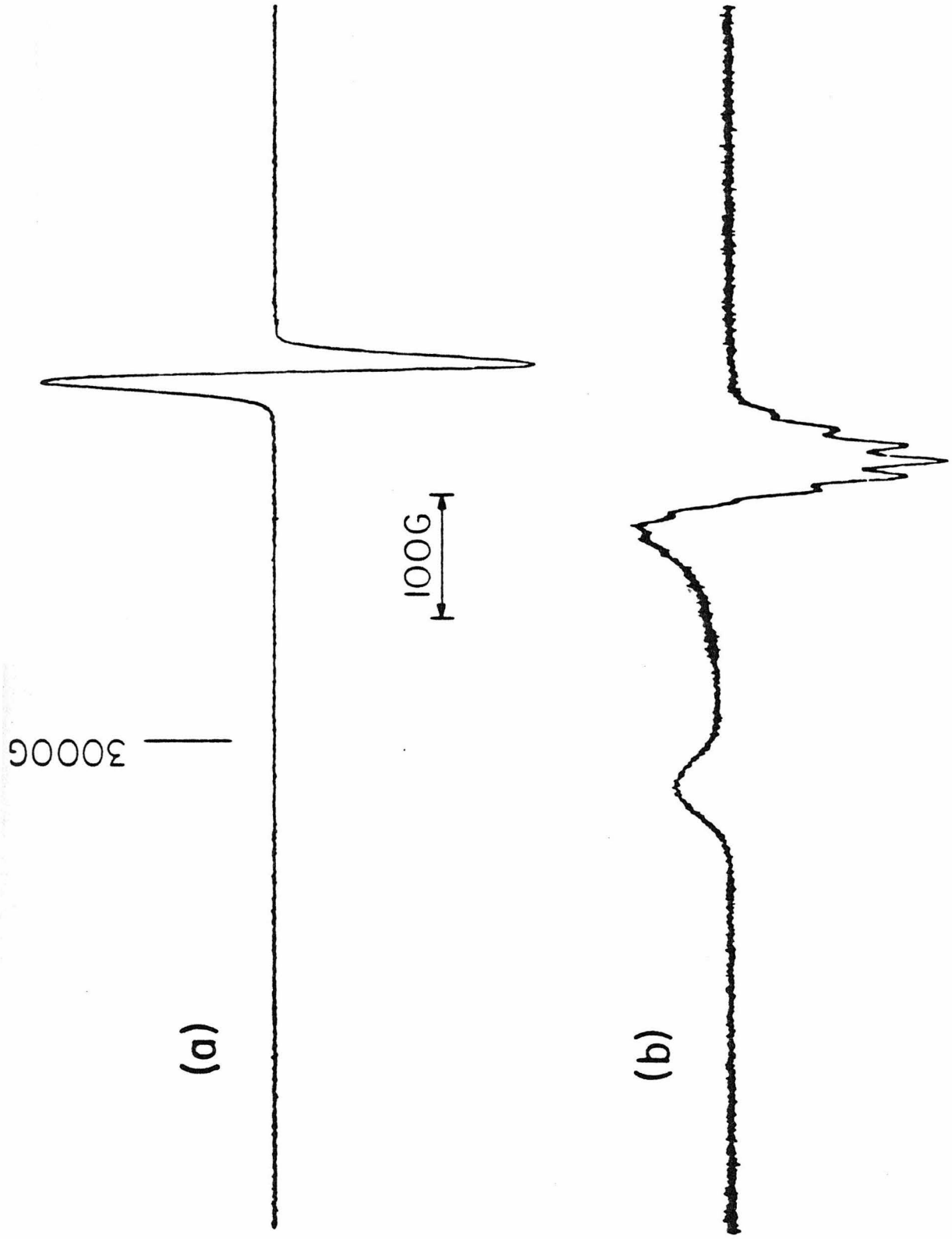

Figure 1

adduct 6 is a paramagnetic, five-coordinate, Ni(I) complex, analogous to 3. The conversion of the four-coordinate, nickel(II)-ligand radical anion, 5, to a nickel(I)-CO adduct appears to be an example of ligand-to-metal intramolecular electron transfer. The electron transfer process may be promoted by geometrical changes upon binding CO.[14]

That complexes 2 and 5 represent two extreme forms of reduced nickel species suggested the challenge of designing a single Ni(II)-macrocyclic ligand complex which upon reduction would exhibit both forms in equilibrium. Complex 7 was prepared as the perchlorate salt by condensing 2, 3-butanedionemonoxime with 1, 4-diaminobutane followed by reaction with $Ni(II)(ClO_4)_2 \cdot nH_2O$, then BF_3. Reduction with cobaltocene[13] gave the one-electron reduction product, NiL, 8.[17]

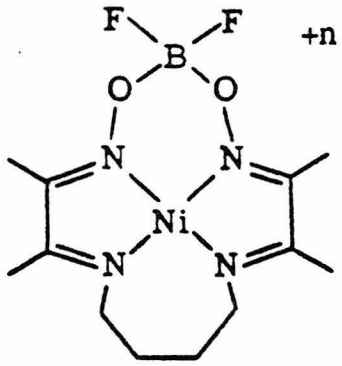

7, n = 1, Ni(II)

8, n = 0, Ni(II) and Ni(I)

Solutions of $\underset{\sim}{8}$ in propylene carbonate (295 K) give EPR spectra (Figure 2) having two signals, one attributable to Ni(I) at g = 2.113 and a second at g = 2.048 assignable to a Ni(II)-ligand-radical anion species. We propose that complex $\underset{\sim}{8}$ exists as two conformational forms in solution, equation 1,

$$Ni(II)(L^{-\cdot}) \underset{}{\overset{K = 0.27}{\rightleftharpoons}} Ni(I)L \qquad (1)$$

That the two EPR signals are indeed due to two interconvertible species is supported by two observations. Firstly, several preparations of complex $\underset{\sim}{8}$ give identical EPR spectra with a constant peak height ratio. Double integration of the first derivative EPR signals gave K = 0.27 ± 0.05, (ΔG = 0.75 ± 0.15 kcal/mole) eq 1.[18] Secondly, the relative intensities of the two EPR signals vary as a function of temperature. On cooling propylene carbonate solutions of $\underset{\sim}{8}$ the EPR signal at g = 2.113 decreases in intensity with concomitant increase in the signal at lower g-values until, at ~ 233 K, only the lower g-value signal remains.[19] The g = 2.113 signal reappears on warming.

Although apparent intramolecular electron transfer in a mononuclear complex has been reported previously,[15,16] the present complex, $\underset{\sim}{8}$, appears to be the first example of an observed equilibrium between two conformationally distinct electronic forms. Further studies of the intramolecular electron transfer rate and the ligand conformational

Figure 2

EPR Spectrum of $\underset{\sim}{8}$ in Propylene Carbonate at 295 K

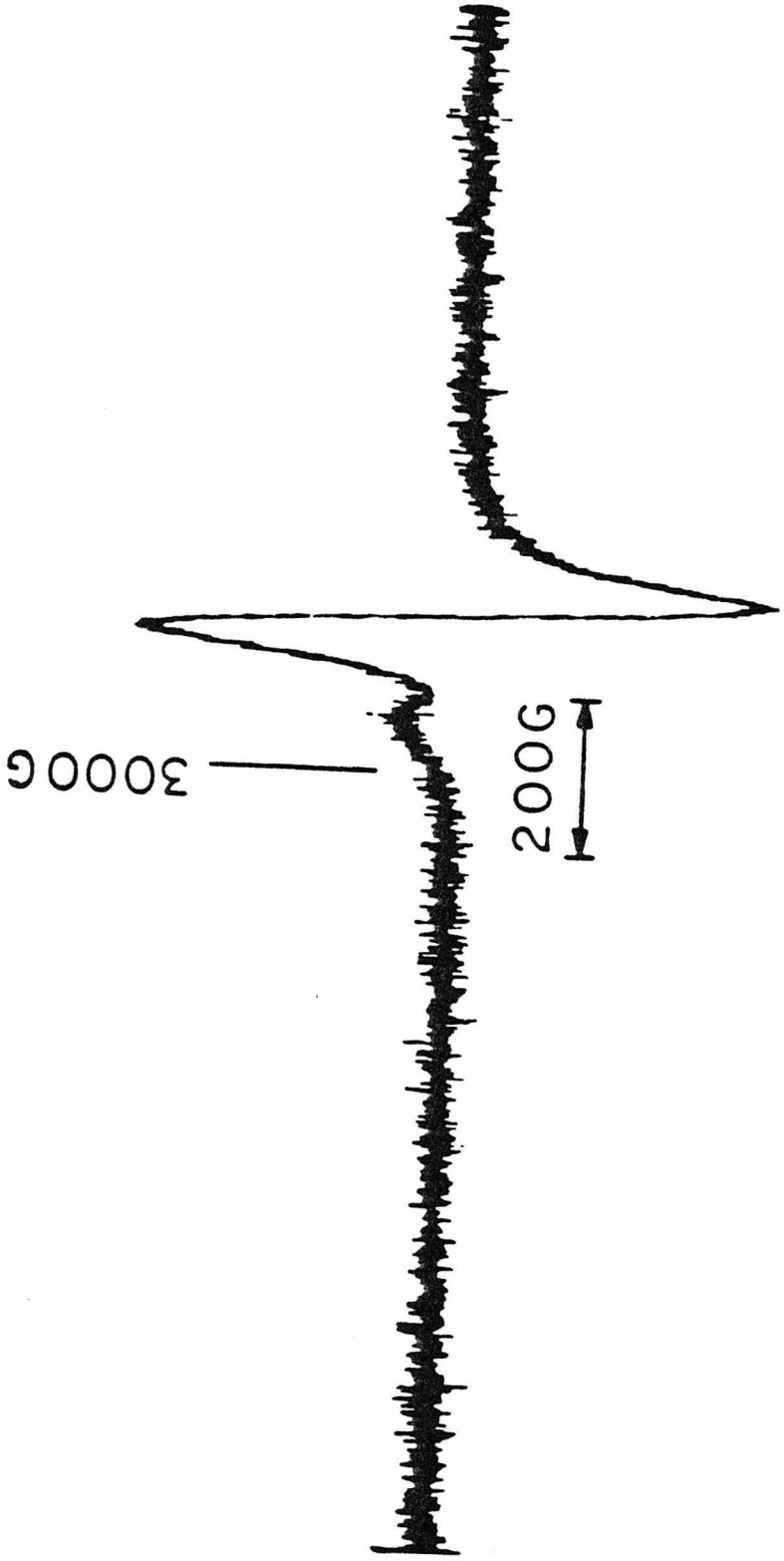

Figure 2

considerations which influence such rates may prove generally useful in understanding electron transfer processes.

Acknowledgment. We appreciate financial assistance from the National Science Foundation and a Sloan Fellowship to R. R. G.

Robert R. Gagné and D. Michael Ingle

Contribution No. 6104 from the

Division of Chemistry and Chemical Engineering

California Institute of Technology

Pasadena, California 91125

References and Notes

(1) Lovecchio, F. V.; Gore, E. S.; Busch, D. H. J. Am. Chem. Soc. 1974, 96, 3109.

(2) Peng, S. M.; Ibers, J. A.; Millar, M.; Holm, R. H. J. Am. Chem. Soc. 1976, 98, 8037.

(3) Olsen, D. C.; Vasilevskis, J. Inorg. Chem. 1969, 8, 1611.

(4) Rillema, D. P.; Endicott, J. F.; Papaconstantinou, E. Inorg. Chem. 1971, 10, 1739.

(5) Curtis, N. F. J. Chem. Soc. 1964, 2644.

(6) All isolated complexes gave satisfactory C, H, N, and Ni analyses.

(7) Carbon monoxide equilibrium binding constants were measured electrochemically as reported recently for copper complexes.[8]

(8) Gagné, R. R.; Allison, J. L.; Ingle, D. M. Inorg. Chem. 1979, 101, 0000.

(9) Gagné, R. R.; J. Am. Chem. Soc. 1976, 98, 6709.

(10) Gagné, R. R.; Allison, J. L.; Gall, R. S.; Koval, C. A. J. Am. Chem. Soc. 1977, 99, 7170.

(11) Gagné, R. R.; Allison, J. L.; Lisensky, G. C. Inorg. Chem. 1978, 17, 3563.

(12) Schrauzer, G. N. Chem. Ber. 1962, 95, 1438.

(13) King, R. B., Ed.; Organometallic Synthesis, Vol. I, p. 70.

(14) For an example of intramolecular electron transfer upon dimerization of a nickel(II) ligand radical anion complex, see reference 2. For an example of phase change dependent intramolecular electron transfer in a Ni(III)/Ni(II) radical cation system, see references 15 and 16.

(15) Johnson, E. C.; Niem, T.; Dolphin, D. Can. J. Chem. 1978, 56, 1382.

(16) Barefield, E. K.; Mocella, M. T. J. Am. Chem. Soc. 1975, 97, 4238.

(17) Complex 8 was also prepared electrochemically (E^f = -0.80 V vs. nhe) with similar results.

(18) Spectra in various solvents gave qualitatively similar results.

(19) Below 233 K the free radical signal begins to decrease in intensity, presumably due to dimerization giving diamagnetic nickel-nickel bonded species.[2] Dimerization does not appear to be significant in the temperature range of 295 K to 233 K, since the total integrated area of the two EPR signals remains constant.

Chapter 2

Synthesis and Properties of Unusual Paramagnetic Four-Coordinate and Five-Coordinate Macrocyclic Ligand Nickel(I) Complexes

Robert R. Gagné
D. Michael Ingle

Synthesis and Properties of Unusual Paramagnetic Four-Coordinate and Five-Coordinate Macrocyclic Ligand Nickel(I) Complexes

ROBERT R. GAGNE* and D. MICHAEL INGLE

Abstract: Mononuclear nickel(II) complexes of tetraaza-macrocyclic ligands undergo one-electron reduction to give either nickel(I) species or species containing nickel(II) complexed to a ligand radical anion. Both reduced species react with carbon monoxide to give paramagnetic, five-coordinate, nickel(I)-carbonyl adducts.

Eleven reduced nickel complexes were studied. Reduction potentials and carbon monoxide binding constants measured electrochemically are reported. EPR parameters obtained in propylene carbonate glass at 100 K are given. Carbonyl stretching frequencies for seven five-coordinate complexes measured in pyridine solution are also tabulated. Two reduced four-coordinate complexes and their corresponding five-coordinate carbonyl adducts have been isolated; solution electronic absorption spectra are reported for the four isolated complexes.

One reduced four-coordinate complex appears to be in thermal equilibrium between two forms: a nickel(II)-stabilized ligand radical and a nickel(I) complex. The variable temperature EPR solution spectrum and electronic absorption spectra of this complex are discussed.

Similarities between the behavior of these nickel complexes and the analogous copper complexes are pointed out. Suggestions for the mode of carbon monoxide binding to the metal are offered.

Introduction

Metal complexes of synthetic tetraaza-macrocycles have received a great deal of attention. The kinetic stability towards dissociation that they impose on their complexes apparently contributes to their unusual chemical and electrochemical properties.[1,2] In addition to kinetic stability, certain macrocycles, such as some of those employed here, lend thermodynamic stability to their metal complexes. Often these macrocyclic ligands stabilize metals in formal oxidation states that normally are not subject to isolation or study in other types of coordination compounds. This affords the opportunity to study the chemical reactivity of uncommon oxidation states in a homeostructural ligand environment and to study the effect of ligand modifications on these chemical properties.

In the 14-membered cyclic tetraaza-ligands, there is an excellent opportunity to study the effect of the degree of ligand unsaturation on the chemical reactivity of the metal complexes.[3,4] Recently, reduced copper complexes, considered as copper(I) species, have been isolated in macrocyclic ligand environments.[5-8] These complexes show varying affinities for binding π-acids as fifth ligands, creating what are best described as 20 electron Cu(I) complexes.[6,7] These diamagnetic complexes have been regarded as copper(I) compounds for both the four-coordinate and the five-coordinate species.[6-9] In an effort to understand more about the bonding at work behind these unusual complexes, we have set out to study the paramagnetic d^9 nickel analogues to the d^{10} copper complexes previously

studied.[6-8] We report here the synthesis and some of the chemical properties of a new class of paramagnetic, presumably five-coordinate, nickel(I)-carbonyl complexes.

Results and Discussion

Electrochemistry: Reduction Potentials and Carbon Monoxide Binding Constants. Reduction of cyclic tetraaza-nickel(II) complexes has been shown to give either nickel(I) complexes or metal-stabilized ligand radicals, depending on the nature of the ligand.[3] Nickel complexes with conjugated α-diimine moieties, used here, undergo one-electron reduction to give nickel-stabilized ligand radicals, Ni(II) $mac^{\cdot}$. Upon exposure to carbon monoxide in solution, these complexes form presumably five-coordinate nickel(I)-carbonyl complexes (eq 1). Ni(II) complexes without

$$\text{Ni(II) mac}^{\cdot} + \text{CO} \overset{K^{CO}}{\rightleftharpoons} \text{Ni(I) mac (CO)} \qquad (1)$$

the conjugated diimines undergo one-electron reduction to give Ni(I) complexes, Ni(I) mac, which also coordinate CO to give presumably five-coordinate nickel(I)-carbonyl complexes (eq 2).

$$\text{Ni(I) mac} + \text{CO} \overset{K^{CO}}{\rightleftharpoons} \text{Ni(I) mac (CO)} \qquad (2)$$

Binding constants for the formation of carbonyl adducts to eleven reduced nickel complexes (shown in Figures 1 and 2) have been

Figure 1

Skeletal Representations for Complexes 1-6

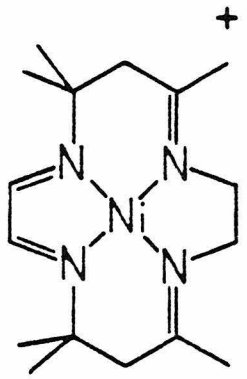

1

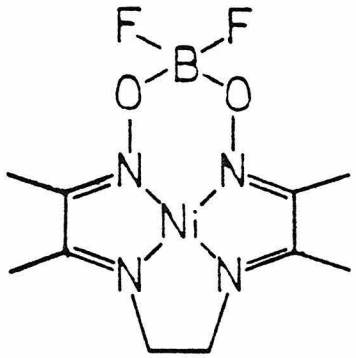

2

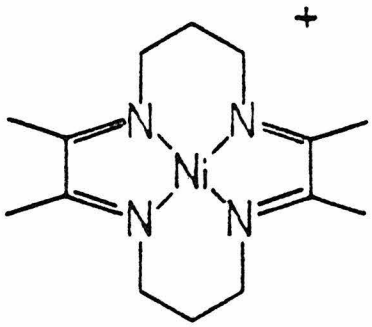

3

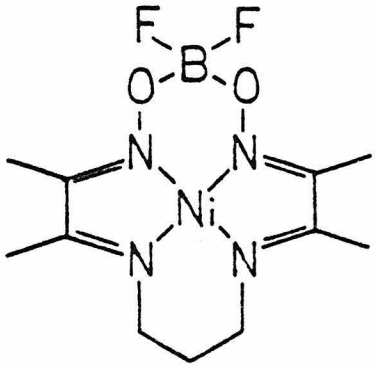

4

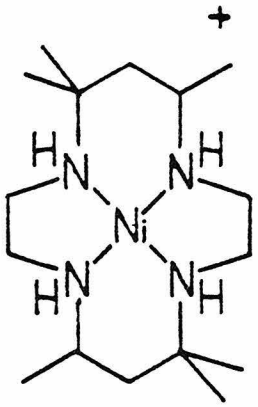

5

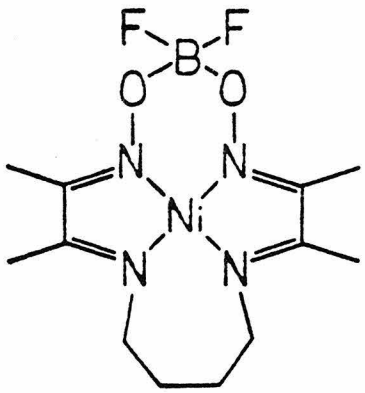

6

Figure 1

Figure 2

Skeletal Representations for Complexes 7-11

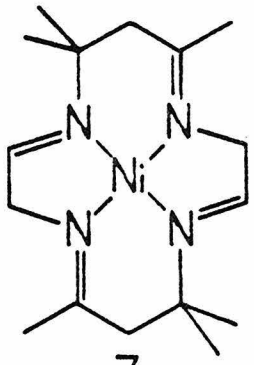

7

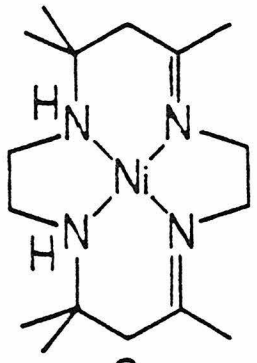

8

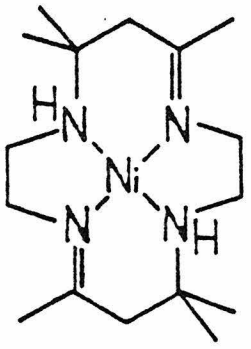

9

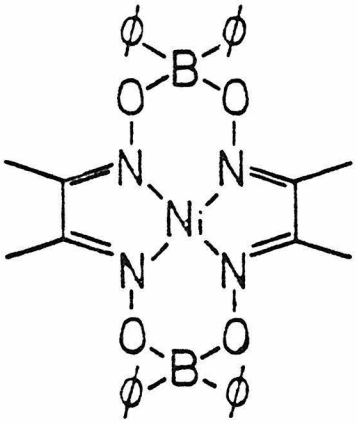

10

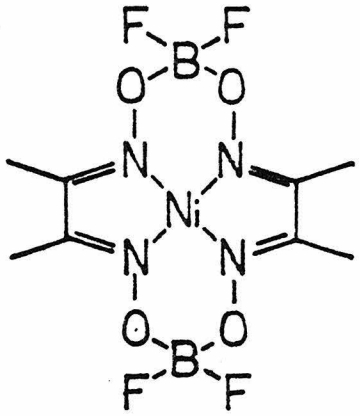

11

Figure 2

measured. The binding constants for these complexes measured in N, N-dimethylformamide (DMF) are given in Table I. The techniques for measuring these binding constants have been described elsewhere.[9]

This electrochemical technique allows for the measuring of the binding constants of CO to the reduced nickel complex by using the readily available nickel(II) compounds as starting materials. Assuming that coordination of CO to the reduced nickel complex is the only equilibrium occurring in solution, application of the Nernst equation yields the electrochemical relationship (eq 3) between the binding constant, K^{CO},

$$K^{CO} = [\exp(\Delta E(nF/RT))-1]/[CO] \qquad (3)$$

the concentration of carbon monoxide, [CO], and the observed difference in the experimentally obtained reduction potentials under argon and CO, ΔE.[10] These reduction potentials were obtained by dc polarography. All nickel complexes reported here undergo reversible or quasi-reversible reductions in DMF. Slopes obtained from the dc polarography indicated one-electron reduction in all cases except for 2 and 4, which show evidence for dimerization as the reduced complex.[11] Constant potential electrolyses indicated that all reductions were one-electron reductions.

Binding constants for CO vary substantially from complex to complex. Compounds 5, 7, 8, and 9, which do not contain conjugated α-diimine moieties, form four-coordinate nickel(I) complexes upon reduction. These four complexes have similar CO binding constants.

Table I. Binding Constants of Various Reduced Nickel Complexes with Carbon Monoxide in DMF.

Nickel Complex	$E_{\frac{1}{2}}$[Ar], V[a]	K^{CO}, M^{-1}[b]
1	-0.456	0[c]
2	-0.478	0[c]
3	-0.527	$1.7(4) \times 10^2$
4	-0.617	$2.7(3) \times 10^3$
5	-1.295[d]	7.8×10^4[d]
6	-0.798	$1.3(1) \times 10^4$
7	-1.081	$4.5(5) \times 10^4$
8	-1.249	$1.8(2) \times 10^4$
9	-1.241	$4.7(5) \times 10^4$
10	-0.979	$5.1(5) \times 10^4$
11	-0.786	$2.8(3) \times 10^5$

[a] vs. nhe

[b] Errors are based on ΔE error of ± 0.0025 V.

[c] $K_f^I \leq 10$ are reported as zero.

[d] Estimated by cyclic voltammetry.

Variations in binding constants may reflect differences in the flexibility of the macrocycle as the complexes are expected to be square-pyramidal with the metal atom displaced some distance out of the plane of the four nitrogen ligands. Crystal structures for the copper(I) complexes $\underset{\sim}{20}$[7] and $\underset{\sim}{21}$[15] (Figure 3) show the metals are displaced out of the plane of the four nitrogens by 0.96 Å and 1.02 Å, respectively; as a result, the macrocycle must distort to accommodate the large out of plane displacement. While it is not likely that the nickel atoms are as far out of the ligand plane as the coppers are, some metal displacement accompanied by ligand distortion is anticipated. For example, complexes $\underset{\sim}{5}$, $\underset{\sim}{7}$, and $\underset{\sim}{9}$ differ only by the degree of unsaturation in the macrocycle; although the three compounds exhibit a marked change in their reduction potentials, the CO binding constants are similar, with the saturated complex, $\underset{\sim}{5}$, having the lowest K^{CO}. With all four nitrogens of $\underset{\sim}{5}$ being saturated, it can be expected that the ligand may be slightly more rigid than the others, possibly accounting for the lowered K^{CO}. In addition, the similarity of CO binding constants suggest that the σ-basicity of the macrocyclic ligand may not make a large contribution to the stability of the five-coordinate complex, although they do affect the stability of the four-coordinate Ni(I) complex.

Complexes which do possess conjugated α-diimine functions show a much wider variation in CO binding constants. Compounds $\underset{\sim}{1}$

Figure 3

Skeletal Representations for Complexes 19-21

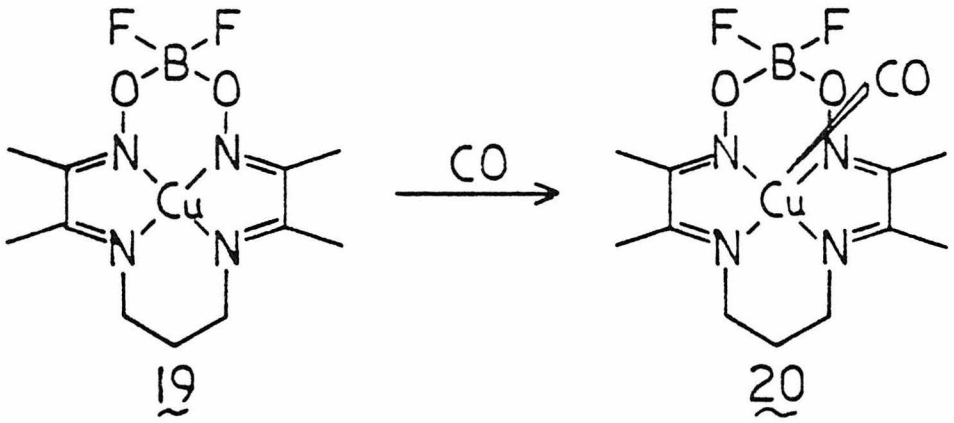

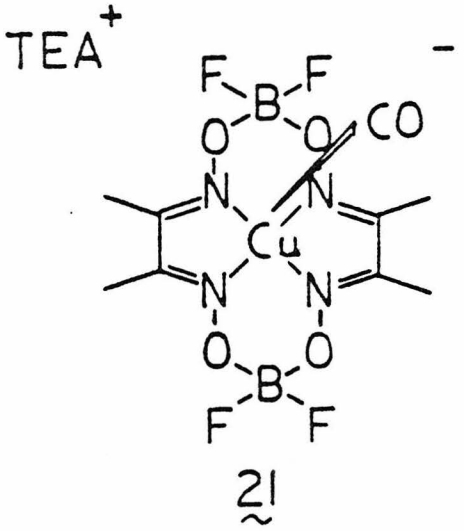

Figure 3

and 2 show no carbonyl adduct formation measurable by the electrochemical method; EPR spectra, vide infra, suggest, however, that there is a small extent of carbonyl formation at low temperatures for those two complexes.

Complexes 2, 4, and 6 represent a series in which the ring size becomes larger, permitting both longer Ni–N bonds and a greater deviation from rigid planarity in the four-coordinate complex. The smallest macrocyclic compound, 2, has the least negative reduction potential of the three compounds. As the macrocyclic size is increased, the reduction potential becomes more negative; the smaller ligand apparently encourages greater stabilization of the ligand-radical by increasing the metal-ligand interaction. Complex 2 also has the smallest CO binding constant of the three complexes. The larger the macrocycle, the greater is its K^{CO}. The smaller macrocycle should be more difficult to distort to give the square-pyramidal nickel(I)-carbonyl complex. An additional factor that may cause the CO binding to vary in these complexes is the extent to which the ligand-radical orbital is stabilized, viz. how far the ligand π^* orbital lies beneath the metal $d_{x^2-y^2}$.[13] The magnitude of this separation between the π^* orbital of the ligand and the metal $d_{x^2-y^2}$ orbital may account for much of the observed trends in carbon monoxide binding constants. This energy separation is of interest particularly for compound 6, which exhibits an equilibrium between the nickel(II) ligand-radical form and the nickel(I) form, where the estimated difference in the two reduced species is 0.75 kcal/mole.[14]

Complexes 3, 4, and 11 show a series in which the trimethylene groups bridging the two α-diimines are replaced successively with difluoroborate groups. Again the reduction potentials, as well as their affinity for CO, varies monotonically over the short series; the least negative reduction potential also corresponds to the smallest K^{CO}. For the analogous copper(I)-carbonyl complexes, where X-ray crystallographic results show possible copper-fluorine interactions for compound 20[7] and compound 21[15] (Figure 3), the suggestion was offered that the higher CO binding constants also observed for copper(I) complexes containing difluoroborate groups were due to a favorable metal-fluorine interaction in the five-coordinate complex.[9] Compound 10, in which the fluorines have been replaced with phenyl groups, exhibits a CO binding constant not significantly smaller than that of 11; this indicates the probable lack of strong metal-fluorine interactions. Another possibility indicated here by the trend of reduction potentials is that the borate bridging groups may raise energy of the ground state of the four-coordinate complex facilitating CO binding; raising the energy of the π^* orbital of the four-coordinate complex would favor the five-coordinate carbonyl adduct if the energy levels of the carbonyl adduct were not altered. Geometrical differences between the alkyl group and borate groups cannot be ignored. Other secondary

forces such as the ligand's ability to distort and solvation effects may also play a role in the binding constant changes.

EPR Spectroscopy. Electron paramagnetic spectra were obtained of the reduced nickel complexes in propylene carbonate glass at 100 K. The results are shown in Table II. Complexes possessing conjugated α-diimine moieties show an isotropic value, indicative of a ligand-radical signal.[3] Upon addition of carbon monoxide (Figure 4), these signals disappear and give rise to the anisotropic spectra of a d^9-metal with axial symmetry.[16] The EPR spectra strongly support the contention for square-pyramidal geometries for the carbonyl-adduct. This process, by which the odd electron is induced to migrate to a largely metal orbital from a predominantly ligand orbital, may be considered an intramolecular electron transfer.[12, 14]

Those complexes lacking conjugated α-diimines (5, 7, 8, and 9) give anisotropic axial EPR spectra as the four-coordinate complex. Upon exposure to carbon monoxide, these complexes give rhombic spectra (Figure 5). Both the four-coordinate and five-coordinate complexes of 5, 7, 8, and 9 appear to be nickel(I) complexes.

All of the five-coordinate carbonyl complexes contain the nickel in the +1 oxidation state. The EPR spectra, as expected, support the $d_{x^2-y^2}$ orbital as the highest energy metal orbital.[16]

Infrared Carbonyl Stretching Frequencies. Infrared stretching frequencies of the carbonyl group for several of these reduced nickel complexes measured in CO-saturated pyridine solution are found in

Table II. ESR Data for Reduced Nickel Complexes in Propylene Carbonate Glass at 100 K

Nickel Complex	Ar[d]	CO[e]
1[a]	2.000(23)[b]	$g_{\|\|} = 2.230$, $g_{\perp} = 2.066$
2[a]	2.002(20)[b]	$g_{\|\|} = 2.227$, $g_{\perp} = 2.063(10)$[c]
3[a]	2.008(35)[b]	$g_{\|\|} = 2.235$, $g_{\perp} = 2.069(12)$[c]
4	2.007(25)[b]	$g_{\|\|} = 2.226$, $g_{\perp} = 2.065(12)$[c]
5	$g_{\|\|} = 2.253$, $g_{\perp} = 2.054$	$g_1 = 2.198$, $g_2 = 2.123$, $g_3 = 2.012$
6	2.020(40)[b]	$g_{\|\|} = 2.242$, $g_{\perp} = 2.068(12)$[c]
7[a]	$g_{\|\|} = 2.190$, $g_{\perp} = 2.056$	$g_1 = 2.238$, $g_2 = 2.159$, $g_3 = 2.066$
8	$g_{\|\|} = 2.235$, $g_{\perp} = 2.086$	$g_1 = 2.305$, $g_2 = 2.151$, $g_3 = 2.056$
9	$g_{\|\|} = 2.220$, $g_{\perp} = 2.063$	$g_1 = 2.201$, $g_2 = 2.123$, $g_3 = 2.018$
11	2.002(16)[b]	$g_{\|\|} = 2.225$, $g_{\|\|} = 2.065(12)$[c]

[a]Generated chemically or electrochemically in situ. [b]Peak-to-peak width (in gauss) of first derivative spectra. [c]Nitrogen superhyperfine (in gauss), where resolvable. [d]Spectra taken in argon-saturated propylene carbonate. [e]Spectra taken in carbon monoxide-saturated propylene carbonate.

Figure 4

EPR Spectra in Propylene Carbonate Glass

at 100 K of $\underset{\frown}{4}$ and $\underset{\frown}{4}$(CO)

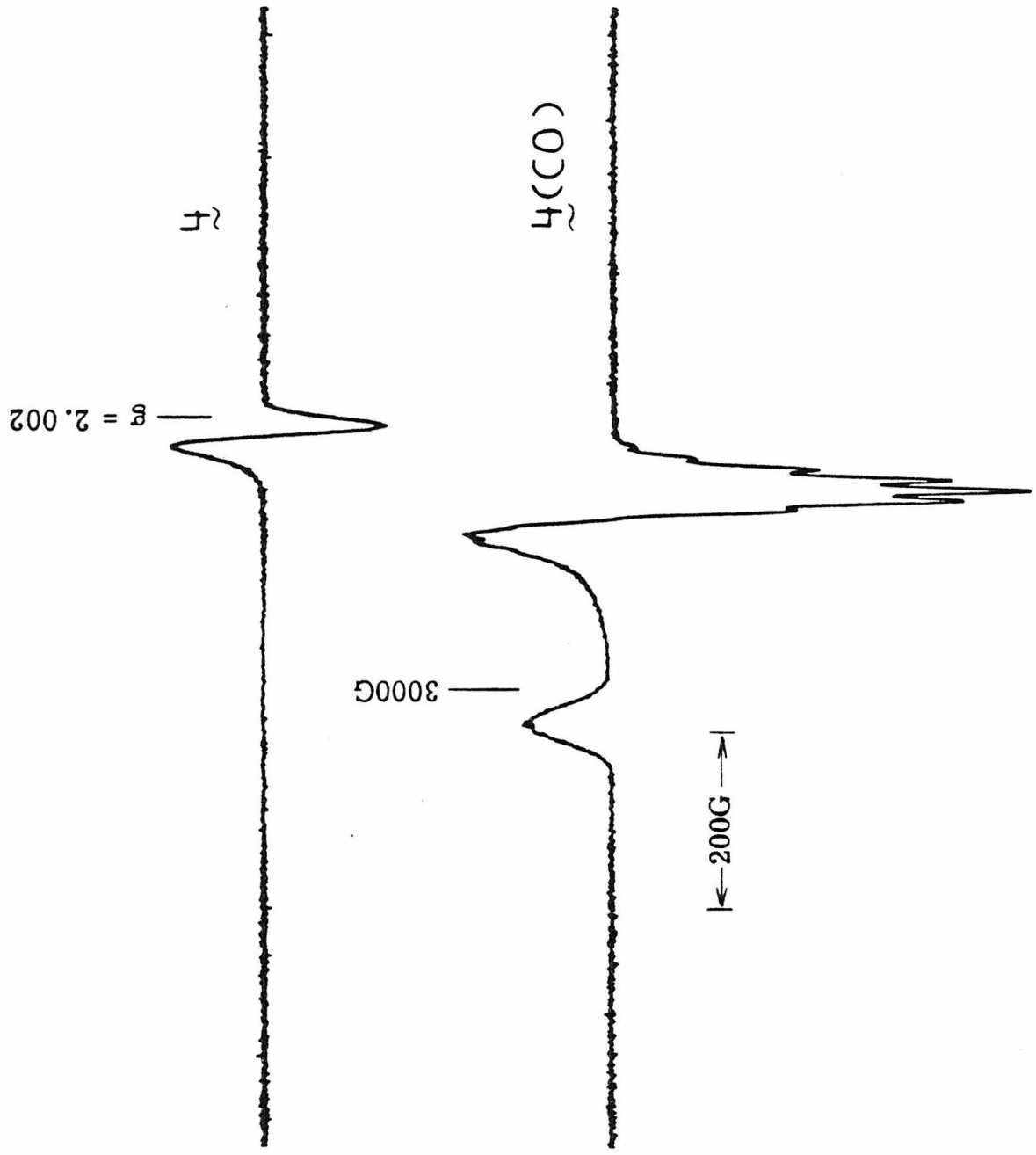

Figure 4

Figure 5

EPR Spectra in Propylene Carbonate Glass

at 100 K of $\underset{\frown}{9}$ and $\underset{\frown}{9}$(CO)

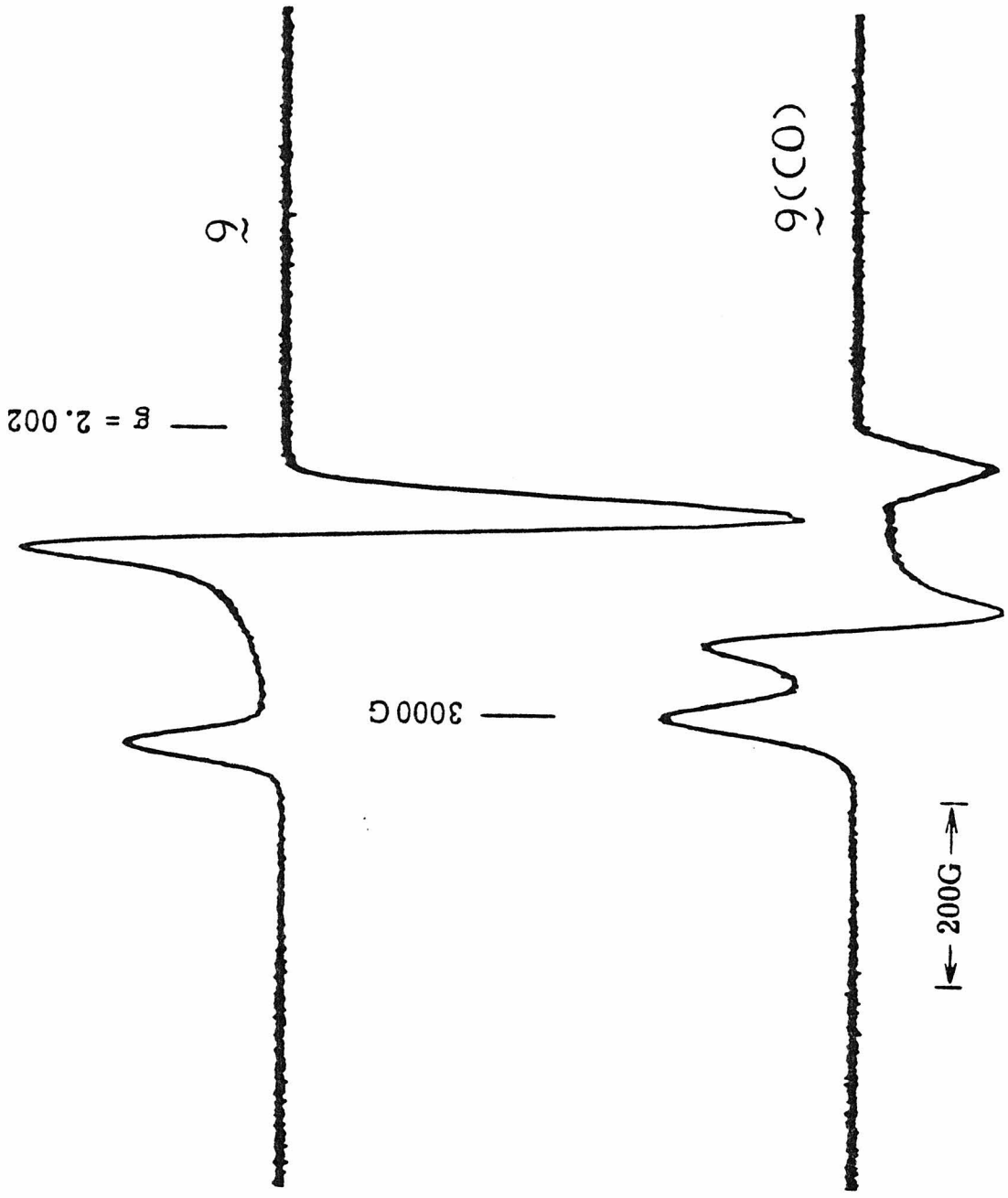

Figure 5

Figure 6

Electronic Absorption Spectra of Compounds

10 (solid line) and 10(CO) (broken line)

in Propylene Carbonate Solution

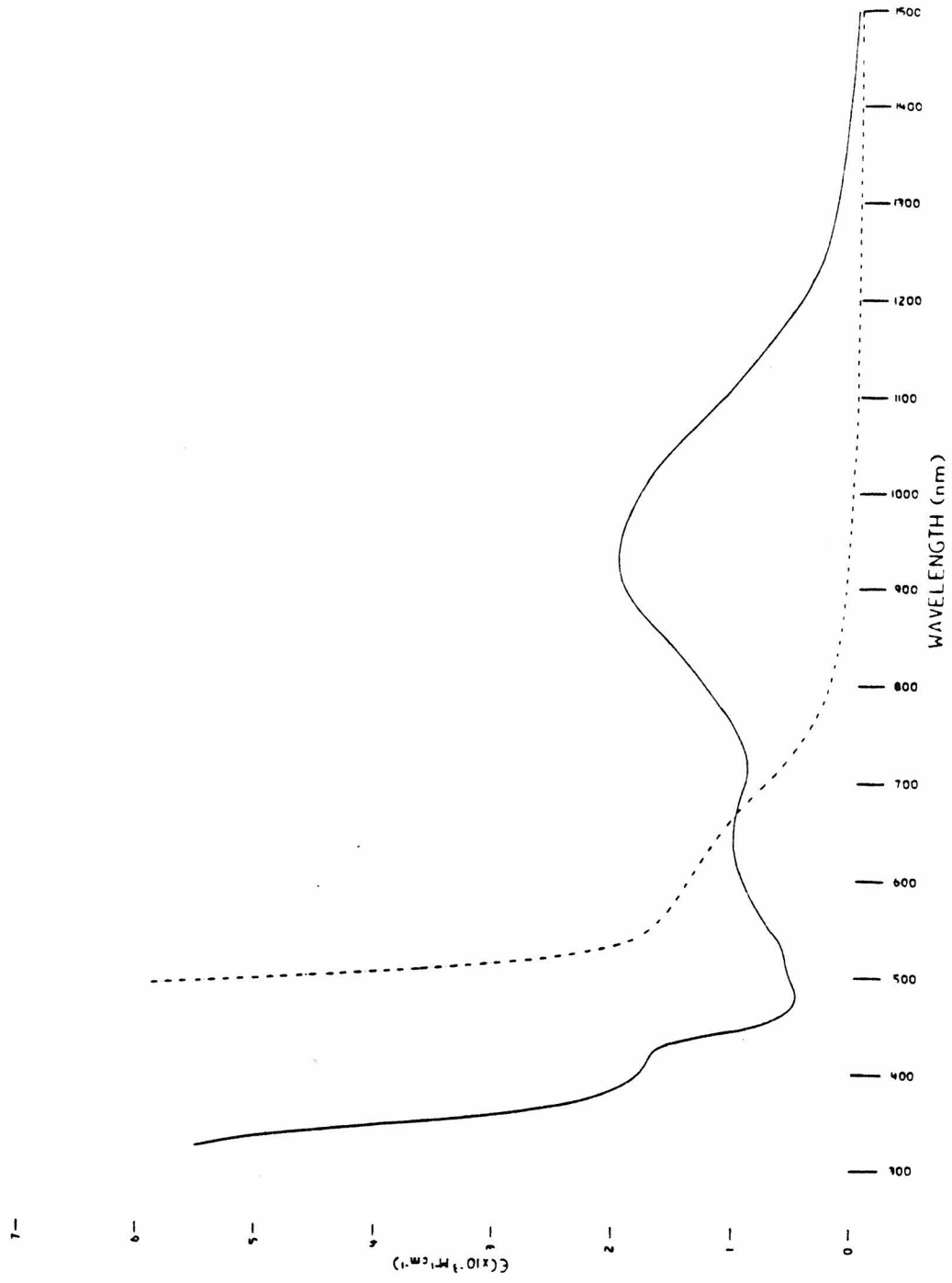
1500
1400
1300
1200
1100
1000
900
800
700
600
500
400
300
WAVELENGTH (nm)
7
6
5
4
3
2
1
0

Figure 6

Figure 7

Electronic Absorption Spectra of Compounds

$\underset{\frown}{9}$ (solid line) and $\underset{\frown}{9}$(CO) (broken line)

in Propylene Carbonate Solution

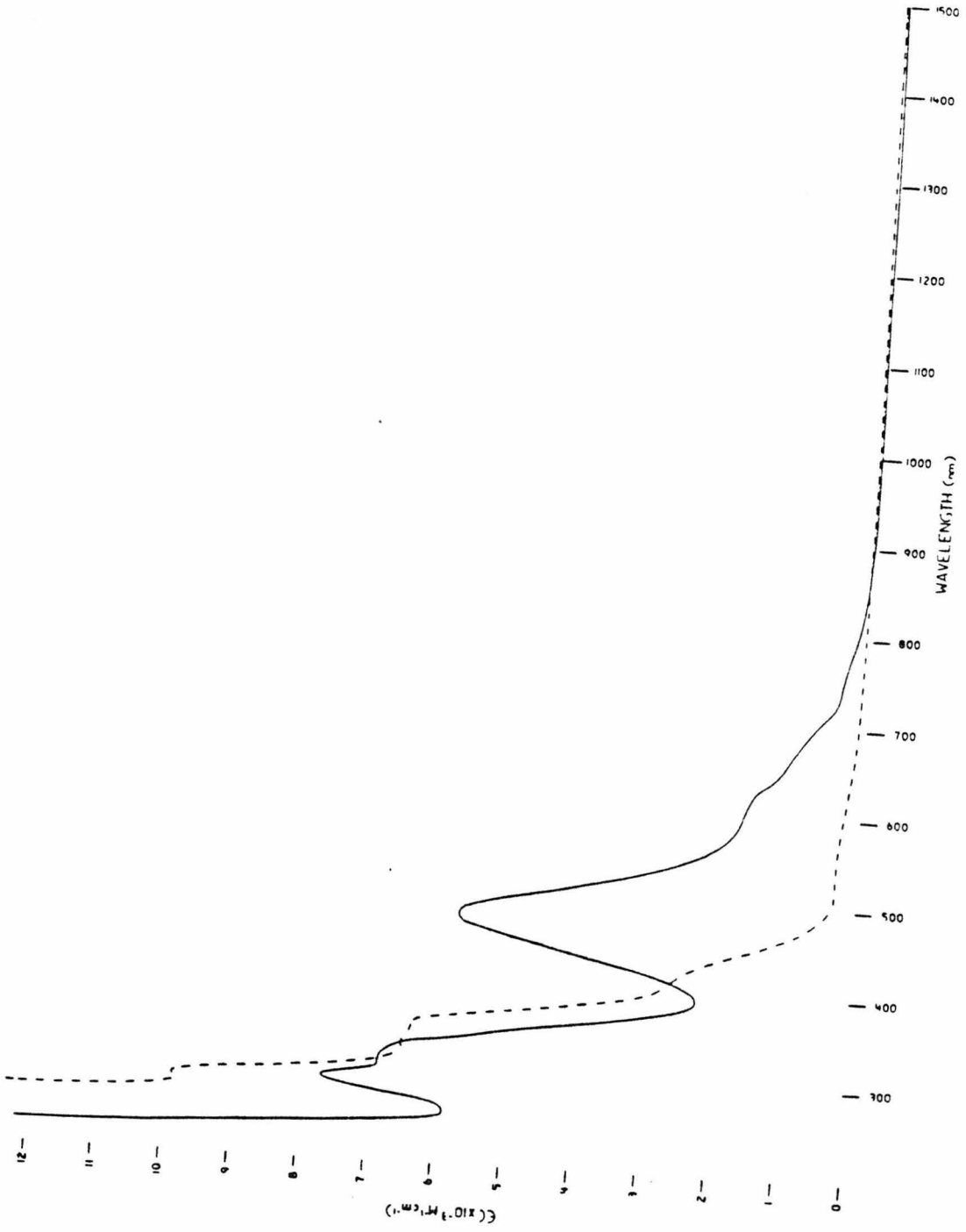
1500
1400
1300
1200
1100
1000
900
800
700
600
500
400
300
WAVELENGTH (nm)
12
11
10
9
8
7
6
5
4
3
2
1
0

Figure 7

Figure 8

EPR Spectrum of $\underset{\frown}{6}$ in Acetonitrile at 298 K

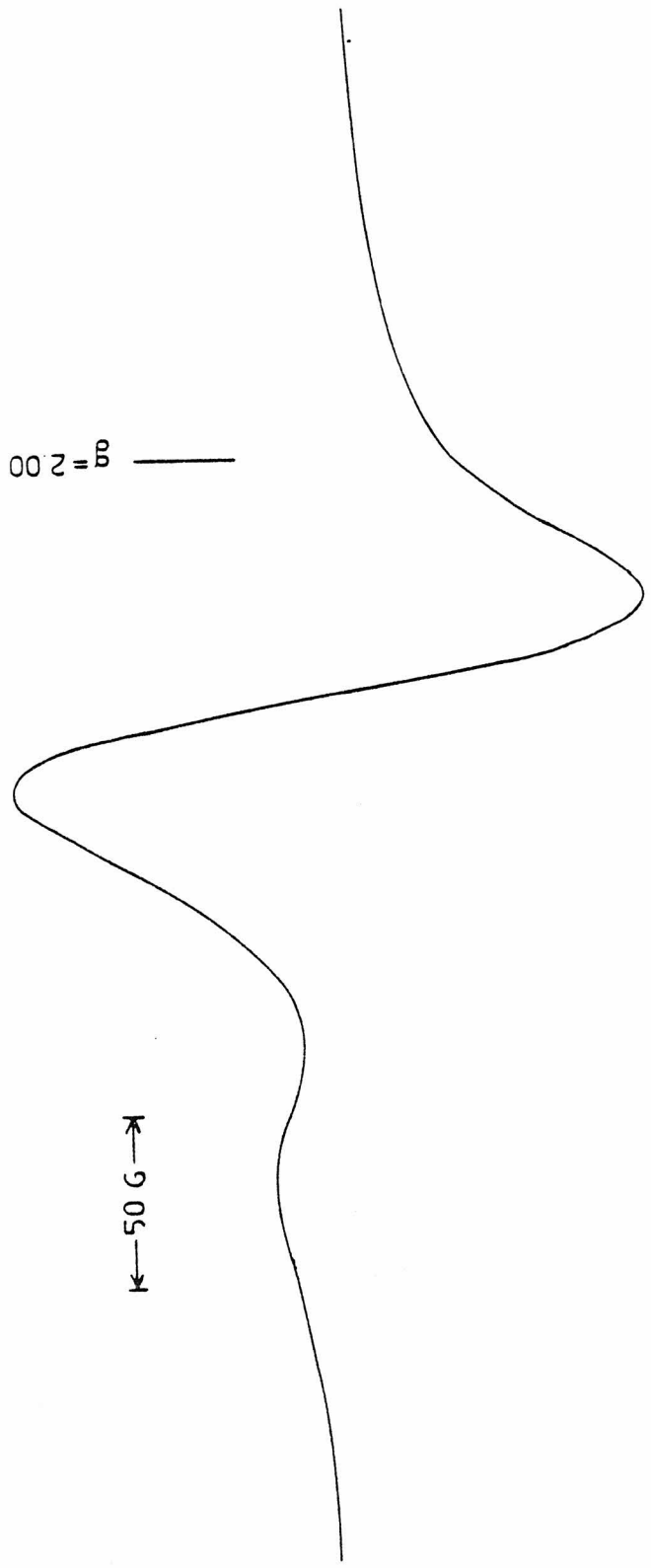

Figure 8

Table III. These complexes fall into three groups. Complexes with four imine nitrogens (conjugated or not) have ν_{CO} near 2020 cm^{-1}; complexes with two imines are near 1960 cm^{-1}; complex $\underset{\frown}{5}$(CO), which has a totally saturated ligand, i. e., no imine nitrogens, has the lowest carbon monoxide stretching frequency, 1949 cm^{-1}. These carbonyl stretching frequencies show no correlation to binding constant. The lack of dependence of carbonyl stretching frequency on K^{CO} suggests that the major contribution to the metal-carbon bond does not involve the metal d-orbitals. This is consistent with the expectation that the binding of late transition series metals to π-acids like CO is primarily through their 4s and 4p orbitals, rather than their d-orbitals.[13] However, minor contributions from the d_{xy} and d_{yz} orbitals to π-back donation is expected to have some contribution in the nickel-carbon bond and thus influence the carbonyl stretching frequencies. In the expected square-pyramidal environment, the metal d_{xz} and d_{yz} orbitals should interact directly with the ligand nitrogen lone pair as well as the carbon monoxide π-antibonding orbitals. Through a symbiotic effect, the harder saturated nitrogens appear to cause a greater delocalization of electron density into the CO π^* orbital by way of the metal d-orbitals than unsaturated nitrogen donors, thus leading to lower carbonyl stretching frequencies for the saturated complex.

Table III. Carbonyl Stretching Frequencies of Nickel(I) Carbonyl Complexes Measured in Pyridine Solution

Nickel Complex	$\nu^{CO}_{cm^{-1}}$
3(CO)[a]	2020
4(CO)[a]	2015
5(CO)[a]	1949
7(CO)[a]	2020
8(CO)[a]	1957
9(CO)[b]	1962 (1961)[c]
11(CO)[b]	2020 (2029)[c]

[a]Carbonyl complexes were generated in situ. [b]Carbonyl complexes were both generated in situ and isolated as crystalline products. [c]IR taken in the solid state (KBr pellet).

Electronic Absorption Spectra. The reduced nickel species are all deeply colored and their electronic absorption spectra consist of moderately intense charge-transfer bands. Nickel(II) ligand-radical complexes are all green and exhibit qualitatively similar spectra; upon formation of the carbonyl adduct, browish-red solutions are formed. Representative spectra taken in propylene carbonate solution are shown in Figure 6. While these charge-transfer bands are not assigned, they are felt to arise from the low energy transition between the ligand π^* orbitals and the $d_{x^2-y^2}$ nickel orbital.

The nickel(I) complexes are all deep brown. Their carbonyl complexes are bright green. Sample solution spectra obtained in propylene carbonate solution are shown in Figure 7.

Temperature-Dependent Behavior of Complex 6. As reported earlier,[14] complex 6 was synthesized and found to exist in two reduced forms: nickel(II) ligand-radical and nickel(I). Those two forms, which are believed to consist of two conformations in equilibrium, give a solution EPR spectrum in acetonitrile and other aprotic solvents showing two g-values (g = 2.113 and g = 2.048) at 25°C (Figure 8), whose relative ratio is temperature dependent. The estimated difference between the nickel(I) and nickel(II)-stabilized ligand-radical forms is 0.75 kcal/mole.

In addition to these observations, temperature-dependent electronic absorption spectra in acetonitrile or propylene carbonate

undergo changes which are ascribed to the same equilibrium process (Figure 9). At 26° C, the two bands centered at 560 and 860 nm are assigned to the nickel(II)-stabilized ligand-radical form; the less intense bands at 790 and 1080 nm are assigned to the nickel(I) form. At reduced temperature (-40° C), the bands associated with the nickel(I) form decrease in intensity. Upon rewarming to 26° C, the original spectrum is obtained.

Summary

Although five-coordinate Ni(I) species are known,[17] carbonyl complexes of metals with a valence electron count greater than eighteen are rare. While the four-coordinate complexes exhibit unusual redox properties, undergoing either metal or ligand reduction--depending on the macrocyclic ligands structure, the five-coordinate carbonyl adducts are all found to be paramagnetic, 19 electron nickel(I) complexes. It is felt that the metal d-orbitals play a minor role in CO binding and that the predominant interaction is through σ-interactions with the metal 4s and 4p orbitals.

Comparisons of compound 6, which appears to be in equilibrium between two reduced forms, and compounds 2 and 4, which appear to be relatively trapped into the nickel(II) ligand-radical form, show that the macrocycle size is an important factor in the stability of the ligand-radical.

These nickel complexes were studied to aid in the understanding of the bonding behind the diamagnetic copper(I) complexes studied

Figure 9

Variable Temperature Electronic Absorption Spectra in Propylene Carbonate of $\underset{\frown}{6}$ at (A) 26°C, (B) -40°, (C) upon rewarming to 26°C

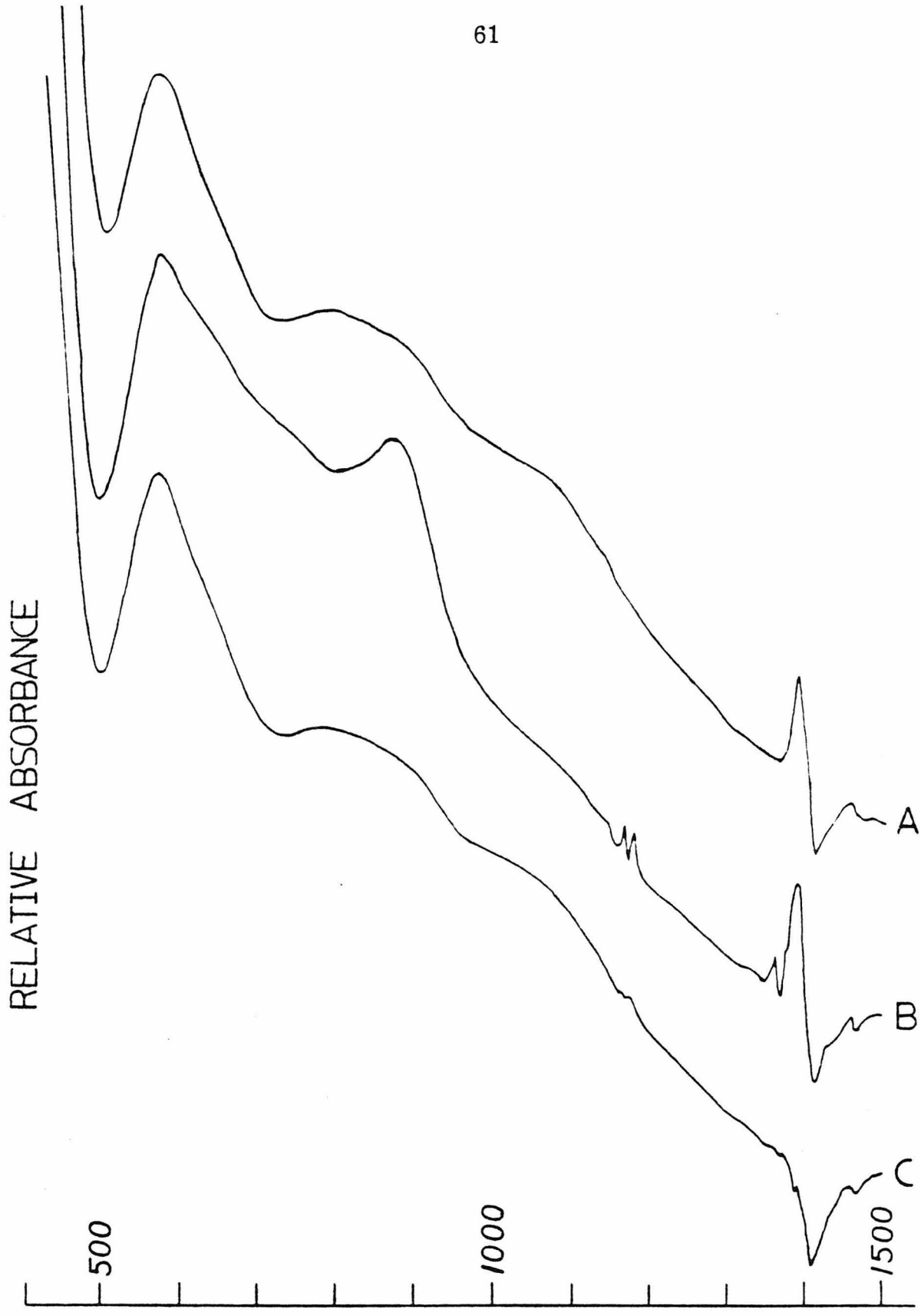

Figure 9

earlier.[6-9] These paramagnetic nickel analogues to the reduced copper systems have given complementary data to help formulate bonding schemes for the carbonyl adducts. In light of a number of similarities between those copper compounds and the nickel(II) ligand-radical and nickel(I)-carbonyl compounds, we are presently reexamining the copper(I) designation for the metal in the reduced four-coordinate copper complexes.

Experimental Section

Materials. All chemicals were reagent grade and were used as received unless otherwise noted. Reagent grade N, N-dimethylformamide (DMF) was dried first over $MgSO_4$, followed by distillation from 4A molecular sieves. Argon, for electrochemical measurements, was purified by passing over hot copper turnings and then through 4A molecular sieves. Carbon monoxide was passed over activated Ridox® and then 4A molecular sieves. Tetrabutylammonium perchlorate TBAP (Southwestern Analytical Chemicals) was dried exhaustively in vacuo before use. Nickel(II) compounds, precursors to complexes 1,[18] 3,[20] 5,[20] 7,[21,22] 8,[21,22] 9,[23] and 11[24], were prepared by the methods given in the references listed. All nickel(II) salts were used as the perchlorate salt, except for the precursor to complex 5, which was used as the tetrafluoroborate salt. CAUTION: PERCHLORATE SALTS MAY BE EXPLOSIVE. All compounds gave acceptable elemental analysis.

Physical Measurements. Samples of air-sensitive materials for physical studies were manipulated in a Vacuum Atmospheres Dri-lab glove box with a helium atmosphere. Solvents were thoroughly deaerated prior to use.

X-Band EPR spectra were recorded on a Varian E-line spectrometer. Temperatures of 100 K were maintained using an Air Products Heli-Tran liquid helium transfer refrigerator. Temperatures near the ambient temperature were maintained using a Varian V-4540 Variable Temperature Controller. Samples were contained in cylindrical quartz tubes (2-mm diameter) equipped with 2-mm oblique-bore vacuum stopcocks and $\overline{\text{S}}$ 14/20 joints. Solutions of the carbonyl adducts were made by evacuating the helium atmosphere in the tube on a vacuum line and then introducing carbon monoxide gas.

Infrared spectra were obtained on a Beckman IR-4240 infrared spectrometer. Solution spectra were obtained using sodium chloride cells (1 mm). Carbon monoxide was introduced into the cell by the insertion of a syringe needle, attached to a tygon tube with a flow of CO passing into serum caps on the solution IR cells until the carbonyl adduct was generated.

Electronic absorption spectra were recorded on a Cary-14 spectrometer. Solution spectra were recorded using quartz cells (0.1 cm or 1 cm) equipped with Kontes teflon® stopcocks to allow for addition of carbon monoxide as described above under the EPR procedure. Temperature control was maintained using a quartz vacuum Dewar and a regulated flow of liquid nitrogen-cooled nitrogen

gas; temperatures were recorded using an iron-constantan thermocouple. NMR spectra were obtained on a Varian EM-390. Chemical shifts are reported relative to internal TMS.

Electrochemistry. The methods and equipment used for polarographic analysis have been described earlier elsewhere.[9]

Synthesis of (3, 6, 10, 13-tetraaza-1-bora-1, 1-difluoro-4, 5, 11, 12-tetramethyl-2, 14-dioxacyclotetradeca-3, 5, 10, 12-tetraenato)-nickel(II) perchlorate, 15 (Precursor to 4). Excess boron trifluoride etherate (7 ml) was added to a slurry of [(3, 3′-trimethylenedinitrilo)-bis(2-butanone oximato)] nickel(II) perchlorate[24] (5g) in dioxane (30 ml). The reaction was heated at reflux for 1 hr. After cooling to the ambient temperature, the reaction mixture was filtered. The yellow-orange solid was washed successively with ethanol and ether. Recrystallization from aqueous acetone gave the yellow-orange microcrystalline solid. Anal. Calcd. for $C_{11}C_{18}BClF_2N_4NiO_6$: C, 29.67; H, 4.07; N, 12.58. Found: C, 30.0; H, 4.3; N, 12.6.

Synthesis of (3, 6, 10, 13-tetraaza-1-bora-1, 1-difluoro-4, 5, 11, 12-tetramethyl-2, 14-dioxacyclotetradeca-3, 5, 10, 12-tetraenato)nickel, 4.[26] In a He atmosphere chamber, 15 (2.3 g) was slurried in acetone (35 ml). Cobaltocene[25] (0.97 g) was added. The reaction was stirred 8 m. The product was then isolated by vacuum filtration. The forest-green crystals were then washed with acetone and dried under a stream of He. Anal. Calcd. for $C_{11}H_{18}BF_2N_4NiO_2$: C, 38.21; H, 5.25; N, 16.20. Found: C, 38.3; H, 5.1; N, 16.2.

Synthesis of cobaltocinium bis(difluoroboroglyoximato)nickel, 11. Under a He atmosphere, nickel(II) bis(difluoroboroglyoximate)[22] (0.40 g) was slurried in acetone (20 ml). Cobaltocene (0.24 g) was added. The reaction was stirred vigorously for 8 min. The product was then isolated by vacuum filtration. The dark green microcrystalline product was then washed with acetone and dried in vacuo. Anal. Calcd. for $C_{18}H_{22}B_2CoF_4N_4NiO_4$: C, 37.68; H, 3.87; N, 9.77; Ni, 10.23. Found: C, 38.1; H, 3.9; N, 10.0; Ni, 10.3.

Synthesis of carbonyl cobaltocinium bis(difluoroboroglyoximate)-nickel, 12. Under a carbon monoxide atmosphere in a Schlenk apparatus, cobaltocene (0.20 g) was dissolved in CO-saturated acetone (5 ml). Nickel(II) bis(difluoroboroglyoxime)(0.33g) was dissolved in CO-saturated acetone (35 ml). The two solutions were combined with stirring under a stream of CO. After 10 min., the reaction was filtered and the brown microcrystalline product was dried under a stream of CO. Anal. Calcd. for $C_{19}H_{22}B_2CoF_4N_4NiO_5$: C, 37.93; H, 3.69; N, 9.31; Ni, 9.76. Found: C, 37.8; H, 3.5; N, 9.5; Ni, 9.7.

Synthesis of carbonyl (5, 7, 7, 12, 14, 14-hexamethyl-1, 4, 8, 11-tetraazacyclotetradeca-4, 11-diene)nickel(I) perchlorate, 13. To sodium amalgam (0.25%, 100 g) under an inert nitrogen atmosphere in a Schlenk apparatus, was added a degassed solution of (5, 7, 7, 12, 14, 14-hexamethyl-1, 4, 8, 11-tetraazacyclotetradeca-4, 11-diene)nickel(II) diperchlorate (1.0 g) in a acetonitrile (50 ml). The reaction mixture was stirred for 6 hr. The dark brown solution was filtered under a nitrogen atmosphere.[1] The filtrate was then stirred under a carbon

monoxide atmosphere. The solution became bright green. The solvent was slowly evaporated off under a stream of carbon monoxide. The remaining solid was washed under a nitrogen atmosphere with oxygen-free water (50 ml). The mixture was rapidly filtered. The dark green solid was dried in vacuo. Anal. Calcd. for $C_{17}H_{24}ClN_4NiO_5$: C, 43.75; H, 6.91; N, 12.01; Ni, 12.58. Found: C, 43.6; H, 6.6; N, 11.9; Ni, 12.5.

Synthesis of (3, 6, 9, 12-tetraaza-1-boro-1, 1-difluoro-4, 5, 10, 11-tetramethyl-2, 13-dioxacyclopentadeca-3, 5, 9, 11-tetraenato)nickel(II) perchlorate · ethanol, 14 (Precurser to 2). Excess boron trifluoride etherate (7 ml) was added to a slurry of [(3, 3′-ethylenedinitrilo)-bis(2-butanone oximato)]nickel(II) perchlorate[24] (5 g) in dioxane (30 ml). The reaction was heated at reflux for 1 hr. After cooling to the ambient temperature, the reaction mixture was filtered. The yellow solid was washed successively with ethanol and ether. Recrystallization from aqueous ethanol gave a red-orange microcrystalline solid. Anal. Calcd. for (4 (14)-ethanol) $C_{41}H_{70}N_{16}O_{25}Cl_4B_4F_8Ni_4$: C, 28.98; H, 4.15; N, 13.19. Found: C, 28.9; H, 4.1; 13.2.

Synthesis of [(3, 3′-tetramethylenedinitrilo)bis-(2-butanone oximato)]nickel(II) perchlorate, 16. 4, 9-Diaza-3, 10-dimethyldodeca-3, 9-diene-2, 11-dione dioxime[9] (10.0 g) was dissolved in hot ethanol (75 ml). A solution of $Ni(ClO_4)_2 \cdot 6H_2O$ (7.6 g) in ethanol (20 ml) was

added to the hot solution of ligand. The reaction was refluxed 1 hr with stirring. Upon cooling to 2° C, the mixture was filtered. The orange solid was vacuum dried. Anal. Calcd. for $C_{12}H_{21}ClN_4NiO_6$: C, 35.20; H, 5.17, N, 13.68. Found: C, 35.0; H, 5.1; N, 13.7.

Synthesis of (3, 6, 11, 14-tetraaza-1-boro-1, 1-difluoro-4, 5, 12, 13-tetramethyl-2, 15-dioxacyclo tri deca-3, 5, 11-13-tetraenato)-nickel(II) perchlorate monohydrate, 17 (Precursor to 6). A slurry of 16 (1.0 g) in dioxane (15 ml) was treated with boron trifluoride etherate (5 ml) and refluxed 4 hr. The reaction mixture was cooled to the ambient temperature. A white crystalline solid was separated off by filtration. The filtrate was taken to dryness on a rotary evaporator. The residue was recrystallized from water with concentrated sodium perchlorate. The bright green crystalline product was collected by filtration. Upon drying in vacuo, the green crystals gave an orange powder. Anal. Calcd. for $C_{12}H_{22}BClF_2N_4NiO_7$: C, 30.19; H, 4.65; N, 11.74. Found: C, 30.4; H, 4.5; N, 11.8.

Synthesis of (3, 6, 10, 13-tetraaza-1, 8-dibora-4, 5, 11, 12-tetramethyl-1, 7, 9, 14-tetraoxa-1, 1, 8, 8-tetraphenylcyclotetradeca-3, 5 10, 12-tetraenato)nickel(II), 18 (Precursor to 10). Nickel(II) dimethylglyoxime (2.0 g) was refluxed with aminoethoxydiphenylborane (2.5 g) in dioxane (25 ml) for two days under a nitrogen atmosphere. The hot reaction mixture was filtered. Upon cooling to the ambient temperature, yellow crystals formed. The product was collected by

vacuum filtration. NMR (d_6-Me_2SO) δ2.07 (s, 3), 7.00 (s, 5). Anal. Calcd. for $C_{32}H_{32}B_2N_4NiO_4$: C, 62.29; H, 5.23; N, 9.08. Found: C, 61.8; H, 5.0; N, 9.1.

Synthesis of (3, 6, 11, 14-tetraaza-1-bora-1,1-difluoro-4,5,12,13-tetramethyl-2,15-dioxacyclopentadeca-3,5,11,13-tetraenato)nickel(I), 6. Under an inert atmosphere, a solution of cobaltocene (0.060 g) in acetonitrile (2 ml) was combined with 17 (0.200 g). The reaction mixture was stirred 8 m. The product was isolated by vacuum filtration. The blue-green microcrystalline product was dried in vacuo. Anal. Calcd. for $C_{12}H_{20}BF_2N_4NiO_2$: C, 40.05; H, 5.6; N, 15.57. Found: C, 39.9; H, 5.3; N, 15.1.

References and Notes

(1) Olson, D. C.; Vasilevslais, J. Inorg. Chem. 1969, 8, 1611

(2) Rillema, D. P.; Endicott, J. F.; Papaconstantinou, E. Inorg. Chem. 1971, 10, 1739.

(3) Lovecchio, F. V.; Gore, E. S.; Busch, D. H. J. Am. Chem. Soc. 1974, 96, 3109.

(4) Millar, M.; Holm, R. H. J. Am. Chem. Soc. 1975, 97, 6052.

(5) Olson, D. C.; Vasilevslais, J. Inorg. Chem. 1971, 10, 463.

(6) Gagné, R. R. J. Am. Chem. Soc. 1976, 98, 6709.

(7) Gagné, R. R.; Allison, J. L.; Gall, R. S.; Koval, C. A. J. Am. Chem. Soc. 1977, 99, 7170.

(8) Gagné, R. R.; Allison, J. L.; Lisensky, G. C. Inorg. Chem. 1978, 12, 3563.

(9) Gagné, R. R.; Allison, J. L.; Ingle, D. M. Inorg. Chem. 1979, 18, 0000.

(10) James, B. R. Ph. D. Thesis, Oxford University, Oxford, U. K., 1960.

(11) Calculating equilibrium constants by the use of shifts in $E_{\frac{1}{2}}$ requires the processes to be chemically and electrochemically reversible. The data reported here were obtained using sampled dc polarography, except for 5 which was done using cyclic voltammetry; reversibility was determined by the requirement that plots of E vs. $\ln[i/(i_d-i)]$ have slopes of $-RT/nF$, i. e., 58. 6 mV at 22° C for a one-electron process.

All complexes studied here gave slopes close to 58.6 mV, except 2, which was 41.5 mV, and 4, which was 45.4 mV. Concentration-dependent electronic spectral changes confirm the proposal that dimerization of 4 occurs in solution. Similar dimerization of reduced conjugated-macrocyclic nickel complexes have been investigated by Ibers, Holm, and co-workers.[12]

(12) Peng, S.-M.; Ibers, J. A.; Millar, M.; Holm, R. H. J. Am. Chem. Soc. 1976, 98, 8037.

(13) Burdett, J. K.; Williams, P. D. private communication.

(14) Gagné, R. R.; Ingle, D. M. submitted for publication to J. Am. Chem. Soc.

(15) Gagné, R. R.; Ingle, D. M.; Kreh, R. P.; McCool, M.; Marsh, R. E. submitted for publication.

(16) Hathaway, B. J.; Billing, D. E. Coord. Chem. Rev. 1970, 5, 143.

(17) Sacconi, L.; Rhilardi, C. A.; Mealli, C.; Zanobini, F. Inorg. Chem. 1975, 14, 1380.

(18) Curtis, N. F. Chem. Commun. 1966, 881.

(19) Tait, A. M.; Busch, D. E. in "Inorganic Synthesis," Doublas B. E., Ed., Wiley-Interscience: New York, 1978; Vol. XVIII, p. 22.

(20) Tait, A. M.; Busch, D. E. Inorg. Nucl. Chem. Lett. 1972, 8, 491.

(21) Curtis, N. F. J. Chem. Soc. 1964, 2644.

(22) Curtis, N. F. J. Chem. Soc. 1965, 924.

(23) Schrauzer, G. N. Chem. Ber. 1962, 95, 1438.

(24) Uhlig, V. E.; Friedaich, M. Z. Anorg. Allg. Chem. 1964, 333, 90.

(25) King, R. B. "Organometallic Synthesis," Academic Press: New York, 1965; Vol. 1, p. 70.

(26) All reduced nickel complexes are air sensitive and must be handled routinely under an inert atmosphere.

Chapter 3

Intramolecular Electron Transfer in Some Tetraazamacrocyclic Ligand Complexes of Copper and Nickel

Robert R. Gagné
Jeremy K. Burdett
D. Michael Ingle
P. D. Williams

Intramolecular Electron Transfer in Some Tetraazamacrocyclic Complexes of Copper and Nickel

R. R. GAGNÉ, J. K. BURDETT, D. M. INGLE, and
P. D. WILLIAMS

Abstract

Infrared spectral studies of four nickel(II) and copper(II) tetraazamacrocyclic complexes, their four-coordinate, one-electron reduction products, and the corresponding five-coordinate nickel(I) and copper(I) carbonyl adducts have been studied. Overall similarities between the nickel and copper complexes cause formulation of the four-coordinate one-electron reduction products of copper(II) complexes containing conjugated α-diimine moieties as copper(III)-ligand dianion species.

Extended Hückel molecular orbital calculations confirms the experimentally-based conclusions. In square-planar complexes M(DOBF$_2$), where M = Cu(I), Ni(I), the $\sigma^*_{x^2-y^2}$

metal orbital lies above the normally unoccupied ligand π^* orbital. For M = Cu(II), Ni(II) or for ligands without conjugated imine groups, the $\sigma^*_{x^2-y^2}$ orbital lies below the ligand π^* orbital. The presence of a small HOMO-LUMO gap in the reduced species favors a tetrahedral distortion (experimentally observed in the crystal structure of $Cu(DOBF_2)$). Upon coordination of CO with the reduced species, the $\sigma^*_{x^2-y^2}$ orbital always lies below the ligand π^* orbitals. This intramolecular electron transfer coincident with geometry change has been experimentally observed.

The CO is attached to the metal mainly through σ-interactions between ligand σ orbitals and metal 4s and 4p orbitals, augmented by stabilization, via unoccupied CO π^* orbitals, of two metal d orbitals (π back-donation). The σ contribution of the metal d orbitals to the metal-carbonyl bond is zero.

Introduction

During the past decade, several investigations into the chemistry of polydentate and macrocyclic complexes have presented the opportunity to observe certain metals in less common oxidation states. Of interest for possible models for copper-containing proteins is the chemistry of copper(I) macrocyclic complexes. Endicott and co-workers[1] have studied the aqueous electrochemistry of copper(II) tetraazamacrocyclic complexes; a highly-reactive, yellow species, which although isolation was not possible, was shown to be a copper(I) complex, was produced. Olson and Vasilevskis,[2] working in acetonitrile solution, were able to electrochemically generate and isolate both copper(I) and copper(III) complexes of tetraazamacrocyclic ligands. Busch and co-workers[3, 4] have investigated a highly conjugated tetraazamacrocyclic copper(II) complex ($Cu(TAAB)^{2+}$), which was proposed to

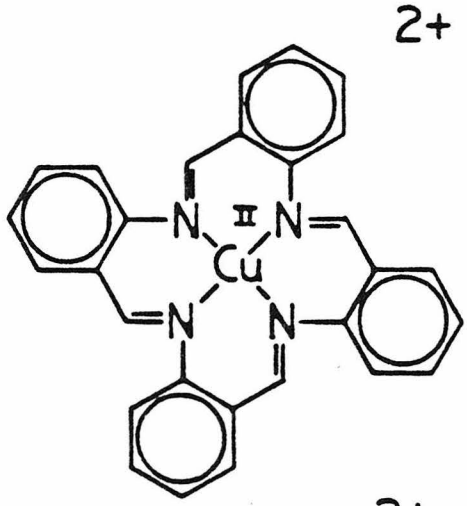

$Cu(TAAB)^{2+}$

yield a blue copper(III) ligand-dianion complex upon reduction. Gagné reported[5, 6] the one-electron reduction of the complex Cu(II) $(DOBF_2)^+$ to give a deep blue, diamagnetic complex, $Cu(DOBF_2)$.

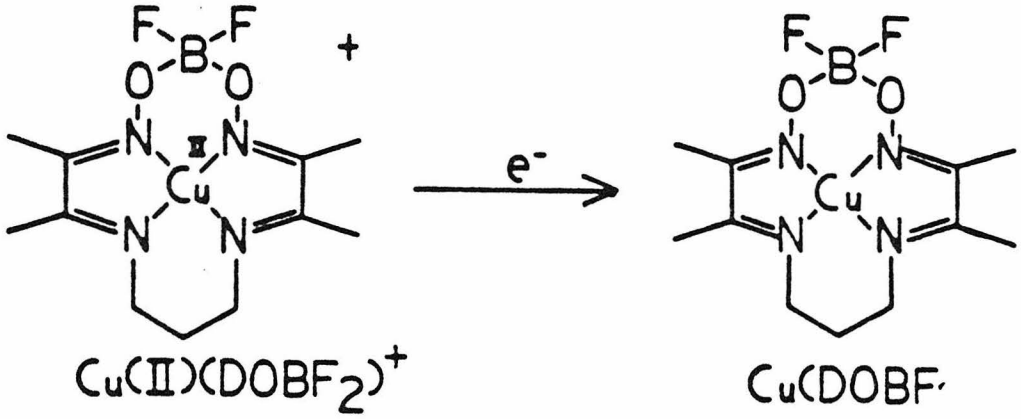

The reduced complex exhibits the novel ability to bind a fifth ligand, i. e., carbon monoxide, to yield a yellow, five-coordinate, 20-electron copper(I) complex, Cu(I) $(DOBF_2)CO$.[6]

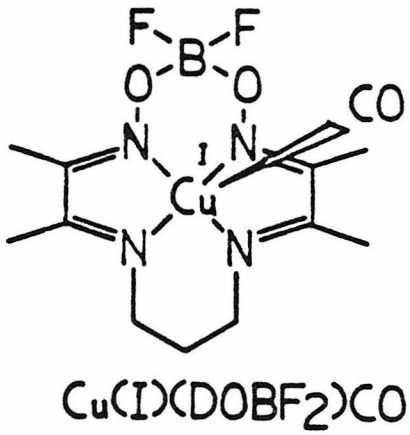

Crystallographic analysis of Cu(I) ($DOBF_2$)CO[6] and tetraethylammonium carbonyl [(1, 8-dibora-3, 6, 10, 13-tetraaza-1, 1, 8, 8-tetrafluoro-4, 5, 11, 12-tetramethyl-2, 7, 9, 14-tetraoxatetradeca-3, 5,10, 12-tetraenato) copper(I)][7], $TEA^+[Cu(I)(DMGBF_2)_2CO]^-$, reveals that the copper atoms are displaced out of the best-plane of the four nitrogen ligands by 0.96 and 1.02 Å, respectively. Furthermore, the ligand

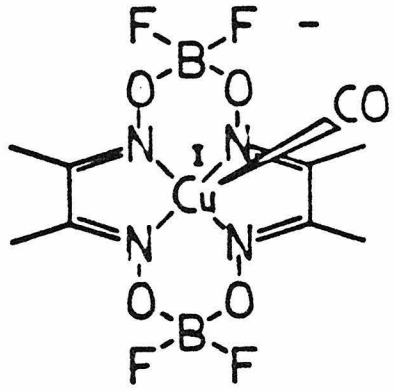

$[Cu(I)(DMGBF_2)_2CO]^-$

assumes an interesting "dome" shape (Figure 1). All available data suggest that Cu(I)($DOBF_2$)CO is a five-coordinate, 20-electron, copper(I)-carbonyl complex. There are no other carbonyl complexes which violate the eighteen electron rule except for $W(\phi C{\equiv}C\phi)_3CO$, for which there is a simple explanation, and the nickel complexes[8, 9] analogous to these copper carbonyl complexes.

Figure 1

ORTEP Drawing of the Structure
of $Cu(I)(DOBF_2)CO$ [6]

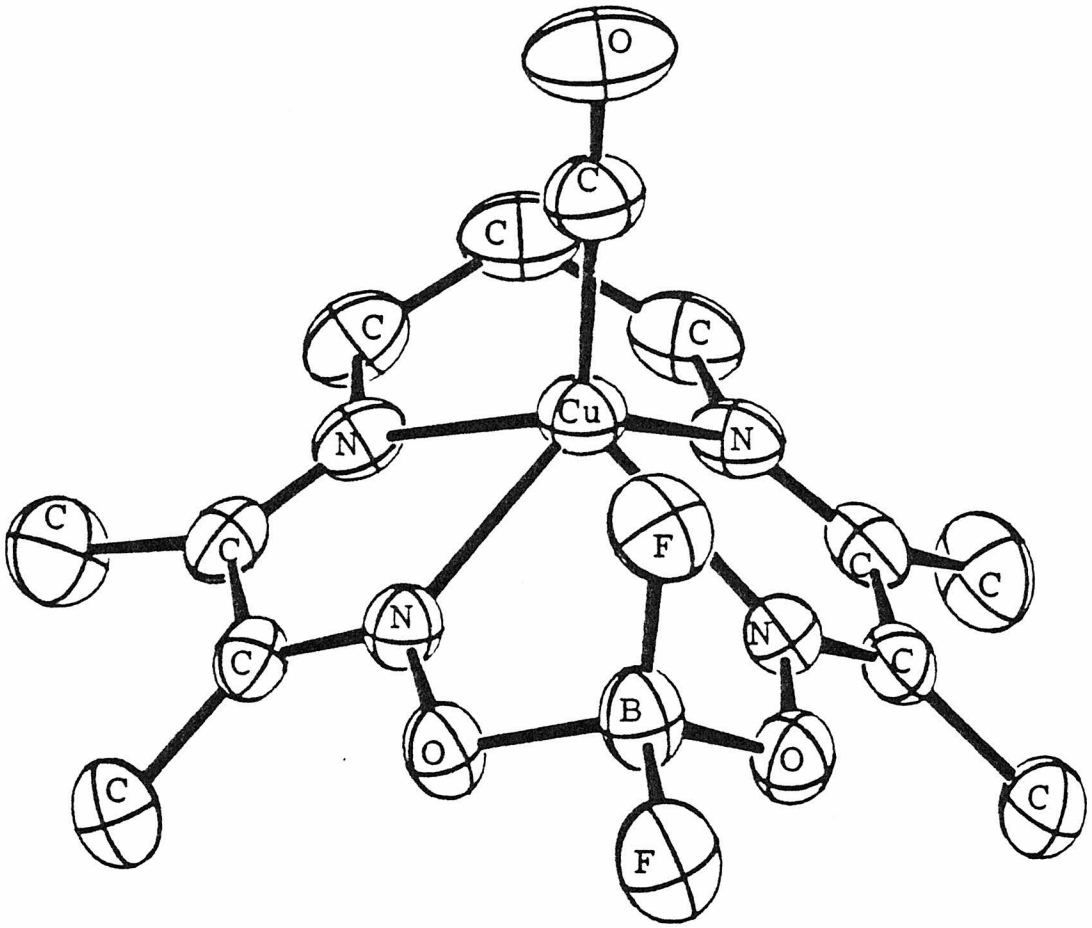

Figure 1

The 18-electron, four-coordinate complex, $Cu(DOBF_2)$, has also been studied crystallographically;[9] the complex is essentially square-planar, but with a tetrahedral distortion towards a local D_{2d} geometry about the CuN_4 unit, which is consistent with the inherent inclination of Cu(I) to assume a tetrahedral geometry. The infrared spectrum of $Cu(DOBF_2)$ demonstrated an unusual feature; the typical imine stretches in the 1600-1650 cm^{-1} region observed for $Cu(II)(DOBF_2)\cdot ClO_4$ were not observed. Three additional bands were, however, observed in the 1250-1500 cm^{-1} region. The usual 1650 cm^{-1} area bands were observed for $Cu(I)(DOBF_2)CO$. This behavior was ascribed to possible π-delocalization from the metal into the ligand π^* orbital. The oxidation state for copper in $Cu(DOBF_2)$ was tentatively regarded as Cu(I)..

Analogous nickel complexes have since been synthesized[10, 11] in a continued effort to elucidate the nature of the four- and five-coordinate copper complexes. We report here an analysis of the infrared spectra of both copper and nickel systems to link the similarities of the two more fully and to establish assignments for the oxidation states of the copper species. Also, the results of molecular orbital calculations using the Extended Hückel method are especially enlightening. There results, which are consistent with experimental observations, suggest that the 20-electron $Cu(DOBF_2)CO$ complex be described as a copper(I) species, while the tetrahedrally-distorted,

18-electron Cu(DOBF$_2$) should best be described as a copper(III) complexed to a doubly reduced ligand.

Results and Discussion

Infrared Spectroscopy. Infrared spectra of isolated, analytically-pure complexes have been studied. The structures of the ligands involved are shown in Figure 2.

The copper(I) complexes studied by Endicott and co-workers[1] and isolated by Olson and Vasilevskis[2] were of the trans-diene ligand. The IR spectra of Cu(II) (trans-diene) · 2 ClO_4 and Cu(I) (trans-diene) · ClO_4 have previously been reported.[2] The Cu(I) (trans-diene)-CO · ClO_4 has not been isolated due to a low carbon monoxide affinity.[12] Imine stretching frequencies for Cu(II) (trans-diene) · 2 ClO_4 and Cu(I) (trans-diene) · ClO_4 are located in the normal imine region (1665 cm^{-1} and 1630 cm^{-1}, respectively).

The analogous nickel complex, Ni(II) (trans-diene) · 2 ClO_4 undergoes a one-electron reduction to give the d^9 complex, Ni(I) (trans-diene) · ClO_4,[13] which in turn binds carbon monoxide to give the five-coordinate, 19-electron Ni(I) (trans-diene)CO · ClO_4.[10, 11] The designation of both of these reduced complexes as nickel(I) species has been demonstrated by EPR spectroscopy.[10, 11, 14] The IR frequencies are listed in Table I. Upon reduction from Ni(II) to Ni(I), the imine band moves only a small amount (from 1665 cm^{-1} to 1640 cm^{-1}). Formation of the nickel(I) carbonyl adduct causes little change ($\nu_{C=N}$ = 1645 cm^{-1}). Comparisons of the behavior of the IR imine band of the

Figure 2

Skeletal Representations of the Ligands

<u>trans</u>-diene and $(DMGBF_2)_2^{2-}$

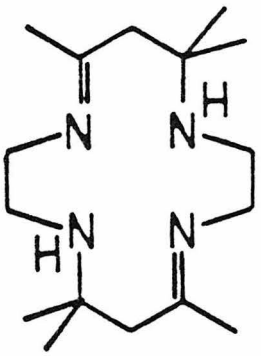

trans-diene

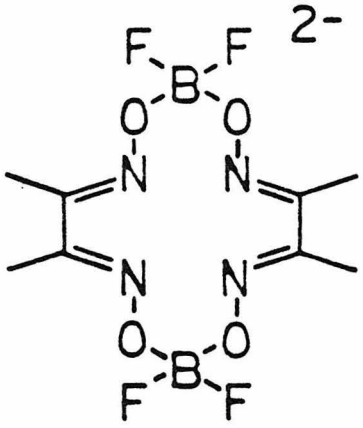

$[(DMGBF_2)_2]^{2-}$

Figure 2

Table I. Infrared Spectra (from 2500 to 1200 cm^{-1})[a]

Cu(trans-diene)$(ClO_4)_2$[b]	Cu(trans-diene)(ClO_4)[b]	Ni(trans-diene)$(ClO_4)_2$[c]	Ni(trans-diene)(ClO_4)[c]	Ni(trans-diene)CO(ClO_4)[d]
				1962 s
1665 s	1630	1665 s	1640 m	1645 s
	1615 m		1610 s	
1485 w	1480 m	1460 s	1570 m	1495 w
1445 m	1470 s	1450 s	1460 s	1470 m
1420 m	1445 s	1430 s	1430 s	1460 m
1410 m	1400 s	1405 s	1380 s	1445 s
1395 s	1385 m	1390 s	1365 s	1425 s
1360 m	1370 s	1370 s	1340 s	1390 s
1305 m	1360 m	1360 s	1285 m	1375 s
1280 w	1330 s	1355 s	1255 m	1295 m
1260 m	1265 s	1305 m	1235 m	1280 m
1240 w	1255 w	1275 m	1220 m	1245 w
1210 w	1245 w	1255 w	1200 w	1235 w
	1230 s	1235 w		1220 m
				1210 w

[a]Abbreviations: s, strong; m, medium; w, weak. [b]Ref. 2.

[c]Ref. 13. [d]This work.

nickel complexes to the copper complexes of trans-diene is unremarkable. No profound changes occur in the imine stretching frequencies; both metals appear to be univalent.

The IR spectra obtained for $Cu(II)(DMGBF_2)_2$, $CoCp_2^+[Cu(DMGBF_2)_2]^-$, and $CoCp_2^+[Cu(DMGBF_2)_2CO]^-$,[15] are shown in Figure 3. The IR spectrum obtained for $Cu(II)(DMGBF_2)\cdot$ dioxane exhibits an imine stretch at 1635 cm^{-1}. The copper(I) carbonyl-adduct, $CoCp_2^+[Cu(DMGBF_2)_2CO]^-$, gives an imine band at 1630 cm^{-1}. The four-coordinate reduced complex, $CoCp_2^+[Cu(DMGBF_2)_2]^-$, however, shows no imine band in the normal region, but instead has new bands at 1330 and 1470 cm^{-1}. This result is similar to that of $Cu(DOBF_2)$, vide supra. The infrared spectral bands are given in Table II.

The IR spectra associated with the $Ni(DMGBF_2)_2$ undergo a reversible one-electron reduction; the product is not the corresponding Ni(I) species, but rather a nickel(II)-stabilized ligand-radical (as shown by EPR).[10,11] This nickel ligand radical binds carbon monoxide, accompanied by intramolecular electron transfer (ligand to metal), to give a paramagnetic, five-coordinate, 19-electron nickel(I) carbonyl complex, $CoCp_2^+[Ni(I)(DMGBF_2)_2CO]^-$.[10,11] The IR spectrum of $Ni(II)(DMGBF_2)_2$ has an imine stretch at 1635 cm^{-1}; $CoCp_2^+[Ni(I)(DMGBF_2)_2CO]^-$ has its imine stretch at 1610 cm^{-1}. The nickel(II)-stabilized ligand-radical, $CoCp_2^+[Ni(DMGBF_2)_2]^-$, has no normal region imine stretching frequency; new bands at 1325 and 1450 cm^{-1} appear instead. Figure 4 shows the IR spectra of these three

Figure 3

Infrared Spectra of $Cu(II)(DMGBF_2)_2 \cdot$ dioxane (upper),

$CoCp^+[Cu(DMGBF_2)_2]^-$ (middle), and

$CoCp^+[Cu(DMGBF_2)_2CO]^-$ (lower)

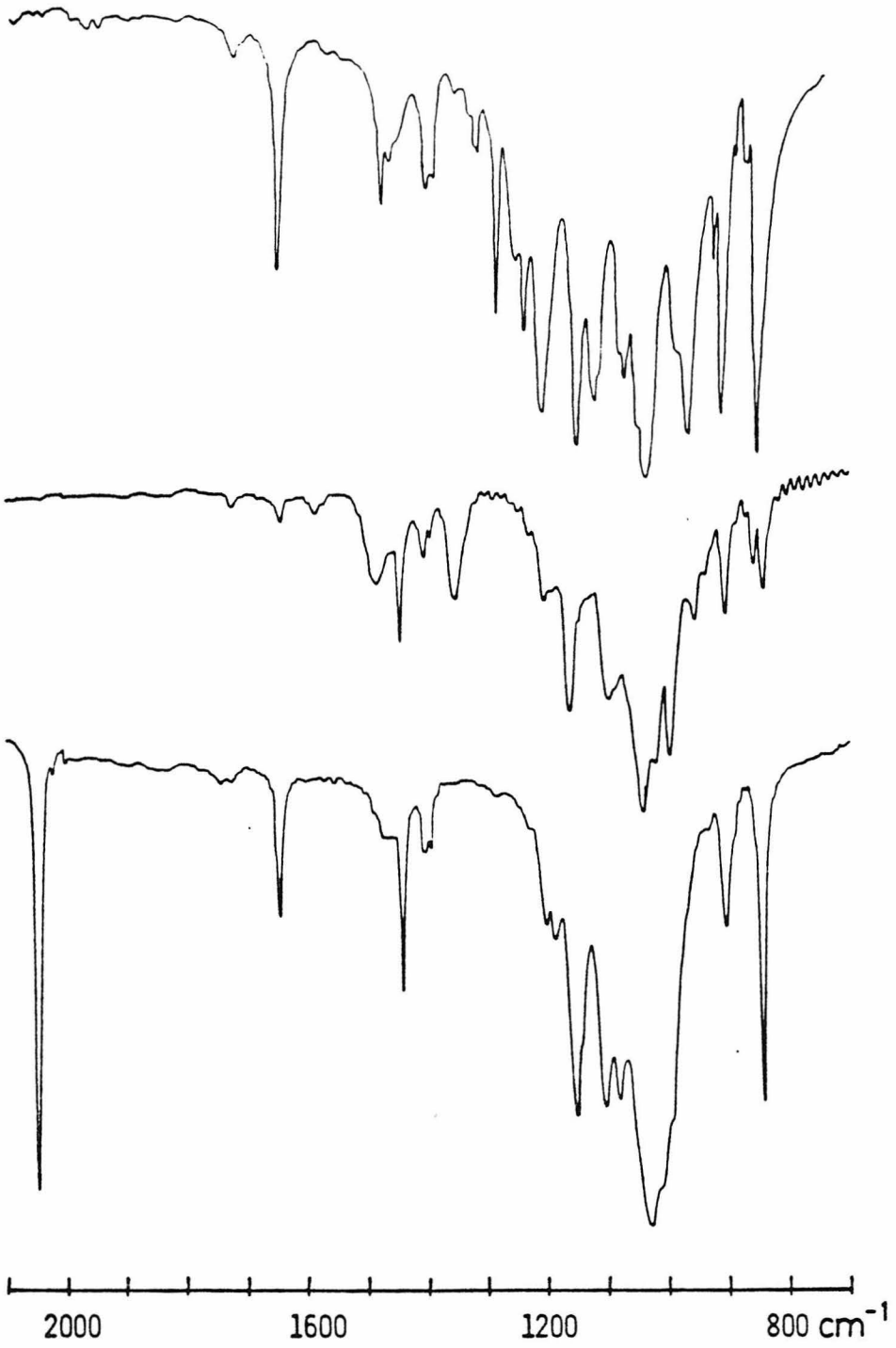

Figure 3

Table II. Infrared Spectra (from 2500 to 1100 cm^{-1})[a]

$Cu(II)(DMGBF_2)_2 \cdot$ dioxane[b]	$CoCp_2^+$ $Cu(DMGBF_2)_2^-$[b]	$CoCp_2^+$ $Cu(I)(DMGBF_2)_2CO^-$[b]	$Ni(II)(DMGBF_2)_2$[b]	$CoCp_2^+$ $Ni(DMGBF_2)_2^-$[b]	$CoCp_2^+$ $Ni(DMGBF_2)_2CO^-$[b]
		2040 s			2015 s
1635 m		1630 m	1635 m		1610 m
1460 w	1470 m	1440 w	1430 w	1450 m	1510 m
1450 w	1420 m	1420 m	1385 m	1420 m	1445 w
1385 m	1385 w	1380 m	1250 m	1380 m	1415 m
1370 w	1370 w	1370 w	1230 m	1325 s	1385 w
1295 w	1330 m	1175 m	1190 s	1215 w	1375 w
1260 m	1175 m	1160 m	1130 m	1140 m	1345 w
1230 m	1135 s	1120 s	1105 s	1100 m	1190 w
1210 m					1160 m
1180 s					1120 s
1120 s					

[a]Abbreviations: s, strong; m, medium; w, weak. [b]This work.

Figure 4

Infrared Spectra of $Ni(DMGBF_2)_2$ (upper),

$CoCp_2^+[Ni(DMGBF_2)_2]^-$ (middle), and

$CoCp_2^+[Ni(DMGBF_2)_2CO]^-$ (lower)

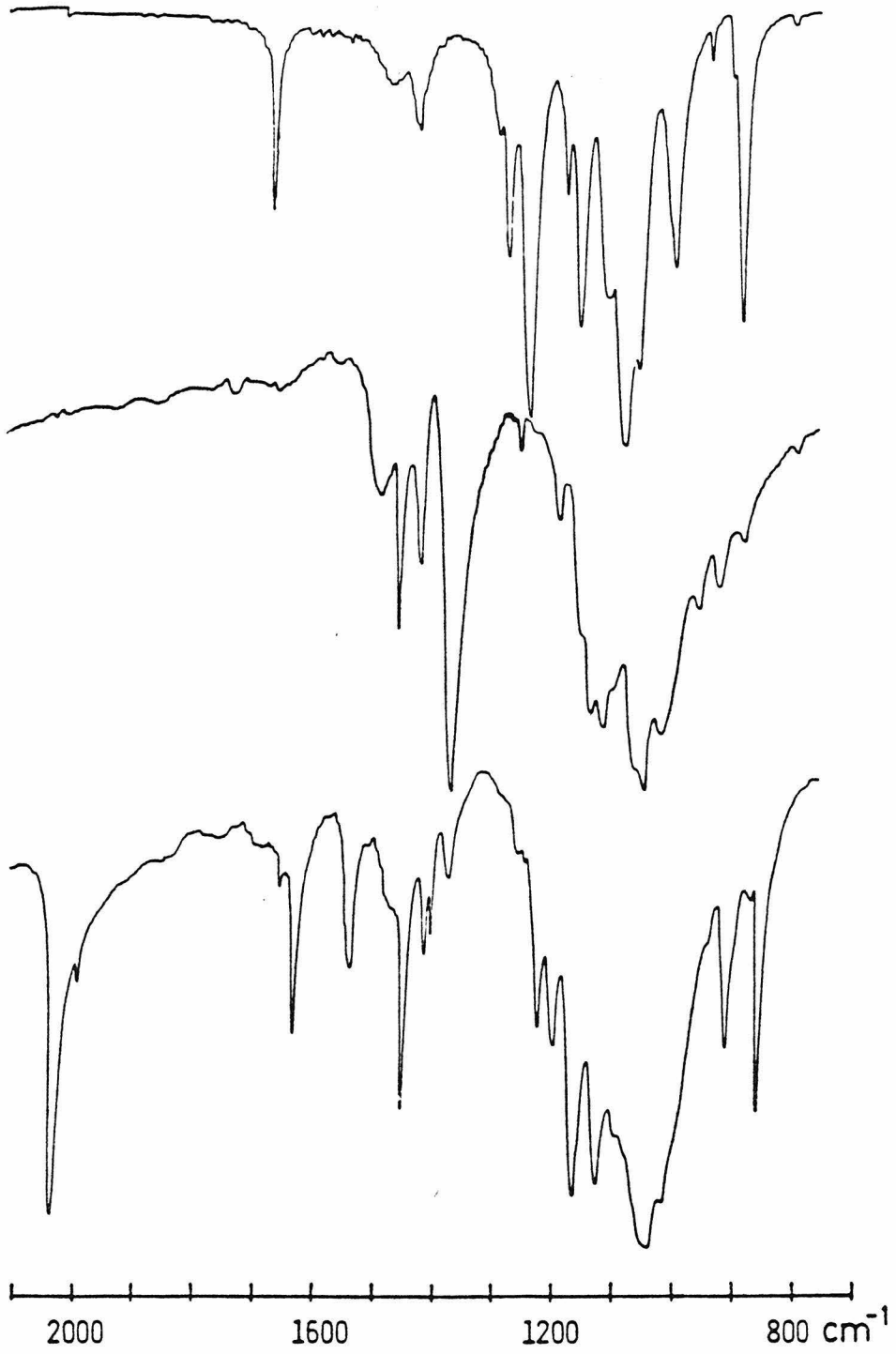

Figure 4

complexes; Table II compiles the infrared spectral bands.

To confirm that the bands discussed here are actually related to the imine group, ^{15}N-substituted $Ni(DMGBF_2)_2$ was synthesized. The IR spectrum of this compound shows an isotopic dependence of the 1635 cm^{-1} absorbance ($\nu_{C=^{15}N}$ = 1615 cm^{-1}). Similarly, $(^{15}N)\,CoCp_2^+[Ni(DMGBF_2)_2]^-$, the nickel(II) ligand-radical, shows a change in the new low energy bands ($\nu_{(^{15}N)}$ = 1310 and 1440 cm^{-1}). Although the bands of interest are affected by the isotopic change, the shift is not as large as for the unreduced nickel(II) species. The ligand-radical bonds are expected to show higher vibronic coupling due to the occupation of the ligand π^* orbital (vide infra). The deviation from a simple harmonic oscillator model is not surprising. Table III gives ^{15}N-substituted IR results.

The similarity between the copper and nickel IR data compels us to formulate the four-coordinate, reduced copper complex as a copper(III)-stabilized ligand-dianion. A formal two-electron intramolecular electron transfer occurs upon binding of carbon monoxide. By analogy to the related nickel chemistry,[10,11] we suggest that reduced complexes of copper with square-planar tetraazamacrocyclic ligands containing at least one α-diimine moiety should also be viewed as a copper(III)-stabilized ligand-dianion.

Molecular Orbital Calculations. Molecular orbital calculations were done on the species shown in Figure 5, using the Extended Hückel method with the parameters given in the Appendix. Results will

Table III. Infrared Spectra for ^{15}N-Substituted $Ni(DMGBF_2)_2$ (from 2500 to 1100 cm^{-1}). [a]

(^{15}N) $Ni(DMGBF_2)_2$	(^{15}N) $CoCp_2^+Ni(DMGBF_2)_2^-$
1615 m	
1430 w	1440 m
1385 m	1415 m
1240 m	1375 m
1215 m	1310 s
1190 s	1195 w
1110 m	1145 m
1100 s	1110 m

[a]Abbreviations: s, strong, m, medium, w, weak.

Figure 5

Skeletal Representations for Metal Complexes

Used in EHMO Calculations

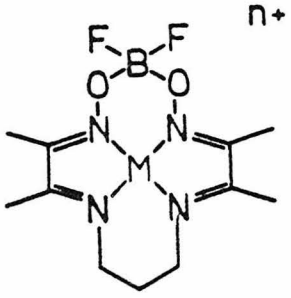

M(DOBF$_2$)$^{n+}$
M = M(I) ; n = 0
M = M(II) ; n = 1

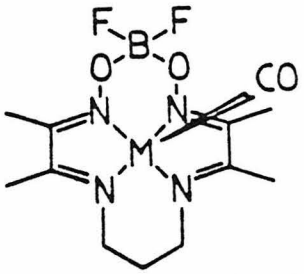

M(I)(DOBF$_2$)CO

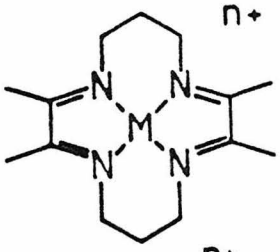

M(TIM)$^{n+}$
M = M(I) ; n = 1
M = M(II) ; n = 2

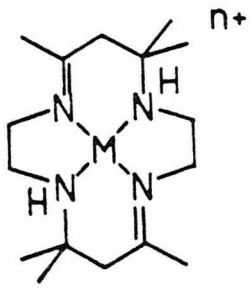

M(<u>trans</u>-diene)$^{n+}$
M = M(I) ; n = 1
M = M(II) ; n = 2

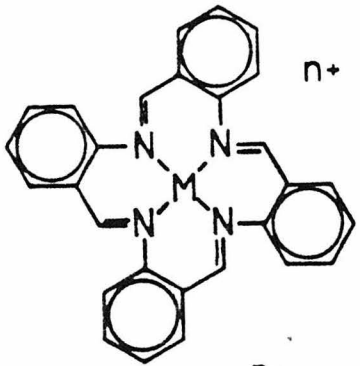

M(TAAB)$^{n+}$
M = M(I) ; n = 1
M = M(II) ; n = 2

Figure 5

be discussed for $Cu(DOBF_2)$; individual attention will be given to the other complexes when relevant to the discussion.

Interactions of metal 3d, 4s, and 4p orbitals with the low-lying nitrogen σ orbitals, which point toward the center of the macrocycle, and four pairs of π orbitals, belonging to the two conjugated α-diimine moieties, are shown in Figure 6 The nitrogen σ's are stabilized by interaction with the metal orbitals in the usual manner.[16] Most notable is the strong destabilization of the $d_{x^2-y^2}$ orbital caused by metal-ligand interactions forming the b_{2g} σ^*[17] (Figure 7). Stabilization of the b_{2g} σ^* is not possible, in the square-planar geometry, by mixing with higher energy metal (4s, 4p) orbitals, because it is of the wrong symmetry. The traditional sort of π-donation (metal-to-ligand) proposed for these complexes[9] is probably not very important as the ligand π^* orbitals show no such stabilization. One of the π^* orbitals, a_{2u} π_1^*, is actually stabilized by an admixture with the metal 4p orbital in a binding fashion (Figure 8); the associated a_{1u} π_2^* (Figure 9) is of the wrong symmetry to interact with any metal orbital and remains unchanged in energy with respect to the free ligand. The relative ordering of the b_{2g} σ^*, the a_{2u} π_1^*, and the a_{1u} π_2^* (hereafter, referred to as $\sigma^*_{x^2-y^2}$, π_1^*, and π_2^*, respectively) causes many of the unusual properties possessed by the four-coordinate complexes.

Figure 6 shows a triad of energetically close orbitals—$\sigma^*_{x^2-y^2}$ (consisting of metal $3d_{x^2-y^2}$ and ligand $\sigma_{x^2-y^2}$),[18] π_1^* (consisting of mostly ligand π^* and a small amount of metal 4p), and π_2^* (which is nearly unaltered ligand π^*). For Ni(II) (d^8), Ni(I) and Cu(II) (d^9), and

Figure 6

Molecular orbital diagram for $Cu(DOBF_2)$ (center) showing its assembly from the diagram for the free ligand (right) and the metal (left). The ligand has an idealized planar skeleton for the complex and the ligand. Only the orbitals which change in energy significantly on complexation have been included. The ligand σ orbitals are labelled with subscripts to indicate with which central atom orbitals they predominantly interact. The orbital occupancies are for the neutral ligand and Cu(I).

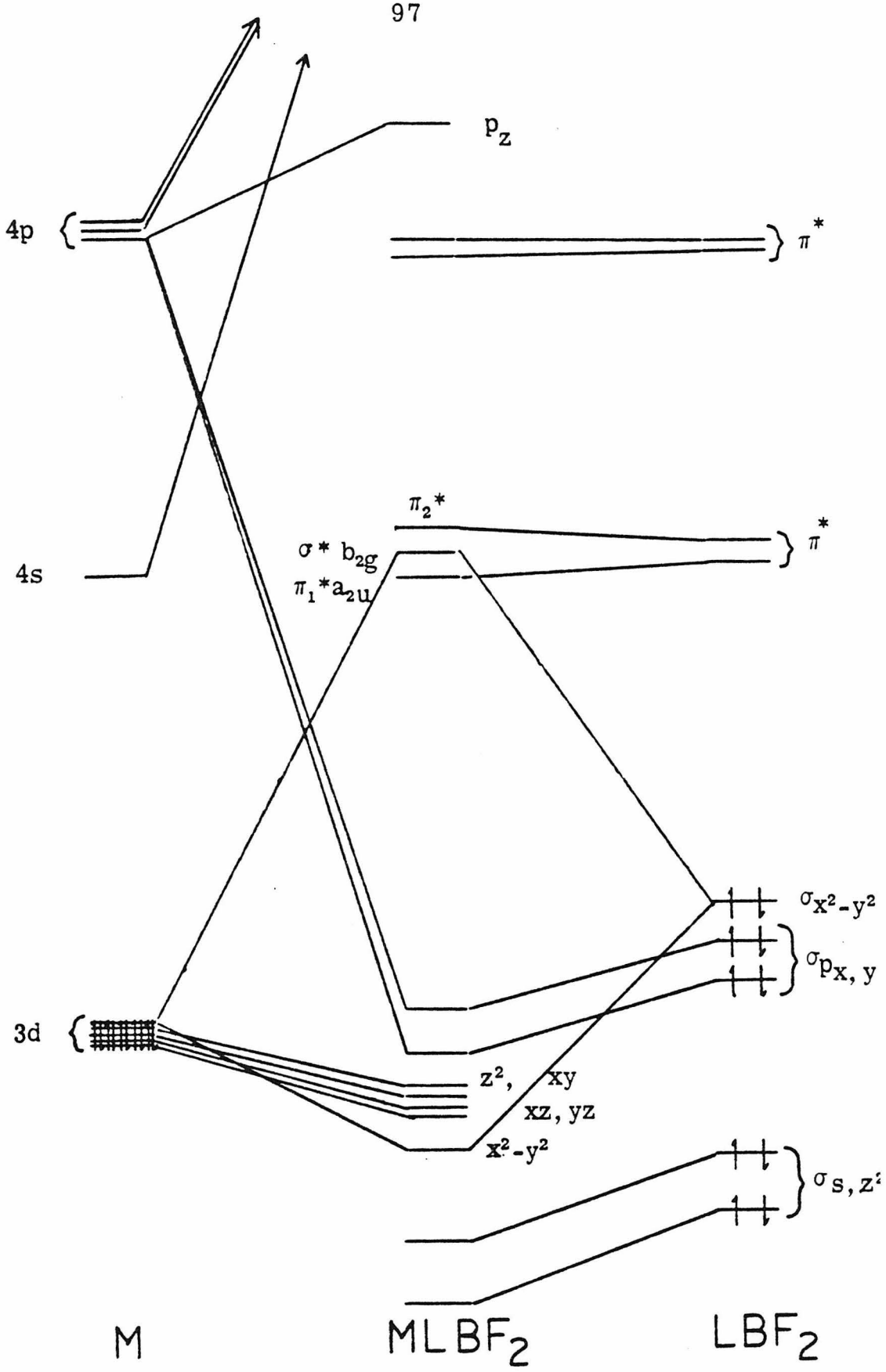
p_z
4p
π^*
π_2^*
σ^* b_{2g}
$\pi_1^* a_{2u}$
4s
π^*
$\sigma_{x^2-y^2}$
$\sigma_{p_x, y}$
3d
z^2, xy
xz, yz
x^2-y^2
σ_{s, z^2}
M
$MLBF_2$
LBF_2

Figure 6

Figure 7

Schematic Representation of the b_{2g} σ^* Orbital

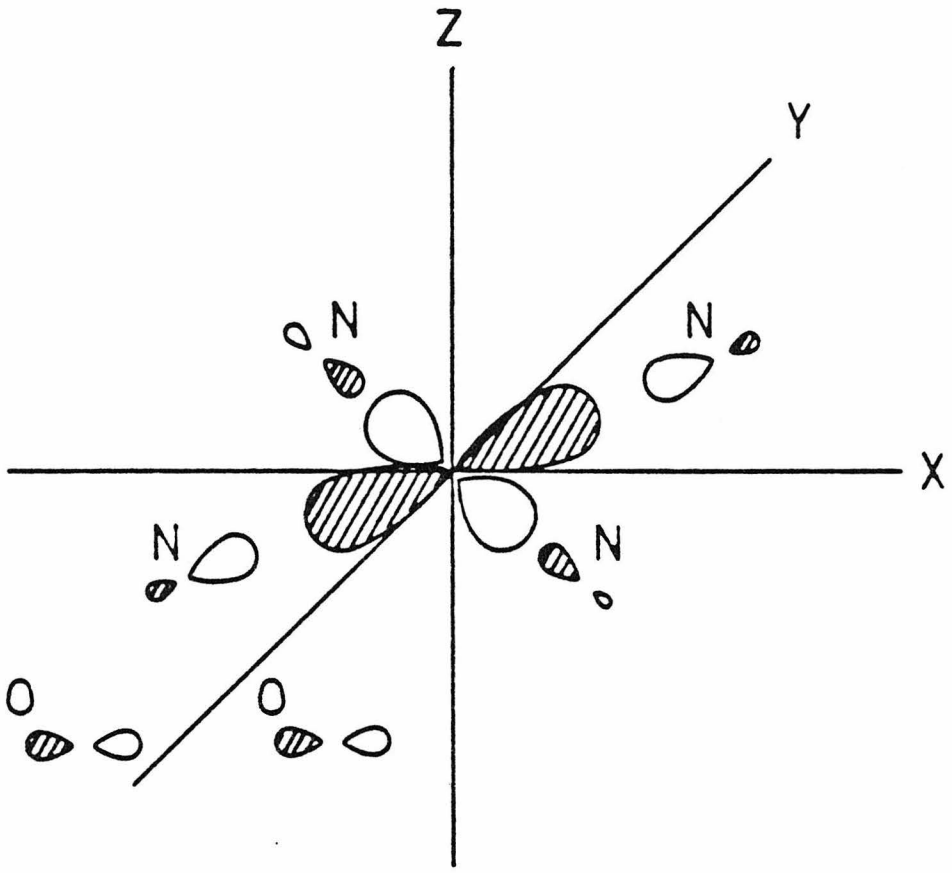

Figure 7

Figure 8

Schematic Representation of the a_{2u} π_1* Orbital

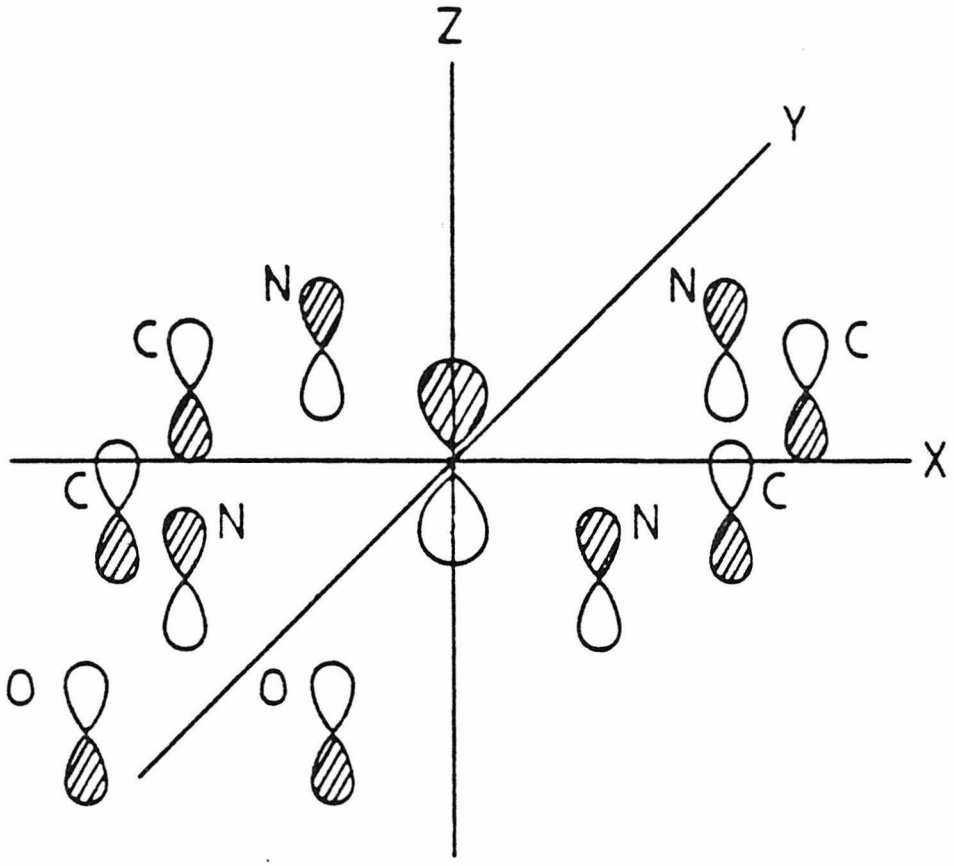

Figure 8

Figure 9

Schematic Representation of the a_{1u} π_2^* Orbital

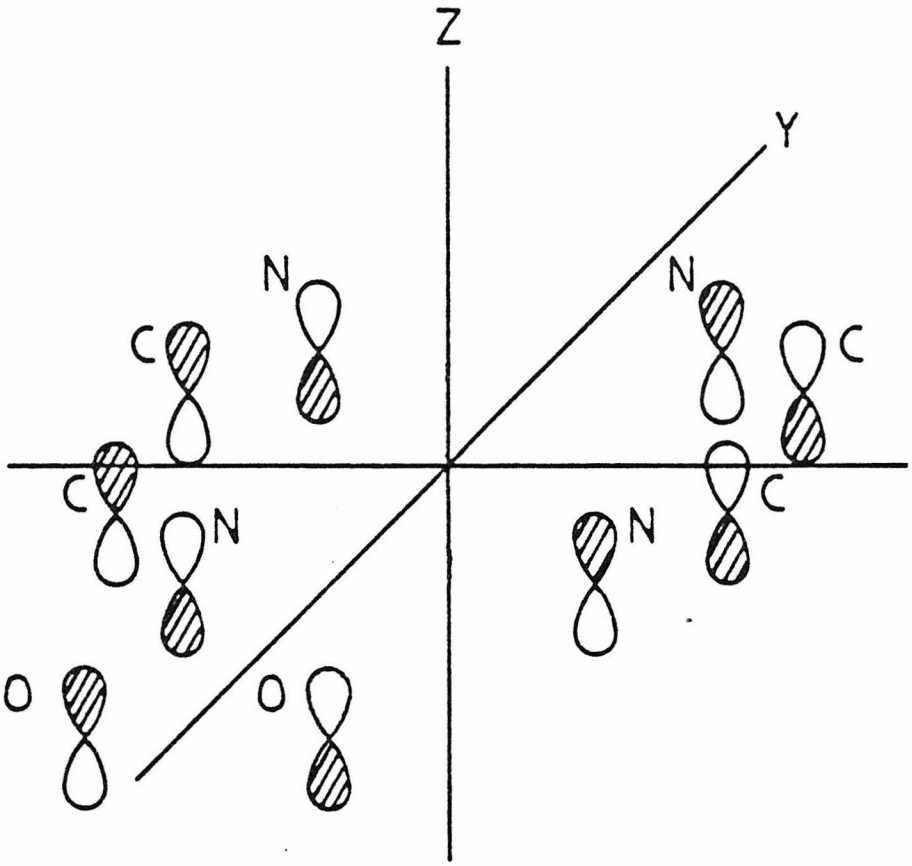

Figure 9

Cu(I) (d^{10}) complexes, these three orbitals contain 0, 1 and 2 electrons, respectively. From the molecular orbital calculations, two different energy level orderings were found (Figure 10). Because the d-orbitals of the divalent metals are more contracted than the corresponding univalent metals, the antibonding interaction between the $d_{x^2-y^2}$ orbital with the nitrogen σ orbitals is less for the divalent ion than for the univalent ion. These calculations show that for Ni(I) and Cu(I) the HOMO for M($DOBF_2$) is the ligand orbital π_1^*. This is consistent with the experimental assertion that these are metal-stabilized ligand-radicals and ligand-dianions, respectively. A population analysis of the C–N bond (Table IV) indicates a decrease of about ten percent in the four-coordinate complex, responsible for lowered imine infrared stretching frequencies. For divalent metals, the π_1^* orbital remains essentially unchanged, but the $\sigma^*_{x^2-y^2}$ becomes lower in energy. Thus for Cu(II), the HOMO is the metal $d_{x^2-y^2}$-containing orbital. Population analysis of the Cu(I)($DOBF_2$)CO shows the ordering of these three levels is qualitatively similar to the Cu(II) species. The question is mute for Ni(II) as all three of these orbitals are empty. For ligands where there are no conjugated α-diimines, <u>trans</u>-diene for example, the π-orbital picture is very different; the π^* orbital is considerably higher in energy (Figure 11), thus the $\sigma^*_{x^2-y^2}$ is always the HOMO. A similar reduction has been proposed[3, 4] to occur for $Cu(TAAB)^+$ containing Cu(I) (or rather $[Cu(III)(TAAB^{2-})]^+$). The vibrational frequency changes upon reduction associated with the imine bonds are

Figure 10

Energy Level Orderings for $M(DOBF_2)^+$ and $M(DOBF_2)$

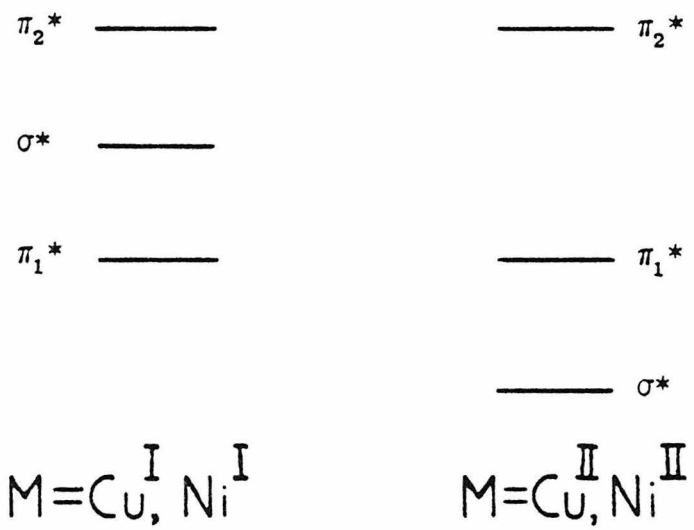

Figure 10

Table IV. C–N Population Analysis

	total	σ	π
$DOBF_2$	1.11	0.80	0.31
square planar $Cu(DOBF_2)$	1.01	0.82	0.19
pyramidal $Cu(I)(DOBF_2)CO$	1.11	0.82	0.29
domed $Cu(I)(DOBF_2)CO$	1.12	0.81	0.31

very much smaller for $Cu(TAAB)^{n+}$ ($Cu(II)(TAAB)^{2+}$, 1562 cm^{-1}; $Cu(TAAB)^{+}$, 1536 cm^{-1})[4] than observed with the $Cu(DMGBF_2)_2$ and $Ni(DMGBF_2)_2$ systems. Molecular orbital calculations on the free ligand, TAAB, show that its π-orbital system forms a group of occupied ligands straddling the energy of the $\sigma^*_{x^2-y^2}$ (Figure 11). Thus for $Cu(TAAB)^{+}$, no electron transfer to the ligand should occur, i. e., no formation of the Cu(III) ligand-dianion is expected to occur.[19]

The square-planar reduced complexes (formally d^9 Ni(I) and d^{10} Cu(I)) of $M(DOBF_2)$ have a small HOMO-LUMO gap. Perturbation theory arguments (or application of the second order Jahn-Teller theorem) lead to the prediction of a b_{1u} distortion of the square-planar geometry to a local D_{2d} point group for the MN_4 unit, i. e., a tetrahedral distortion.[9] The calculations show an overall stabilization for the complex occurs (Figure 12). Stabilization is dominated by relieving the metal $d_{x^2-y^2}$-ligand antibonding interactions.[20] Upon distortion, the HOMO (π_1^* orbital) begins mixing in a contribution from the $d_{x^2-y^2}$ metal orbital. During this process, some of the ligand-located electron density is returned to the metal center. A correlation between the imine stretching frequency and the extent of tetrahedral distortion would be predicted.

Coordination of carbon monoxide to the square-planar complex $Cu(DOBF_2)$ results in a d orbital pattern corresponding to the square-pyramidal geometry. Figure 13 shows the relationship between the energies of the orbitals of the four-coordinate and five-coordinate species, for which the metal has been constrained to remain in the

Figure 11

Molecular Orbital Diagram for the Ligands
$DOBF_2$ and TIM (left),
trans-diene (center), and
TAAB (right).
For reference, the $\sigma^*_{x^2-y^2}$ energy for
$Cu(DOBF_2)$ is included.

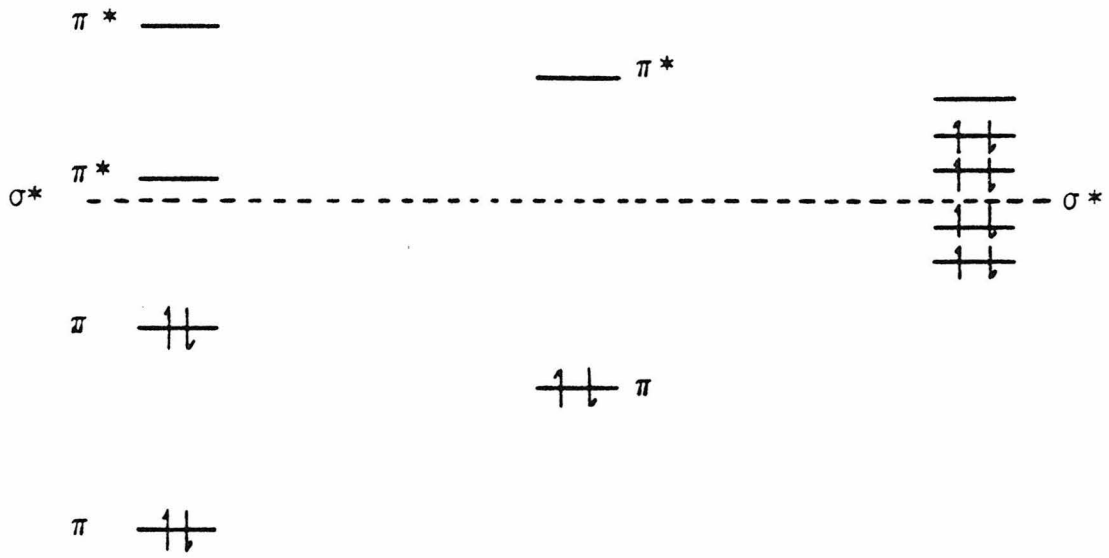

Figure 11

Figure 12

Molecular Orbital Diagram for the $\sigma^*_{x^2-y^2}$ and π_1^* of $Cu(DOBF_2)$, showing the effect of a b_{1u} distortion

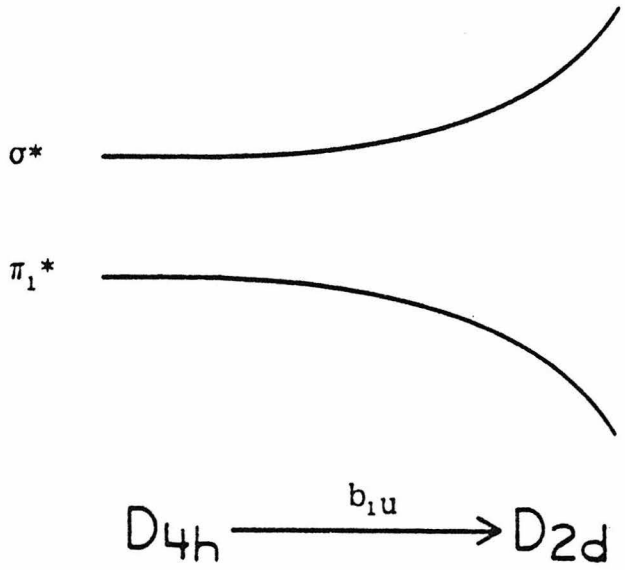

Figure 12

Figure 13

Molecular Orbital Diagram for Cu(I)($DOBF_2$)CO (center)
arising from the interaction of the
Cu($DOBF_2$) orbitals (left) and
the free CO orbitals (right).
The ligand has an idealized planar skeleton
for Cu($DOBF_2$) and Cu(I)($DOBF_2$)CO in which
the metal atom lies in the plane.

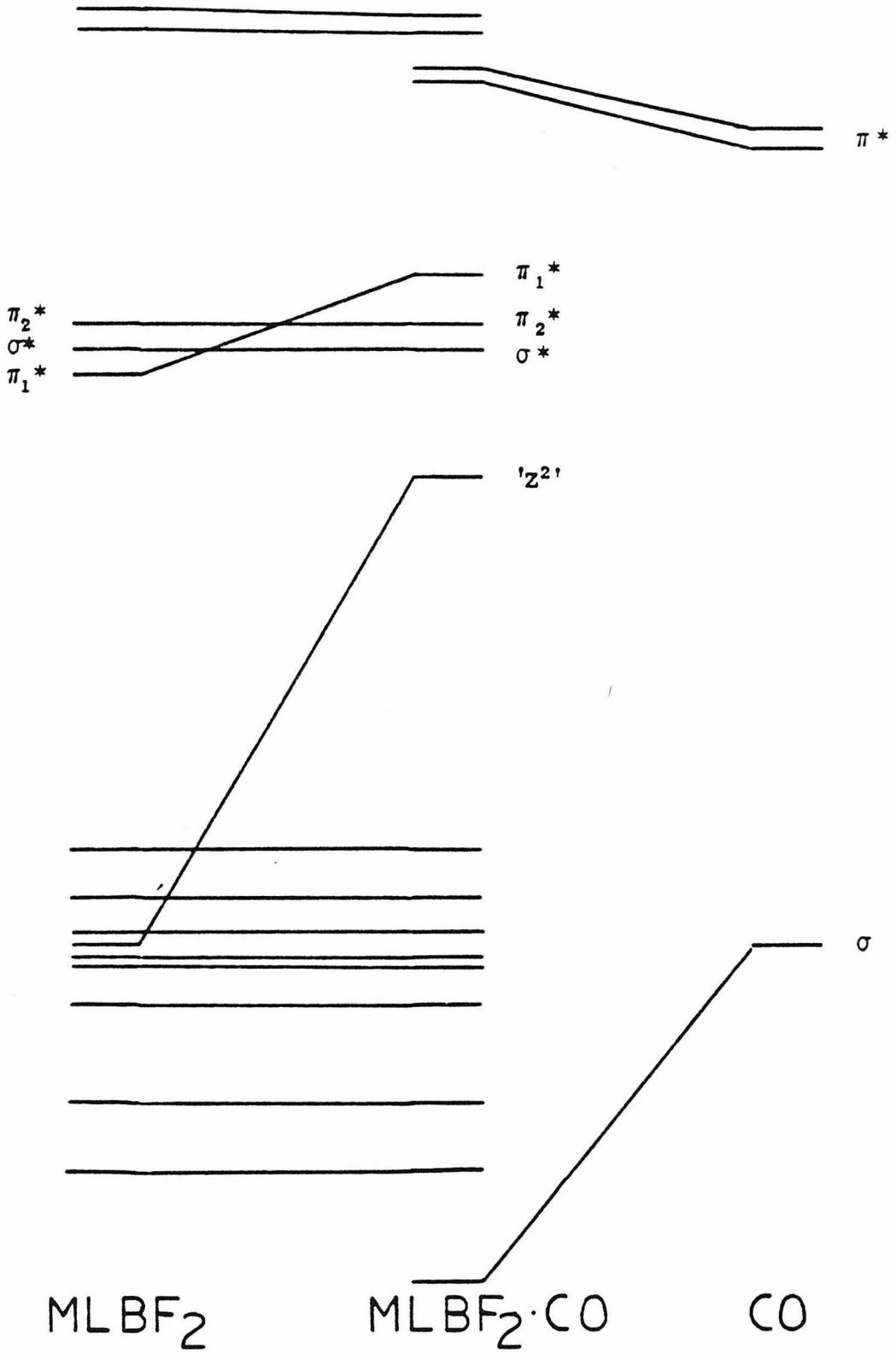

Figure 13

Figure 14

Moleuclar Orbital Diagram for Cu(I)($DOBF_2$)CO showing the idealized square-planar (left) and the observed geometry (right).

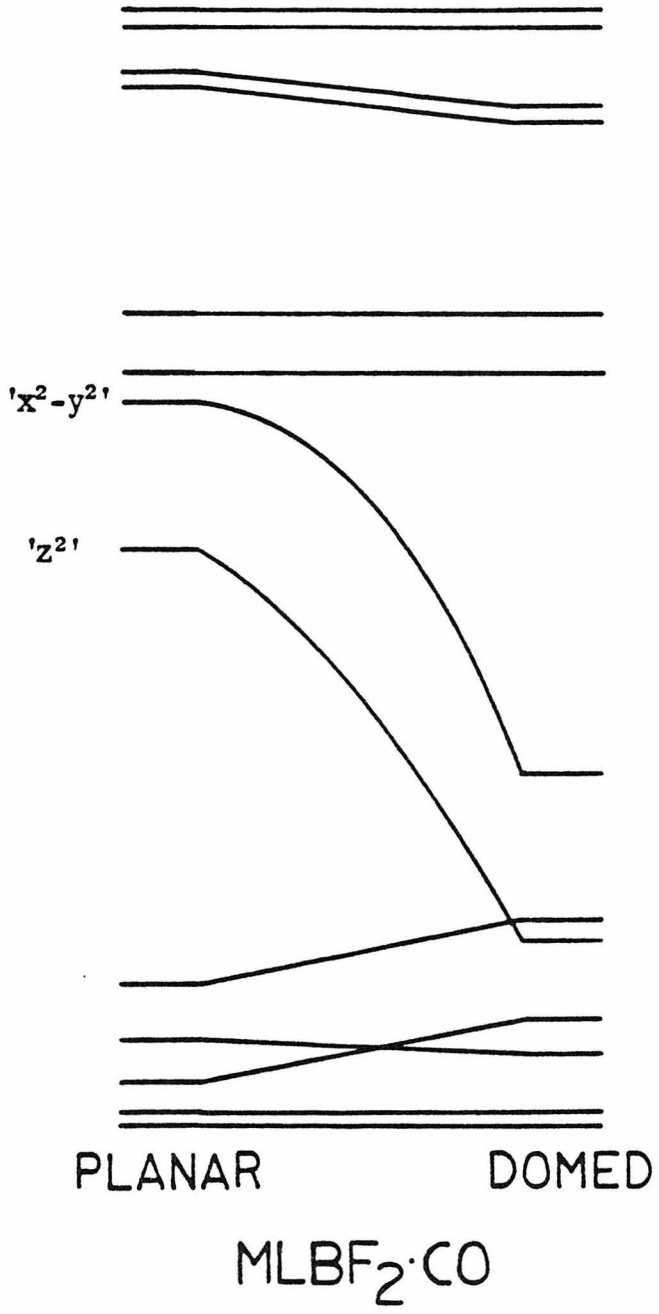

Figure 14

Table V. Cu-X Population Analysis in the Five-Coordinate $Cu(I)(DOBF_2)X$

	Total	σ(s, p)	σ(d)	π(d)	π(p)
square-planar Cu-CO	0.55	0.45	0.02	0.07	0.01
observed geometry Cu-CO	0.66	0.54	0	0.08	0.02
square-planar $Cu-Cl^-$	0.34	0.41	0.01	-0.08	0

plane of the square-planar ligand. Two major changes have occurred: (1) the reduced symmetry has allowed the metal to mix 3d, 4s, and 4p orbitals, (2) the metal d_{z^2} has been highly destabilized due to antibonding interactions with the carbonyl σ orbital. As the metal ion is moved out of the plane of the ligand, while holding the macrocycle in a fixed planar position, the system is strongly stabilized; the metal $d_{x^2-y^2}$ and d_{z^2} are considerably stabilized upon moving the metal out of the ligand plane, due to the relief of metal-ligand antibonding forces.[21] An additional, but smaller stabilization is found as the ligand assumes the "domed" geometry observed crystallographically (Figure 14).[6,7] Other distortions, including bending the difluoroborate and alkyl bridges away from the metal side of the complex are highly disfavored.[22]

Since the metal d_{z^2}-carbonyl σ-interaction is an antibonding interaction, a long apical bond might be expected.[23] This is not the case, as shown by crystallography.[6,7] A population analysis of the Cu(I)($DOBF_2$)CO complex (Table V) indicates that the carbon monoxide is primarily attached to the metal by strong σ-interactions with the metal 4s and 4p orbitals. Interaction of ligand σ and metal d orbitals leads to negligible stabilization. A small stabilization is seen by interaction of the carbon monoxide π^* orbitals with the filled metal d_{xz} and d_{yz} orbitals--M-CO π back-donation. A similar mechanism for CO attachment is formed with all the ligands mentioned above (Figure 5).[25] The σ-interactions of importance for the formation of these metal carbonyls are similar to those between CO and the main

group species BH_3. The ability of the metal d-orbitals to π back-donate to CO gives a ν_{CO} (2068 cm^{-1}), which is less than that of free CO (2143 cm^{-1}) and much less than for BH_3CO (2164 cm^{-1}). Certain Cu(I)-carbonyl complexes have been reported to be higher (ranging from 2160 to 2185) than free CO.[26] Copper 4s and 4p orbitals σ-interactions are also shown by population to be the major contributors to the Cu-N linkages. Hoffmann and co-workers[27-28] have noted the importance of (n+1)s and p orbitals in the bonding interactions between closed-shell species Cu(I)/Cu(I) and Pt(0)/Pt(0). The importance of the s and p orbitals suggests comparison to a square-pyramidal main group species, $SbPh_5$; inclusion of Sb 4d electrons reveals this is a 20-electron complex. The general importance of higher orbitals on determining the properties of transition metal complexes is an unanswered question. Although parameter dependent, the results reported here suggest that for these copper-carbonyl complexes they are quite important.

Calculations were also done for the Cu(I)$(DOBF_2)Cl^-$ species to investigate the effect of the coordination of a σ-donor as a fifth ligand. From the population analysis (Table V), the attachment of chloride is also by σ orbitals and the copper 4s and 4p orbitals. In contrast to the stabilizing π-interactions for the copper-carbonyl complex, the π-interactions are actually destabilizing for the chloride complex. This π-bonding, resulting from occupation of both Cu-Cl bonding and anti-bonding orbitals, has been noted for other macrocyclic complexes by Okawa and Busch.[29] These results for chloride attachment are

consistent with the observations[6, 12] of larger equilibrium constants, K^L, for binding a π-acceptor ligand as fifth ligand than for a σ-donor ligand.

$$Cu(DOBF_2) + L \overset{K^L}{\rightleftharpoons} Cu(DOBF_2)L$$

$$L = CO,\ K = 1.2 \times 10^5\ M^{-1}$$

$$L = 1\text{-methylimidazole},\ K = 1.6 \times 10^1\ M^{-1}$$

Summary

EHMO calculations as well as experimental infrared results indicate that reduced tetraazamacrocyclic copper complexes containing conjugated α-diimine moieties may best be described as copper(III) complexed to a ligand dianion.[32] Corresponding reduced nickel species have been shown to be nickel(II)-stabilized radical anions. Although this formalism might seem to suggest a very electropositive metal, the tetrahedral distortion observed serves to mix the HOMO-LUMO pair, returning some electron density, and thus copper(I) "character," back to the metal center. One might speculate that this intramolecular electron transfer process, which may be suitably altered by adjustment of molecular parameters,[10, 11, 12] plays an important role in the mechanism for electron transport in copper containing proteins, for which there are presently no detailed descriptions of the role of the copper site.

Experimental

Infrared spectra were obtained on a Beckman IR-4240 infrared spectrometer. Samples, contained in KBr pellets, were prepared under an inert atmosphere as much as possible. Spectra of KBr pellet samples were comparable to the spectra of nujol mull samples prepared under a helium atmosphere in a Vacuum Atmospheres Dri-Lab glove box. All nickel[10, 13] and copper[2, 5, 7, 12] complexes gave satisfactory analytical analyses.

Isotopically substituted ^{15}N-$Ni(DMG)_2$ was prepared by stirring 2, 3-butanedione (56 mg), ^{15}N)-hydroxylamine hydrochloride (70 mg), and nickel(II) acetate · dihydrate (240 mg) in 4 ml ethanol at the ambient temperature overnight. Subsequent syntheses were as described elsewhere.[10, 11]

Appendix

The calculations were carried out on the parent molecule $Cu(LBF_2)$ with dimensions given. It

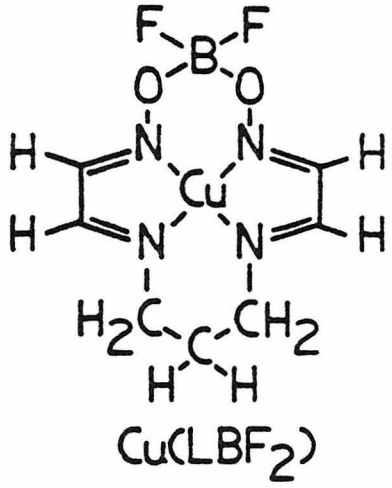

$Cu(LBF_2)$

differs from the ligand used in the experimental work by replacement of some terminal methyl groups by hydrogen atoms. The parameters of the Extended Hückel calculations[30] are given in Table VI. For the M(I) and M(II) species (M = Cu, Ni) the double ζ Slater functions of Richardson and co-workers[31] were used for the metal 3d orbitals. The explanation of the experimental results above derive from a particular level ordering in the complexes obtained using these radical functions. Calculations are parameter dependent as alternate choices of d-orbital functions, for example single ζ, do not give the same results. Values of the metal 4s and 4p orbital exponents and s, p, and d VSIP's are those used by Hoffmann and Mehrota.[27]

Table VI. Extended Hückel Parameters

Atom	Orbital	Exponent		H_{ji} (eV)
H	1s	1.300		-13.60
B	2s	1.300		-15.20
B	2p	1.300		-8.50
C	2s	1.625		-21.40
C	2p	1.625		-11.40
N	2s	1.950		-26.00
N	2p	1.950		-13.40
O	2s	2.275		-32.30
O	2p	2.275		-14.80
F	2s	2.475		-40.00
F	2p	2.475		-18.10
Cl	3s	2.033		-30.00
Cl	3p	2.033		-15.00
M	4s	2.200		-11.40
M	4p	2.200		-6.06
Cu(I)	3d	5.95 (0.5933)[a]	2.30 (0.5744)	-14.00
Cu(II)	3d	5.95 (0.6062)	2.50 (0.5371)	-14.00
Ni(I)	3d	5.75 (0.5817)	2.20 (0.5890)	-14.00
Ni(II)	3d	5.75 (0.5959)	2.40 (0.5497)	-14.00

[a]The 3d orbitals are in double ζ form with expansion coefficients in parentheses.

References and Notes

(1) Palmer, J. M.; Papaconstantinou, E.; Endicott, J. F. Inorg. Chem. 1969, 8, 1516.

(2) Olson, D. C.; Vasilevskis, J. Inorg. Chem. 1971, 10, 463.

(3) Tokel, N. E.; Katovic, V.; Farmery, K.; Anderson, L. B.; Busch, D. H. J. Am. Chem. Soc. 1970, 92, 400.

(4) Katovic, V.; Taylor, L. T.; Urbach, F. L.; White, W. H.; Busch, D. H. Inorg. Chem. 1972, 11, 479.

(5) Gagné, R. R. J. Am. Chem. Soc. 1976, 98, 6709.

(6) Gagné, R. R.; Allison, J. L.; Gall, R. S.; Koval, C. A. J. Amer. Chem. Soc. 1977, 99, 7170.

(7) Gagné, R. R.; Ingle, D. M.; Kreh, R. P.; McCool, M.; Marsh, R. E. manuscript submitted for publication.

(8) Laine, R. M.; Moriarty, R. E.; Bau, R. J. Am. Chem. Soc. 1972, 94, 1402.

(9) Gagné, R. R.; Allison, J. L.; Lisensky, G. C. Inorg. Chem. 1978, 17, 3563.

(10) Gagné, R. R.; Ingle, D. M. submitted for publication in J. Am. Chem. Soc.

(11) Gagné, R. R.; Ingle, D. M. manuscript in preparation.

(12) Gagné, R. R.; Allison, J. L.; Ingle, D. M. Inorg. Chem. 1979, 18, 0000

(13) Olson, D. C.; Vasilevskis, J. Inorg. Chem. 1969, 8, 1611.

(14) Lovecchio, F. V.; Gore, E. S.; Busch, D. H. J. Am. Chem. Soc. 1974, 96, 3109.

(15) "$CoCp^+$" represents the counter ion cobaltocinium.

(16) Elian, M.; Hoffmann, R. Inorg. Chem. 1975, 14, 1058.

(17) For convenience, D_{4h} labels for the square-planar species are used.

(18) A population analysis for the $\sigma^*_{x^2-y^2}$ orbital for the reduced copper system reveals this is mostly a metal $d_{x^2-y^2}$ orbital: $d_{x^2-y^2}$, 0.7; σ^*_N, 0.5.

(19) Alternatively, one might speculate that for Cu(II), Ni(I), or Ni(II) the reverse process, electron transfer from the ligand to the metal, might occur.

(20) The π_1^* orbital being lower than the $\sigma^*_{x^2-y^2}$ orbital for the reduced species allows for an avoided crossing on distortion.

(21) Smaller out-of-plane displacements found experimentally for the Cu(II) species in the present system is understandable. With the $\sigma^*_{x^2-y^2}$ orbital half-occupied, the driving force for out-of-plane movement of the metal is less. This molecular orbital result is detailed elsewhere.[15]

(22) Since the Cu-N distance change significantly (~0.20 Å)[6] on going from the four-coordinate Cu(DOBF$_2$) to the five-coordinate calculations should not be relied on to accurately predict the extent of distortion. However, the general trends suggested here are in accord with experimental observations.

(23) The low-spin d^8 $Ni(CN)_5^{3-}$ is such a case: $Ni\text{-}CN_{ap}$ = 2.168 Å, $Ni\text{-}CN_{bas}$ = 1.87 Å.[24]

(24) Raymond, K. N.; Corfield, P. W. R.; Ibers, J. A. Inorg. Chem. 1968, 7, 1362.

(25) $Cu(I)(TAAB)^+$ experimentally shows very little attraction for binding π-acids.[11] The overall rigidity of this complex may inhibit formation of five-coordinate complexes.

(26) Souma, Y.; Iyoda, J.; Sano, H. Inorg. Chem. 1976, 15, 968.

(27) Mehrota, P. K.; Hoffmann, R. Inorg. Chem. 1978, 17, 2187.

(28) Dedieu, A.; Hoffmann, R. J. Am. Chem. Soc. 1978, 100, 2074.

(29) Okawa, H.; Busch, D. H. Inorg. Chem. 1979, 18, 1555.

(30) Hoffmann, R. J. Chem. Phys. 1963, 39, 1397.

(31) Richardson, J. W.; Nieuwpoort, W. C.; Powell, R. R.; Edgell, W. E. J. Chem. Phys. 1962, 36, 1057.

(32) Consideration of these complexes as copper(III)-ligand dianions must be done bearing in mind that the metal-ligands are very covalent[18] and that distortion towards tetrahedrality introduces further "copper(I)-character" into the system.

Summary

Summary

These investigations of nickel macrocyclic ligand complexes have revealed certain facts. To enumerate, they are:

(1) Four-coordinate nickel(I) complexes of certain tetraaza-macrocyclic ligands can bind carbon monoxide to form nineteen electron, paramagnetic, presumably five-coordinate nickel(I) carbonyl complexes.

(2) Four-coordinate nickel(II)-stabilized ligand radical complexes of several tetraazamacrocyclic ligands containing conjugated α-diimine moieties can also bind carbon monoxide to form nineteen electron, paramagnetic, presumably five-coordinate nickel(I) carbonyl complexes. Intramolecular electron transfer apparently occurs upon the complex going from four-coordinate to five-coordinate as seen by EPR and IR spectroscopy.

(3) One complex, $Ni(DOBF_2)Bn$, displays both the nickel(I) and the nickel(II)-stabilized ligand radical at ambient temperatures. From variable temperature EPR, the nickel(I) form is estimated to be 0.75± 0.15 kcal/mole higher in energy than the nickel(II) ligand radical.

(4) Carbon monoxide binding constants, EPR parameters, electronic absorption spectra, and infrared spectra of the four-coordinate and five-coordinate reduced nickel complexes have been reported.

(5) On the basis of similarities in the infrared spectra between the reduced nickel and analogous reduced copper complexes, the previously known four-coordinate reduced copper complexes having conjugated α-diimines can be regarded as copper(III)-stabilized ligand dianion complexes, having a large amount of "copper(I)-character." EHMO calculations are related that are consistent with this view.

Appendix I

Unusual Structural and Reactivity Types for Copper(I): Equilibrium Constants for the Binding of Monodentate Ligands to Several Four-Coordinate Copper(I) Complexes

Robert R. Gagné
Judith L. Allison
D. Michael Ingle

Unusual Structural and Reactivity Types for Copper (I): Equilibrium Constants For the Binding of Monodentate Ligands to Several Four-Coordinate Copper(I) Complexes

ROBERT R. GAGNÉ*, JUDITH L. ALLISON, and D. MICHAEL INGLE

Abstract: Equilibrium binding constants, K^I, were measured for the reaction: $Cu(I)mac^{+n} + L \rightleftharpoons Cu(I)mac(L)^{+n}$, in which $Cu(I)mac^{+n}$ is a four-coordinate Cu(I) complex of a polydentate ligand, L is a monodentate ligand, and $Cu(I)mac(L)^{+n}$ is a five-coordinate Cu(I) complex. Equilibrium constants have been obtained for reactions between isonitriles, phosphites, CO, phosphines and amines with a single, four-coordinate, copper(I) macrocyclic ligand complex. Reactions between CO and twelve different four-coordinate copper(I) complexes were also studied. In all cases equilibrium constants were obtained using a simple electrochemical technique. Sampled dc polarography was used to obtain $E_{\frac{1}{2}}$ for the $Cu(mac)(II/I)^{+n}$ redox couple in the absence and in the presence of a monodentate ligand, L. The observed shift in $E_{\frac{1}{2}}$ was then used to calculate equilibrium constants. In general, five-coordination for Cu(I) was found to be

favored for π-acid ligands, such as isonitriles, phosphites, CO and phosphines. Five-coordinate adducts are apparently accessible from a variety of four-coordinate Cu(I) complexes. Tetradentate ligands which enforce a near square-planar, yet flexible, ligand geometry for Cu(I), seem to promote five-coordination.

Introduction

The four-coordinate copper(I)-macrocyclic ligand complex, 1, has been shown to have tetrahedrally distorted, square-planar coordination.[1] Besides an uncommon copper(I) geometry, the complex also exhibits unusual reactivity, binding monodentate ligands to give five-coordinate adducts, 2, equation 1.[2-4] The first fully characterized five-coordinate copper(I) complex, a carbonyl adduct, 3 (2 with

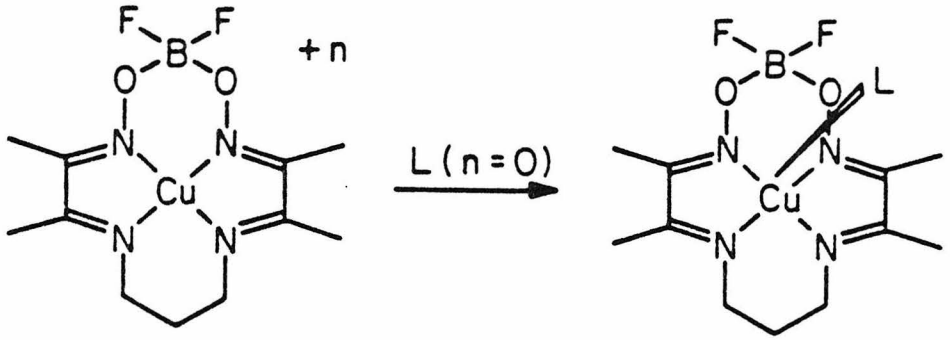

(1)

1, Cu(I), n = 0
4, Cu(II), n = 1

2

L = CO) was shown by X-ray structural analysis to exist in a distorted square-pyramidal configuration.[3] The carbonyl complex, 3, has a

copper-carbon bond length of 1.78 Å, but long copper-nitrogen bonds (2.14-2.16 Å) accompanied by an extraordinary 0.96 Å) displacement of copper(I) from the mean plane of the four coordinated nitrogen atoms.[3]

Initial spectroscopic, structural and reactivity studies (L = CO, 1-MeIm, CH_3CN) have suggested that these species, 1 and 2, be regarded as copper(I) complexes, but have not explained the unusual reactivity or structures.[1-3] Equilibrium binding constant studies, reported here, help to define the nature of copper binding to both axial (L) and macrocyclic ligands. This paper presents experimentally determined equilibrium constants obtained with a wide range of monodentate ligands reacting with several copper-macrocyclic ligand complexes.

Determination of Equilibrium Constants

Equilibrium constants, K^I, equation 2, were measured for a

$$Cu(I)\,mac + L \overset{K^I}{\rightleftharpoons} Cu(I)\,mac\,(L) \qquad (2)$$

variety of copper(I)-macrocyclic complexes, Cu(I)mac, and monodentate ligands, L, in acetone or N,N-dimethylformamide (DMF). All determinations were made using electrochemical methods. Since this technique has not been widely applied for monitoring ligand

binding a detailed description of the procedure is given here.

From the Nernst equation, equation 3, an expression can be

$$E = E^{o} + \frac{RT}{nF} \ell n \frac{[Cu(II)]}{[Cu(I)]} \tag{3}$$

derived that relates reduction potentials and copper(II) and copper(I) equilibrium binding constants. If the equilibria given in equations 4 and 6 are the only equilibria in solution, the derived electrochemical

$$Cu(II)mac + L \rightleftharpoons Cu(II)mac(L) \tag{4}$$

$$K^{II} = \frac{[Cu(II)mac(L)]}{[Cu(II)mac][L]} \tag{5}$$

$$Cu(I)mac + L \rightleftharpoons Cu(I)mac(L) \tag{6}$$

$$K^{I} = \frac{[Cu(I)mac(L)]}{[Cu(I)mac][L]} \tag{7}$$

relationship in equation 8 results, where $E_{\frac{1}{2}}(L)$ is the half-wave

$$E_{\frac{1}{2}}(L) = E_{\frac{1}{2}} + \frac{RT}{nF} \ell n \left[\frac{1+K^{I}[L]}{1+K^{II}[L]}\right] \tag{8}$$

potential measured with some mondentate ligand L present and $E_{\frac{1}{2}}$ is the corresponding potential in the absence of ligand. Derivation

of this relationship has been described elsewhere.[4-7]

Experimentally, half-wave potentials were determined for a copper(II) solution under argon and with various concentrations of monodentate ligand, L. The binding constants, K^{II} and K^{I}, were calculated using a form of equation 8, given in equation 9

$$\frac{1}{e^{\Delta E(nF/RT)}-1} = \frac{1}{K^{I}-K^{II}}\left(\frac{1}{[L]}\right) + \frac{K^{II}}{K^{I}-K^{II}} \qquad (9)$$

where

$$\Delta E \equiv E_{\frac{1}{2}}(L) - E_{\frac{1}{2}} \; . \qquad (10)$$

A plot of the reciprocal of the exponential term, $e^{\Delta E(nF/RT)}-1$, *vs.* the reciprocal of $[L]$ has a slope equal to $1/(K^{I}-K^{II})$ and an ordinate intercept equal to $K^{II}/(K^{I}-K^{II})$. The binding constants, K^{I} and K^{II}, can be determined from the slope and intercept by solving simultaneous equations.

A simpler expression can be used when either $K^{II}[L]$ or $K^{I}[L]$ approaches zero. As $K^{II}[L]$ approaches zero, equation 8 becomes equation 11

$$e^{\Delta E(nF/RT)}-1 = K^{I}[L] \; . \qquad (11)$$

One potential shift measurement due to a single L concentration thus allows calculation of K^I.[8]

Half-wave potentials for the reduction of copper(II) to copper(I) were evaluated from sampled dc polarograms.[8] Figure 1 shows polarograms for the copper(II) compound, $\underset{\sim}{4}$, in N,N-dimethylformamide (DMF) with argon and carbon monoxide atmospheres. The half-wave potential of a cathodic wave was evaluated using the relationship given in equation 12, where i is the mean current and i_d is the mean

$$E = E_{\frac{1}{2}} - \frac{RT}{nF} \ell n \left[\frac{i}{i_d - i}\right] \qquad (12)$$

diffusion current, measured as indicated in Figure 1. Diffusion current constants, I_d, characteristic of a compound in a particular solvent, were calculated using the measured mean diffusion current, i_d, and the relationship given in equation 13

$$I_d = \frac{i_d}{[Cu_B] m^{\frac{2}{3}} t^{\frac{1}{6}}} \; . \qquad (13)$$

In equation 13, $[Cu_B]$ is the bulk concentration of electroactive species in mM, m is the mercury flow rate in mg/s, and t is the drop time in seconds. Half-wave potentials, $E_{\frac{1}{2}}$, were determined as the intercepts of E <u>vs.</u> $\ln[i/(i_d - i)]$ plots. Theoretically, such

Figure 1

Sampled dc polarograms with curves smoothed of complex $\underset{\frown}{4}$, (0.5 mM), in DMF with carbon monoxide, $E_{\frac{1}{2}} = -0.296$ V, and argon, $E_{\frac{1}{2}} = -0.456$ V.

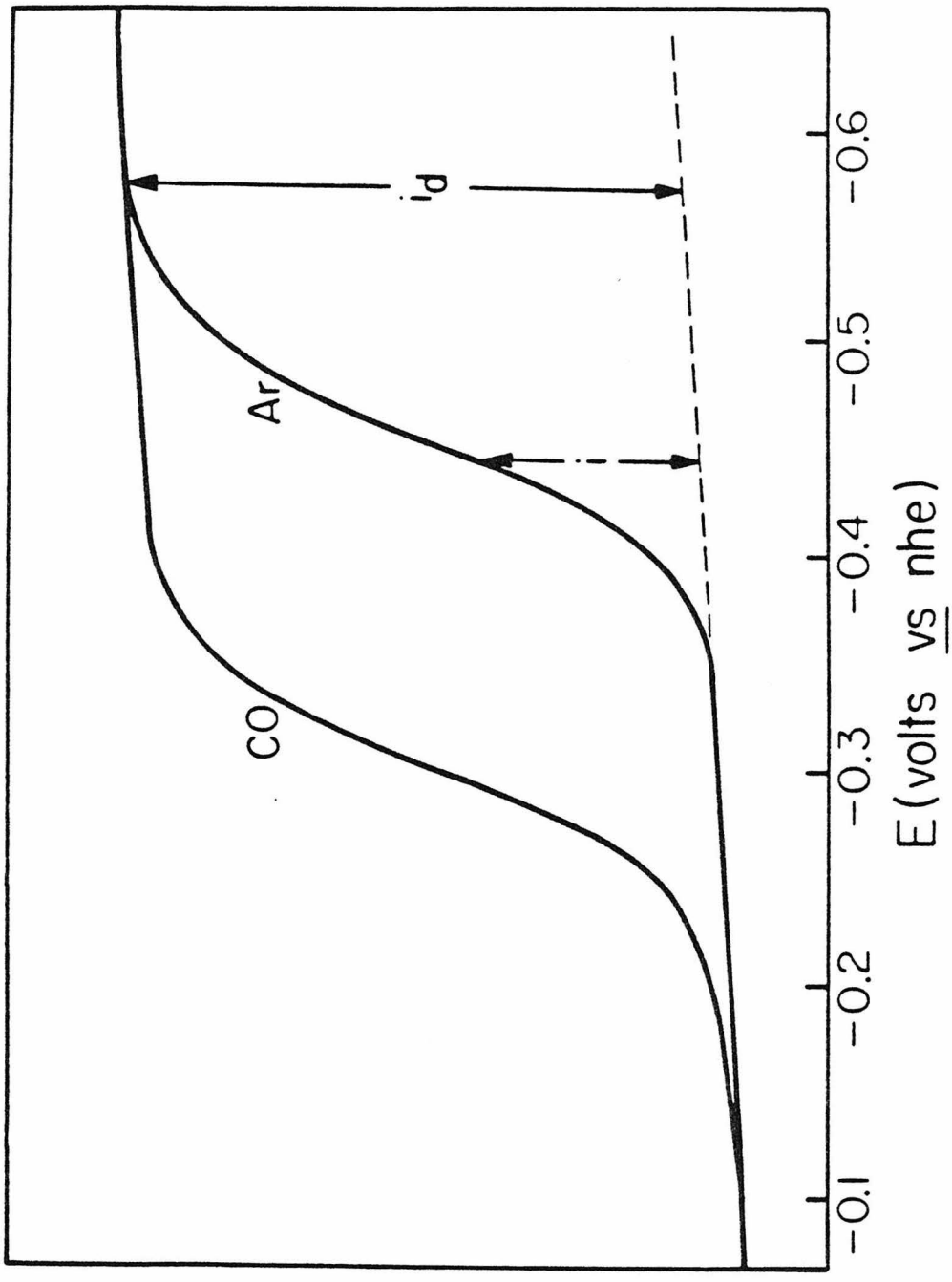

Figure 1

plots should have a slope -RT/nF for a reversible electrochemical process. In practice the measured slopes of E vs. $\ln[\, i/(i_d-i)]$ plots were used as one indication of electrochemical reversibility. Logarithmic analysis of polarograms of $\underset{\sim}{4}$, with added ligands at initial concentration, $[\, L\,]_i$, resulted in values for I_d, slope, and $E_{\frac{1}{2}}(L)$, presented in Tables I (DMF as solvent) and II (acetone as solvent). For some ligands other than $P(\underline{p}\text{-}C_6H_4Cl)_3$ and pyridine a series of different ligand concentrations were examined, but the data presented are representative.

The negative slope should be 58.6 mV at 22 °C for n=1. For the reduction of copper(II) to copper(I) in the presence of ligand, L, negative slopes varying from 54.8 to 81.5 mV were found, Table I. The majority of slopes are close to 58.6 mV consistent with electrochemically reversible reduction processes. The glaring exceptions (in DMF) are $P(O\text{-}Bu)_3$ (-79.2 mV), $P(O\text{-}C_6H_{11})_3$ (-81.5 mV), and $P(\underline{p}\text{-}C_6H_4Cl)_3$ at low $[L]_i$ (-67.2 to -72.1 mV). At low $[L]_i$ or at very high K^I a problem exists which is mirrored by the slope value. If the reduction process is reversible without L, on addition of L, a reversible process will occur only if there is a sufficient excess of L to effectively maintain the electrode surface concentration, $[L]_s$, at the initial level, $[L]_i$, throughout the polarographic run. For ligands which bind especially strongly to Cu(I) a high concentration of L was

Table I. Representative Sampled dc Polarographic Results for 4 and Fifth Ligands in DMF.[a]

Ligand, L	$[L]_i \times 10^3$ (M)	I_d[b]	-slope[c]	r^2[c]	$E_{\frac{1}{2}}(L)$[e]
No ligand[d]	0.0	1.70	56.8	0.9993	-0.456
p-NC(C_6H_4)NC	5.03	1.61	58.5	0.9992	-0.166
p-NO_2(C_6H_4)NC	5.08	1.69	64.5	0.9996	-0.168
P(O-C_6H_{11})$_3$	1.99	1.64	81.5	0.9995	-0.251
P(O-Bu)$_3$	2.06	1.65	79.2	0.9995	-0.270
P(O-p-C_6H_4Cl)$_3$	2.00	1.67	59.6	0.9995	-0.304
CO	4.64	1.70	57.3	0.9997	-0.296
P(O-p-$C_6H_4CH_3$)$_3$	1.03	1.60	67.0	0.9999	-0.349
P(O-o-$C_6H_4CH_3$)$_3$	2.41	1.53	58.7	0.9998	-0.337
P(p-C_6H_4Cl)$_3$	5.00	1.56	56.9	0.9998	-0.327
	2.00	1.71	62.9	0.9998	-0.352
	0.960	1.69	67.2	0.9998	-0.375
	0.800	1.64	68.2	0.9993	-0.380
	0.640	1.70	72.1	0.9997	-0.389
P(p-$C_6H_4CH_3$)$_3$	2.00	1.56	64.0	0.9989	-0.360
P(C_6H_5)$_3$	2.00	1.71	62.6	0.9999	-0.363
P(o-$C_6H_4OCH_3$)$_3$	2.00	1.67	58.7	0.9994	-0.458
P(o-$C_6H_4CH_3$)$_3$	2.00	1.68	57.1	0.9995	-0.459

[a] $[Cu(II)] = 5.00 \times 10^{-4}$ M. Temperature, average value, 22°C. Drop time, t, 5 s.

[b] I_d, $\mu A\ s^{\frac{1}{2}}\ (mM)^{-1}\ (mg)^{-\frac{2}{3}}$

[c] From linear regression fit of plot of E vs. $\ln[i/(i_d-i)]$: -slope, mV; r^2, coefficient of determination; $E_{\frac{1}{2}}(L)$, ordinate intercept, in volts vs. nhe, assuming $E^f_{ferrocene} = 0.400$ V.

[d] Average values.

Table II. Representative Sampled dc Polarographic Results for 4 and Fifth Ligands in Acetone.[a]

Ligand, L	$[L]_i \times 10^3$ (M)	I_d[b]	-slope[c]	r^2[c]	$E_{\frac{1}{2}}(L)$[c]
no ligand[d]	0.0	2.93	59.0	0.9991	-0.400
$P(O\text{-}Bu)_3$	2.05	2.70	59.9	0.9987	-0.168
$P(O\text{-}\underline{p}\text{-}C_6H_4Cl)_3$	2.73	2.65	60.3	0.9925	0.205
$P(C_6H_5)_3$	3.18	2.57	57.6	0.9999	-0.270
pyridine	100.4	2.78	57.3	0.9994	-0.462
	50.8	2.83	58.3	0.9990	-0.450
	33.5	2.81	58.0	0.9995	-0.440
	25.4	2.81	58.7	0.9995	-0.435
	20.3	2.80	58.0	0.9993	-0.431
	16.7	2.78	57.3	0.9991	-0.427
$4\text{-}(CH_3)_2N$pyridine	100.0	2.62	59.9	0.9994	-0.532
$(CH_3)_2N(C_6H_5)$	50.5	2.64	54.8	0.9995	-0.401
$4\text{-}CH_3O_2C$pyridine	116.9	2.60	56.9	0.9997	-0.434

[a] $[Cu(II)] = 4.99 \times 10^{-4}$ M. Temperature, average value, 22° C. Drop time, t, 5 s.

[b] I_d, $\mu A\ s^{\frac{1}{2}}\ (mM)^{-1}\ (mg)^{-\frac{2}{3}}$.

[c] From linear regression fit of plot of E vs. $\ln[i/(i_d-i)]$: -slope, mV; r^2, coefficient of determination; $E_{\frac{1}{2}}(L)$, ordinate intercept, in volts vs. nhe, assuming $E^f_{ferrocene} = +0.400$ V.

[d] Average values.

necessary to maintain $[L]_s$ effectively constant throughout the reduction. Unfortunately, measuring the current, i, from plots of E *vs.* $\ln[i/(i_d-i)]$ was difficult for higher concentrations due to background current problems (discussed below) so that polarograms at higher concentrations could not be quantitatively analyzed. This may account for the large negative slopes of certain logarithmic plots, viz. those of the strongly binding phosphites $P(O\text{-}Bu)_3$ and $P(O\text{-}C_6H_{11})_3$. The data for $P(\underline{p}\text{-}C_6H_4Cl)_3$, Table I, illustrate the gradual approach of the negative slope to 58.6 mV with increasing ligand concentration.

Low concentrations of phosphine ligands were used due to background currents that increase with increasing ligand concentrations. Even with only 2 mM ligand, the polarogram of $P(\underline{p}\text{-}C_6H_4CH_3)_3$ had nonparallel background and diffusion currents. The background current had a greater slope (i/E) initially due to the current from an oxidation wave of the ligand,[7,9] which did not affect the more negative diffusion current of the copper(II) reduction. With increased ligand concentration, the very rapidly growing background current began to overwhelm the slope of the copper(II) reduction, and accurate determination of the half-wave potential became difficult. Low concentrations of L were used to minimize the background current slope.

Problematically, however, low ligand L concentrations led to variation in the slopes of the E *vs.* $\ln[i/(i_d-i)]$ plots from -58.6 mV,

and also inaccuracy in $E_{\frac{1}{2}}$ determinations, Table I. The value of $[L]_s$ at equilibrium is not equal to the bulk or initial concentration of L, $[L]_i$, but is lowered by χ, the concentration of Cu(I)L formed (equations 6 and 14). With $[L]_i$ and ΔE, an initial equilibrium

$$Cu(I)\,mac + L \rightleftharpoons Cu(I)\,mac\,(L) \tag{6}$$

$$K^I = \frac{\chi}{([Cu(I)]_i - \chi)([L]_i - \chi)} \tag{14}$$

constant, K_i^I, was calculated (equation 11). This constant, K_i^I, and $[L]_i$ were used to initiate an iterative calculation of χ. The equilibrium or final concentration of L within the diffusion layer, $[L]_f$, is equal to $[L]_i$ minus the converged value of χ. This value was used to determine K_f^I, the final equilibrium constant.

The calculated $[L]_f$ values for five concentrations of $P(p\text{-}C_6H_4Cl)_3$ are given in Table III. Figure 2 graphically illustrates the difference between $[L]_i$ and $[L]_f$ in a plot of $e^{\Delta E(nF/RT)}-1$ *vs.* $[L]$ (see equation 11). The calculated ordinate intercepts of the two plots are -8.29, $[L]_i$, and -0.42, $[L]_f$. For any ligand at $[L] = 0$, ΔE is zero and the plot should pass through the origin. The use of $[L]_f$ adjusted the ordinate-intercept closer to zero, with minimal change in slope (3.33×10^4 to $3.34 \times 10^4\ M^{-1}$).

Table III. Iterative Ligand Reduction Results for $\underset{\wedge}{4}$ and P(p-$C_6H_4Cl)_3$ in DMF[a]

$[L]_i \times 10^3$ (M)[b]	$(e^{\Delta E(nF/RT)} - 1)$[c]	$K_i^I \times 10^{-4}$ (M^{-1})[d]	$[L]_f \times 10^3$ (M)[b]	$K_f^I \times 10^{-4}$ (M^{-1})[d]
5.00	158.3	3.17	4.74	3.33
2.00	58.63	2.93	1.75	3.34
0.960	23.15	2.41	0.720	3.21
0.800	18.84	2.35	0.563	3.35
0.640	12.93	2.02	0.408	3.17

[a] For the reaction: Cu(I)mac, $\underset{\wedge}{1}$ + P(p-$C_6H_4Cl)_3 \overset{K^I}{\rightleftharpoons}$ Cu(I)mac[P(p-$C_6H_4Cl)_3$].

[b] $[L]_i$, $[L]_f$ = initial and final L concentrations, respectively.

[c] $\Delta E \equiv E_{\frac{1}{2}}(L) - E_{\frac{1}{2}}$.

[d] K_i^I, K_f^I = initial and final equilibrium constants, respectively. $K_{i,f}^I = (e^{\Delta E(nF/RT)} - 1)/[L]_{i,f}$.

Figure 2

Graph of $e^{\Delta E(nF/RT)}-1$ vs. $[L]$ for five concentrations of $P(\underline{p}\text{-}C_6H_4Cl)_3$ in DMF with 0.5 mM complex 4. $\Delta E \equiv E_{\frac{1}{2}}[P(\underline{p}\text{-}C_6H_4Cl)_3]-E_{\frac{1}{2}}$. The top line is the plot using $[L]_f$, the corrected ligand concentration. The slope is $3.34 \times 10^4\ M^{-1}$, the ordinate-intercept is -0.42, and r^2 is 0.9999. The lower line is the plot using $[L]_i$, the initial ligand concentration. The slope is $3.33 \times 10^4\ M^{-1}$, the ordinate-intercept is -8.29, and r^2 is 0.9999.

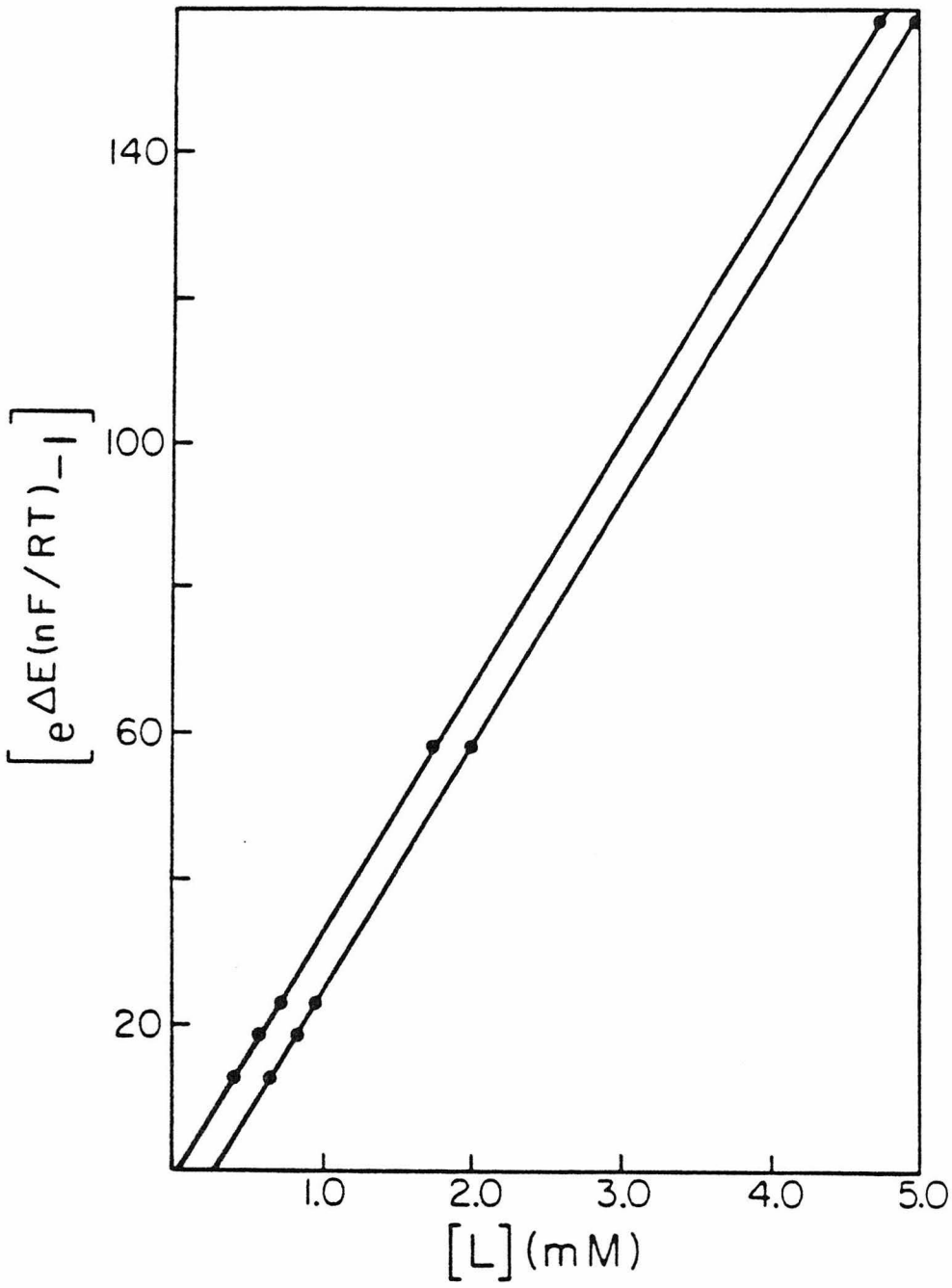

Figure 2

The other difficulty encountered with low concentrations of ligand was ambiguity in the position of the half-wave potential. The $E_{\frac{1}{2}}$ values determined from E *vs.* $\ln[i/(i_d-i)]$ plots and $[L]_f$ values calculated iteratively were used to find K_f^I (equation 11). When several initial concentrations of L were examined, a plot of $e^{\Delta E(nF/RT)}-1$ *vs.* $[L]_f$ (as in Figure 2) was constructed and the slope, equal to K_f^I, was determined. The coefficient of determination, r^2, is an indication of the linearity of the data pairs. Table IV condenses the results of both simple calculations of K^I from a single ΔE, $[L]_f$ pair and the linear regression calculations of slopes, intercepts and coefficients of determination for a series of ΔE, $[L]_f$ pairs. With the assumption that K^{II} is zero, K^I values were calculated and the r^2 values indicate a good data fit, Table IV. Because of the correlation of high and low ligand concentration data, the error in determination of $E_{\frac{1}{2}}$ appears to be smaller than the theoretically predicted error, $\Delta E'$ (equation 15).[7] The error, $\Delta E'$, is

$$\Delta E' \approx \frac{RT[Cu(II)]}{2nF[L]} \qquad (15)$$

± 0.0015 V with $[Cu(II)] = 5\times10^{-4}$ M and $[L] = 2\times10^{-3}$ M. An error of ± 0.0025 V in $E_{\frac{1}{2}}(L)$ has been estimated, corresponding to $[L] = 1.25\times10^{-3}$ M or, as intended, large enough to include instru-

Table IV. Determination of Equilibrium Binding Constants, K^I, with Assumption, $K^{II} = 0$.[a]

Ligand, L	Solvent	Points[b]	r^2[c]	b[c]	$K^I(M^{-1})$[a,c,d]
p-NC(C_6H_4)NC	DMF	3	0.99942	-2500.	1.9×10^7
p-NO_2(C_6H_4)NC	DMF	3	0.9996	-620.	1.7×10^7
P(O-C_6H_{11})$_3$	DMF	2			1.8×10^6
P(O-Bu)$_3$	DMF	2			8.3×10^5
	acetone	2			5.1×10^6
P(O-p-C_6H_4Cl)$_3$	DMF	5	0.99970	8.6	2.2×10^5
	acetone	2			8.6×10^5
CO	DMF	2			1.2×10^5
P(O-C_6H_5)$_3$	DMF	5	0.9960	-2.6	1.1×10^5
P(O-p-$C_6H_4CH_3$)$_3$	DMF	4	0.9946	0.74	8.7×10^4
P(O-o-$C_6H_4CH_3$)$_3$	DMF	2			4.9×10^4
P(p-C_6H_4Cl)$_3$	DMF	6	0.9999	-0.60	3.3×10^4
P(p-$C_6H_4CH_3$)$_3$	DMF	5	0.9986	-0.66	2.4×10^4
P(C_6H_5)$_3$	DMF	5	0.9984	0.59	2.1×10^4
	acetone	2			5.6×10^4
P(o-$C_6H_4OCH_3$)$_3$	DMF	2			0
P(o-$C_6H_4CH_3$)$_3$	DMF	2			0

[a] For the reactions: Cu(I)mac, $\underset{\sim}{1}$ + L $\overset{K^I}{\rightleftharpoons}$ Cu(I)mac(L) and Cu(II)mac$^+$, $\underset{\sim}{4}$ + L $\overset{K^{II}}{\rightleftharpoons}$ Cu(II)mac(L)$^+$.

[b] Points = number of ΔE, [L] points used to determine K^I. This number includes (0, 0) which was used in each K^I calculation.

[c] Plot of $e^{\Delta E(nF/RT)}-1$ vs. [L]; $\Delta E = E_{\frac{1}{2}}[L] - E_{\frac{1}{2}}$. Coefficient of determination = r^2, ordinate intercept = b, slope = K^I.

[d] $K^I = 0$ indicates an equilibrium constant of ≤ 10.

mental and technique errors at all L concentrations.

With an estimation of error in $E_{\frac{1}{2}}(L)$ the question of equilibrium binding constant values can be addressed. Equilibrium constants were evaluated using the assumptions $K^{II} = 0$ (Table IV) and $K^{I} = 0$ (Table V). Equation 16 was used, with $\Delta E = [E_{\frac{1}{2}}(L) - E_{\frac{1}{2}}]$,

$$e^{\Delta E(n\ /RT)} - 1 = K_f^{I,II}[L]_f \qquad (16)$$

to calculate either K^{I} or K^{II}. Each calculation included the point (0, 0) and the linearity of all the points is indicated by the coefficient of determination, r^2, and the closeness of the ordinate intercept to zero. The fit was good in most cases. In only two cases were the data better fit by removal of the assumption that K^{I} or K^{II} is equal to zero. These cases are given in Table VI with the binding constant values, calculated using equation 9. Finally, Table VII summarizes the best fit K^{I} and K^{II} values with errors (error in $E_{\frac{1}{2}}(L) = \pm 0.0025$ V).

Four-coordinate copper(I)-macrocyclic ligand complexes other than 1 were found to also bind monodentate ligands, L, to form five-coordinate adducts. Electrochemical measurements were used to study the binding of carbon monoxide and of p-$NO_2(C_6H_4)NC$ with various copper complexes. Collection and analysis of electrochemi-

Table V. Determination of Equilibrium Binding Constants, K^{II}, for 4, with Assumption, $K^{I} = 0$.[a]

Ligand, L	Solvent	Points[b]	r^2[c]	b[c]	$K^{II}(M^{-1})$[c,d]
$P(o\text{-}C_6H_4OCH_3)_3$	DMF	2			4.1×10^1
$P(o\text{-}C_6H_4CH_3)_3$	DMF	2			6.4×10^1
pyridine	acetone	7	0.9929	0.24	1.0×10^2
4-$(CH_3)_2$Npyridine	acetone	7	0.9901	28.00	1.6×10^3
$(CH_3)_2N(C_6H_5)$	acetone	2			0
4-CH_3O_2Cpyridine	acetone	6	0.9926	-0.09	2.7×10^1

[a] For the reactions: $Cu(I)mac, 1 + L \overset{K^I}{\rightleftharpoons} Cu(I)mac(L)$ and $Cu(II)mac^+, 4 + L \overset{K^{II}}{\rightleftharpoons} Cu(II)mac(L)^+$.

[b] Points = number of ΔE, [L] points used to determine K^I. This number includes (0, 0) which was used in each K^{II} calculation.

[c] Plot of $e^{\Delta E(nF/RT)} - 1$ vs. [L]; $\Delta E = E_{\frac{1}{2}} - E_{\frac{1}{2}}(L)$. Coefficient of determination = r^2, ordinate-intercept = b, slope = K^{II}.

[d] $K^{II} = 0$ indicates an equilibrium constant ≤ 10.

Table VI. Determination of Equilibrium Constants, K^{I} and K^{II}, for $\underset{\sim}{4}$[a]

Ligand, L	Solvent	Points[b]	r^2[c]	$K^{I}(M^{-1})$[c]	$K^{II}(M^{-1})$[c]
$P(O\text{-}\underline{p}\text{-}C_6H_4Cl)_3$	DMF	4	0.9977	2.5×10^{5}	2.2×10^{1}
$4\text{-}(CH_3)_2N$pyridine	acetone	6	0.9815	1.5×10^{1}	4.3×10^{3}

[a] For the reactions: $Cu(I)mac, \underset{\sim}{1} + L \overset{K^{I}}{\rightleftharpoons} Cu(I)mac(L)$ and

$Cu(II)mac^{+}, \underset{\sim}{4} + L \overset{K^{II}}{\rightleftharpoons} Cu(II)mac(L)^{+}$

[b] Points = number of ΔE, [L] points used to determine $K^{I,II}$. The point (0, 0) was not used in these calculations.

[c] Plot of $1/(e^{\Delta E(nF/RT)}-1)$ vs. $1/[L]$; $\Delta E = |E_{\frac{1}{2}}(L) - E_{\frac{1}{2}}|$. For $K^{I} > K^{II}$, ordinate-intercept = $K^{II}/(K^{I} - K^{II})$, slope = $1/(K^{I} - K^{II})$. For $K^{II} > K^{I}$, ordinate-intercept = $K^{I}/(K^{II} - K^{I})$, slope = $1/(K^{II} - K^{I})$. Coefficient of determination = r^2.

Table VII. Final Equilibrium Constants of Ligands with 4.

Ligand, L	Solvent	$K^{I}(M^{-1})^{a,b,c,f}$	$K^{II}(M^{-1})^{b,c,d,f}$
p-NC(C_6H_4)NC[e]	DMF	$1.9(4) \times 10^{7}$	0
p-NO_2(C_6H_4)NC	DMF	$1.7(2) \times 10^{7}$	0
P(O-C_6H_{11})$_3$	DMF	$1.8(2) \times 10^{6}$	0
P(O-Bu)$_3$	DMF	$8.3(8) \times 10^{5}$	0
	acetone	$5.1(5) \times 10^{6}$	0
P(O-p-C_6H_4Cl)$_3$	DMF	$2.5(3) \times 10^{5}$	$2.2(3) \times 10^{1}$
	acetone	$8.6(9) \times 10^{5}$	0
CO	DMF	$1.2(2) \times 10^{5}$	0
P(O-C_6H_5)$_3$	DMF	$1.1(2) \times 10^{5}$	0
P(O-p-$C_6H_4CH_3$)$_3$	DMF	$8.7(10) \times 10^{4}$	0
P(O-o-$C_6H_4CH_3$)$_3$	DMF	$4.9(5) \times 10^{4}$	0
P(p-C_6H_4Cl)$_3$	DMF	$3.3(4) \times 10^{4}$	0
P(p-$C_6H_4CH_3$)$_3$	DMF	$2.4(3) \times 10^{4}$	0
P(C_6H_5)$_3$	DMF	$2.1(3) \times 10^{4}$	0
	acetone	$5.6(6) \times 10^{4}$	0
P(o-$C_6H_4OCH_3$)$_3$	DMF	0	$4(6) \times 10^{1}$
P(o-$C_6H_4CH_3$)$_3$	DMF	0	$6(6) \times 10^{1}$
$(CH_3)_2N(C_6H_5)$	acetone	0	0
pyridine	acetone	0	$1.0(3) \times 10^{2}$
4-$(CH_3)_2$Npyridine	acetone	$1.5(2) \times 10^{1}$	$4.3(4) \times 10^{3}$
4-CH_3O_2Cpyridine	acetone	0	$2.7(8) \times 10^{1}$

[a] For the reaction: Cu(I)mac, 1 + L $\overset{K^{I}}{\rightleftharpoons}$ Cu(I)mac(L).

[b] $K^{I}, K^{II} = 0$ indicates an equilibrium constant ≤ 10.

[c] Bonding is assumed to have been through carbon since NC(C_6H_5) at 3×10^{-2} M did not shift the copper reduction wave in DMF.

[d] For the reaction: $Cu(II)mac^{+}$, 4 + L $\overset{K^{II}}{\rightleftharpoons}$ $Cu(II)mac(L)^{+}$.

[e] Values in parentheses represent estimated standard deviations.

[f] $K^{I, II} = 0$ indicates an equilibrium constant ≤ 10.

cal data was performed as described in detail for 4. Table VIII presents the resulting equilibrium constants for the binding of carbon monoxide to various copper(I) complexes in DMF, along with data from other sources. Table IX presents equilibrium constants found for the reaction of p-$NO_2(C_6H_4)NC$ with five copper(I) complexes in DMF. The copper (II) complexes are depicted in Figures 3 and 4.

Discussion

Methods. Previous investigations demonstrated the ability of the distorted square-planar copper(I) complex, 1, to bind monodentate ligands (CO, 1-methylimidazole, CH_3CN, pyridine, CN^-) forming five-coordinate adducts, 2, equation 1.[1-4] For carbon monoxide in acetone comparable equilibrium binding constants, K^I, equation 2, were obtained using both electrochemical ($K^I = 6.7 \times 10^4 M^{-1}$) and spectral ($K^I = 4.7 \times 10^4 M^{-1}$) techniques.[3] Spectral measurements required the isolation of pure copper(I) complex, 1, whereas the electrochemical technique utilized the copper(II) species, 4. The electrochemical method entailed, simply, measurement of the copper(II/I) reduction potential first in the absence of coordinating monodentate ligands ($E_{\frac{1}{2}}$) then with varying concentrations of ligands, ($E_{\frac{1}{2}}(L)$).

The present study has relied on electrochemical measurements

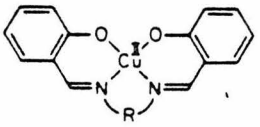

5, R = $-CH_2CH_2-$

6, R = 

7, R = $-CH_2CH_2CH_2-$

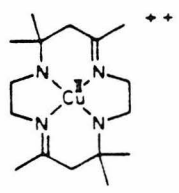

8

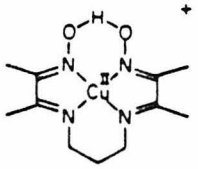

9

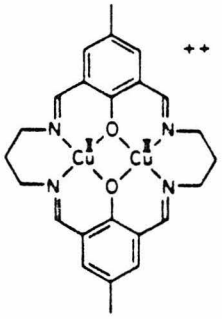

10

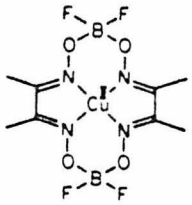

11

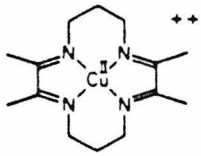

12

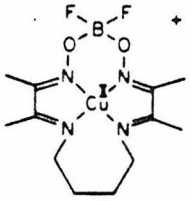

13

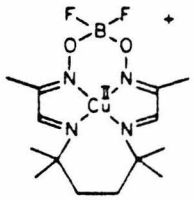

14

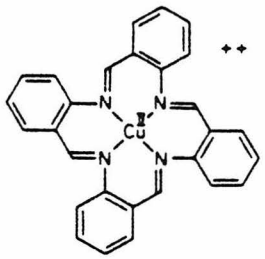

15

Table VIII. Equilibrium Binding Constants of Various Copper Complexes in DMF, for the Reaction:
$Cu(I)mac^{+n} + CO \overset{K^I}{=} Cu(I)mac(CO)^{+n}$.

Complex	$E_{\frac{1}{2}}$[a]	$K^I(M^{-1})$[b]	Reference
5	-1.303	$2.6(3) \times 10^3$	10
6	-1.191	$4.7(30) \times 10^1$	10
7	-1.099	$2.1(3) \times 10^3$	10
8	-0.656	$4.7(30) \times 10^1$	c
9	-0.614	$5.8(30) \times 10^1$	c
10	-0.517[d]	$3.1(3) \times 10^4$	12,13
4	-0.456	$1.2(2) \times 10^5$	c
11	-0.438	$8.8(9) \times 10^5$	c
12	-0.404	$4.2(30) \times 10^1$	c
13	-0.270	$1.2(2) \times 10^3$	c
14	-0.169	$5.3(5) \times 10^3$	c
15	-0.010	0	c

[a] Potentials are given in volts vs. nhe, assuming $E^f_{ferrocene} = +0.400$ V.

[b] Errors are based on an $E_{\frac{1}{2}}(L)$ error of ± 2.5 mV.

[c] This work.

[d] $E_{\frac{1}{2}}$ is for the process: $Cu(II)Cu(II)mac^{+2} + e^- \rightleftharpoons Cu(II)Cu(II)mac^+$;
K^I is for the process: $Cu(II)Cu(I)mac^+ + CO \rightleftharpoons Cu(II)Cu(I)mac(CO)^+$.

to measure equilibrium binding constants, equation 2, for a variety of complexes and monodentate ligands. The binding of eighteen different monodentate ligands, L, to the copper(II/I) redox pair, $\underset{\sim}{4}$ and $\underset{\sim}{1}$, has been studied, Table VII. Equilibrium constants have also been determined for CO and $\underline{p}$-$NO_2(C_6H_4)NC$ binding to several other copper(I)-macrocyclic ligand complexes, Tables VIII and IX.

These extensive studies manifest several advantages of electrochemically auditing metal-ligand interactions. Many copper(I) complexes are sensitive to dioxygen and many are not solution stable, disproportionating rapidly. The electrochemical technique permitted facile use of copper(II) complexes requiring only quasi-reversible redox processes and that copper(I) be stable as a transient species in the absence of dioxygen.[8] Indeed, we have been unable to isolate several copper(I) derivatives, including those of complexes $\underset{\sim}{5}$, $\underset{\sim}{6}$ and $\underset{\sim}{7}$, due to disproportionation complications, yet electrochemical measurements have resulted in estimated copper(I) equilibrium constants. The electrochemical technique was also useful, of course, when copper(II) complexes were more readily available than the copper(I) analogues. Finally, equilibrium constants for both copper(II) and copper(I) could be extracted from a single set of measurements.

The electrochemical technique also has its shortcomings. Precision was found to be limited, as indicated in Tables VII, VIII

Table IX. Equilibrium Binding Constants of Three Copper Complexes in DMF, for the Reaction:

$$Cu(I)mac^{+n} + p\text{-}NO_2(C_6H_4)NC \overset{K^I}{=} Cu(I)mac(p\text{-}NO_2(C_6H_4)NC^{+n}$$

Complex	$E_{\frac{1}{2}}$[a]	$K^I(M^{-1})$[b,c]
8	-0.656	$1.3(2) \times 10^4$
9	-0.614	$8.2(8) \times 10^3$
4	-0.456	$1.7(2) \times 10^7$
12	-0.404	$7.6(7) \times 10^4$
15	-0.010	0

[a] Potentials are given in volts vs. nhe, assuming $E^f_{ferrocene} = 0.400$ V.

[b] Errors are based on an $E_{\frac{1}{2}}(L)$ error of ± 2.5 mV.

[c] $K^I = 0$ indicates an equilibrium constant ≤ 10.

and IX, especially with small equilibrium constants ($K < 10^2\ M^{-1}$). Large equilibrium constants ($K > 10^5\ M^{-1}$) also presented problems. The mathematical analysis utilized assumed that the concentration of ligand L did not change as copper(I) was produced and reacted with L. For large equilibrium constants a more complex, iterative computation was necessary. Presumably, larger equilibrium constants would prove even more troublesome. Finally, but perhaps most limiting, the redox species involved had to exhibit at least quasi-reversible electrochemical redox processes. The electrochemical technique has probably proved adequate for these studies since only a single bond, the copper to axial ligand bond, is involved. Moreover the rate of bond making and breaking was, apparently, sufficiently rapid that equilibrium could be approached during the course of the electrochemical measurement.[8] The entire electrochemical approach to measuring equilibrium constants, as described herein, is based on the assumption that the only two equilibria occurring in solution are represented by equations 4 and 6. This assumption would probably be invalid for substitution labile copper(I) and copper(II) if non-polydentate ligand complexes were involved. Conversely, monitoring reactions which achieve equilibrium only slowly would be difficult.

Equilibrium Constants. Two salient conclusions can be drawn

from the equilibrium constants given in Tables VII, VIII, and IX. Firstly, the four-coordinate copper(I) complex, 1, can bind various monodentate ligands other than CO, forming five-coordinate adducts. Secondly, five-coordination for copper(I) appears to be not limited to adducts of complex 1 but rather is accessible from a variety of four-coordinate copper(I) species.

A more detailed inspection of the measured equilibrium constants may afford some insight into the nature of bonding in five-coordinate copper(I). It should be noted, however, that although equilibrium constants may reflect changes in the copper-ligand (L) bond strength, they are also a function of other geometrical and solvation changes which occur on adduct formation, equation 2. Direct comparison of two equilibrium constants is not invalid but the analysis of observed trends may be more meaningful.

Reactions with Complex 1. The equilibrium constants listed in Table VII suggest that the prime requirement for strong ligand binding by L to complex 1, equation 1, appears to be that L be a good π-acid. The strongest π-acids studied, substituted phenyl isonitriles, exhibit the highest equilibrium constants, $\sim 10^7$ M^{-1}. Amines, including 1-methylimidazole (1-MeIm) are regarded as poor π-acids and they have been found to bind only weakly ($K \sim 16$ M^{-1} for 1-MeIm). Pyridine and methyl isonicotinate may bind but the equilibrium con-

stants are smaller than the experimental error of the electrochemical technique ($K < 10\ M^{-1}$). Carbon monoxide and phosphites, regarded as good π-acids, have been found to exhibit equilibrium constants in the medium range, 10^4 - $10^6\ M^{-1}$, with phosphines binding more weakly ($\sim 10^4\ M^{-1}$).

The overall order of equilibrium constants suggests that complex $\underset{\sim}{1}$ binds better to π-acceptors than to σ-bases. In addition, it may be possible to discriminate between certain steric and electronic effects in binding phosphines or phosphites to the four-coordinate complex $\underset{\sim}{1}$.

Crystallographic analysis[3] of the carbonyl adduct of complex $\underset{\sim}{1}$ shows the copper displaced 0.96 Å out of the mean plane of the four coordinated nitrogen atoms. The macrocyclic ligand assumes a boat conformation with the BF_2 bridge and a methylene of the propyl bridge extending upwards towards copper and CO. Bulky ligands such as $P(\underline{o}\text{-}C_6H_4OCH_3)_3$ and $P(\underline{o}\text{-}C_6H_4CH_3)_3$ may not bind due to steric interactions with the macrocyclic ligand. By the same token, steric hindrance may account for the poorer binding of $P(O\text{-}\underline{o}\text{-}C_6H_4CH_3)_3$ <u>vs.</u> $P(O\text{-}\underline{p}\text{-}C_6H_4CH_3)_3$ and $P(\underline{o}\text{-}C_6H_4CH_3)_3$ <u>vs.</u> $P(\underline{p}\text{-}C_6H_4CH_3)_3$. In contrast, steric concerns are probably minor for <u>para</u>-substituted phenyl phosphite and phosphine ligands. For such ligands substituent effects may be primarily electronic in nature. Thus substituents which either

increase the π-acidity or decrease the σ-basicity of a ligand apparently promote larger equilibrium constants, K^{I}, for binding to complex $\underset{\sim}{1}$.[14]

The copper(II) binding constants (Table VII) follow the expected σ-base order: 4-$(CH_3)_2$N-pyridine > pyridine > 4-CH_3O_2C-pyridine. The binding of 4-$(CH_3)_2$N-pyridine to copper(II) appears to be strictly through the pyridine nitrogen since the potential ligand, $(CH_3)_2N(C_6H_5)$, did not shift the copper(II) reduction potential in acetone. The equilibrium constants correlate with para-Hammett constants, $\sigma_p^{+,-}$, for -$N(CH_3)_2$, -H, and -CO_2CH_3.[16] The plot of $\log_{10}K^{II}$ vs. $\sigma_p^{+,-}$ has a ρ factor of -0.932 and an $r^2 = 0.9991$. The negative ρ factor indicates a reaction in which electron-donating substituents increase the equilibrium constant. Weak binding to copper(II) was found for $P(O\text{-}p\text{-}C_6H_4Cl)_3$, $K^{II} = 2.2(3) \times 10^{1}\ M^{-1}$, which is insignificant relative to K^{I} [$2.5 \times 10^{5} M^{-1}$].

The overall ligand binding trends indicate that copper(II) binds better to σ-bases and copper(I) binds better to π-acceptors. Furthermore, the copper(I) binding constants measured indicate that other ligands bind to complex $\underset{\sim}{1}$, as well as carbon monoxide. If the copper-carbon bond is a covalent bond with π-character, as suggested earlier,[1-3] the copper-L bonds may have similar covalent character.

Reactions with other copper(I) complexes. The most significant

conclusion to be drawn from the measured equilibrium constants K^I for the copper(I) forms of complexes 5 to 15, Tables VIII and IX, is that a host of copper(I)-polydentate ligand complexes apparently form five-coordinate adducts. There appears to be no basis for the notion that there is some unique feature of complex 1 which promotes five-coordination for copper(I).

The complexes examined exhibit a range of reduction potentials, $E_{\frac{1}{2}}$, from -0.01 V to -1.3 V vs. nhe, Table VIII. For the most part the range and order of these reduction potentials can be explained. Patterson and Holm have shown that rigidly planar structures and oxygen ligands tend to favor copper(II).[17] Busch has demonstrated that increased ligand unsaturation favors lower oxidation states.[18] The salicylaldehyde derivatives, 5, 6 and 7, are the most difficult to reduce, presumably due to the presence of oxygen ligands and the resulting negative charge for copper(I). Complexes 8 and 10 also have relatively hard ligands but an overall positive charge, resulting in more facile reduction. Complexes 13, 14, and 15 are the easiest to reduce, probably due to the flexibility of the first two, promoting tetrahedrality, and the highly delocalized nature of the TAAB ligand in 15. The reduction potentials of complexes 4, 11 and 12 are curious. Despite a changing overall charge (from +1, to 0, to -1 on the copper(I) derivative) the observed values for $E_{\frac{1}{2}}$ are rather similar. Sterically,

complexes 4, 11 and 12 are probably comparable, all three ligands being fairly rigid, planar moieties. The invariance in $E_{\frac{1}{2}}$ for 4, 11 and 12 may be attributable to the macrocyclic ligand charge in 4 and 11 being somewhat localized on the BF_2 bridges. Complexes 4, as Cu(I), and 11, as Cu(II), are neutral overall but they may be better viewed as being zwitterionic in character. The net result is that the four nitrogen ligands in 4, 11 and 12 probably present electronically similar coordination environments.

Comparing CO equilibrium binding constants for complexes 4, 11 and 12 is especially enlightening. Having sterically and electronically comparable coordination environments, as suggested above, all three complexes might be expected to exhibit similar affinities for CO. In fact, complexes 4 and 11 gave values of K^I of the same order of magnitude ($1.2 \times 10^5 M^{-1}$ vs. $8.8 \times 10^5 M^{-1}$, Table VIII). In contrast, complex 13 gave a much smaller value of K^I ($4.2 \times 10^1 M^{-1}$). These differences in K^I may arise from the presence of BF_2 bridges in complexes 4 and 11. The molecular structures of the carbonyl adducts of 4^3 and of 11^{23} both consist of both square-pyramidyl coordination geometries with copper(I) displaced far out of the four-nitrogen plane (0.96 Å and 1.02 Å for the CO adducts of 4 and 11, respectively). In addition, both have a fluorine of the BF_2 bridges extended toward copper, approximately 3 Å distant. That complex 12 exhibits

only poor affinity for CO suggests that the BF_2 bridges in 4 and 11 may help to stabilize five-coordinate adducts by copper-fluorine interactions. Complexes 8 and 9 were examined to further test this hypothesis. As shown in Table VIII the Cu(I) forms of complexes 8 and 9 bind CO only weakly ($K^I = 4.7 \times 10^1 M^{-1}$ for 8, $5.8 \times 10^1 M^{-1}$ for 9) despite a coordination environment and overall charge type for 9 comparable to that of complex 4. Similar trends are seen on examining para-nitrophenylisonitrile equilibrium constants, Table IX. The Cu(I) form of complex 4, with a BF_2 bridge, binds p-$NO_2(C_6H_4)NC$ quite strongly ($K^I = 1.7 \times 10^7 M^{-1}$) but Cu(I) derivatives of 8, 9 and 12, with no BF_2 bridges, exhibit significantly smaller values for K^I (8.2×10^2 to $7.6 \times 10^4 M^{-1}$). Further structural studies, presently in progress, should help to further clarify the role of the BF_2 bridge in these complexes.

It is difficult to further account for variations in the measured equilibrium constants, K^I, for CO or p-$NO_2(C_6H_4)NC$ binding to the copper(I) forms of 4-15. Carbon monoxide equilibrium constants are 10^3 to $10^5 M^{-1}$ for most of the complexes studied. For these complexes variations probably reflect several factors including: a) electron density on copper(I), with high electron density promoting coordination of a π - acid ligand; b) the geometry of the four-coordinate precursor, with square-planar structures favoring five-coordination;

c) the ability of the five-coordinate complex to assume a square pyramidal configuration; and d) solvation effects as they relate to the change in coordination geometry.

Summary

The four-coordinate copper(I) complex, 1, reacts with a variety of monodentate ligands to form five-coordinate adducts. Equilibrium constants for the reaction suggest that the copper(I)-fifth ligand bond strength correlates with ligand π-acidity in the order: isonitriles > phosphites ~CO > phosphines > amines. It thus appears that metal to ligand π-backbonding may be a significant component of the copper(I)-fifth ligand bond.

In fact, a variety of four-coordinate copper(I) complexes apparently react with CO or p-$NO_2(C_6H_4)NC$ to form five-coordinate adducts. Five-coordination for copper(I) appears to be promoted by near square-planarity for the four-coordinate precursor yet sufficient ligand flexibility to permit distortion to a square-pyramidal coordination geometry. The presence of difluoroboron bridges on the periphery of certain macrocyclic ligands may further promote five-coordination via copper-fluorine interactions.

Experimental

Materials. Tetrabutylammonium perchlorate, TBAP (Southwestern Analytical Chemicals) was dried exhaustively in vacuo before use. Ferrocene was recrystallized from benzene. For electrochemical measurements DMF was dried first over $MgSO_4/CaSO_4$ then over 4A molecular sieves and vacuum distilled. Spectroquality acetone was used for electrochemical measurements without further purification. Argon was purified by passing it first over hot copper turnings then over 4A molecular sieves. Carbon monoxide was passed over activated Ridox® and molecular sieves. Complexes 4,[3] 5,[18] 6,[20] 7,[21] 8,[22] 10,[12,13] 11[23] and 15[24] were prepared by the methods given in the references listed. Compounds 4, 8 and 9 were used as the perchlorate salts. CAUTION: PERCHLORATE SALTS MAY BE EXPLOSIVE. Complex 15 was used as the nitrate salt. All complexes gave satisfactory elemental analyses.

Synthesis of (2,3,9,10-tetramethyl-1,4,8,11-tetraazacyclotetradeca-1,3,8,10-tetraene)copper(II) diperchlorate (12). To a solution of 1,3-propanediamine (9.0 g) in methanol (300 ml) was added perchloric acid (16.7 g, 60%), followed by 2,3-butanedione (8.6 g). After stirring for 30 m at the ambient temperature, Cu(II) $(CH_3CO_2)_2 \cdot H_2O$ (10.0 g) was added. The reaction was stirred for 6 hours. Perchloric acid

(21.5 ml, 60%) was added. The red-brown reaction mixture was then concentrated on a rotary evaporator to a red oil containing a light precipitate. The mixture was filtered. The filtrate was diluted with H_2O (50 ml). A saturated aqueous sodium perchlorate solution (25 ml) was added. Upon cooling to 2° C, a red microcrystalline solid was obtained. Recrystallization from acetone-ethanol gave wine red needles, which was dried in vacuo. Anal. Calcd. for $C_{14}H_{24}Cl_2CuN_4O_8$: C, 32.92; H, 4.74; N, 10.97; Cu, 12.44. Found: C, 33.0; H, 5.0; N, 11.0; Cu 12.5.

4,9-Diaza-3,10-dimethyldodeca-3,9-diene-2,11-dione dioxime, 16, the free ligand of complex 13. 1,4-Diaminobutane (8.82 g, 0.10 mole) was added to a refluxing solution of 2,3-butanedionemonoxime (20.2 g, 0.20 mole) in ethanol (75 ml). After boiling for two hours the solution was reduced in volume to about 50 ml. When the solution was allowed to cool to the ambient temperature a solid precipitated. The product was isolated by vacuum filtration, washed with ethanol and diethyl ether, and air dried. Yield of white product: 6.7 g, 26%. H NMR (d_6-DMSO) δ 1.67 (m, 2), 1.98 (s, 3), 2.08 (s, 3), 3.35 (m, 2), 11.28 (s, 1).

Complex 13. A hot solution of $Cu(ClO_4)_2 \cdot 6H_2O$ (3.7 g, 0.01 mole) in ethanol (20 ml) was slowly added to a hot solution of the free ligand, 16 (5.1 g, 0.02 mole), in ethanol (50 ml). The resul-

ting red-brown solution was heated at reflux for five minutes, then cooled to the ambient temperature. The resulting dark solid was isolated by vacuum filtration, washed with ethanol and diethyl ether, and recrystallized from a minimum volume of acetone. A boiling dioxane solution (50 ml) of the product (1.5 g, 3.6 mmole) was then treated with boron trifluoride etherate (5 ml, 0.04 mole) and kept at reflux for one hour. After cooling a light-purple solid was isolated by vacuum filtration and washed with dioxane and diethel ether. The complex was recrystallized by slowly adding dioxane to a saturated acetone solution. Anal. Calcd. for $C_{14}H_{24}BClCuF_2N_4O_5$: C, 33.09: H, 4.76: N, 11.03. Found: C, 33.2; H, 4.9; N, 11.0.

Synthesis of 4,9-Diaza-5,5,8,8,-tetramethyldodeca-3,9-diene-2,11-dionedioxine (17), the free ligand of complex 14. 2-Oximinopropanal (0.65 g), made from 2-oximinopropanal dimethyl acetal, was dissolved in ethanol (4 ml). To this was added 2,5-dimethyl-2,5-hexanediamine (0.50 g). The mixture was heated to reflux for 15 minutes. Upon cooling to 2° C, white crystals were formed. The product was isolated by filtration and washed with ether (3 ml). NMR (d_6-DMSO) δ 1.10 (s, 6), 1.38 (s, 2), 1.89 (s, 3), 7.76 (s, 1), 11.50 (br, 1).

Synthesis of 14. To a warm solution of 17 (0.47 g) in ethanol (4 ml) was added a warm solution of Cu(II) $(ClO_4)_2 \cdot 6H_2O$ (0.41 g) in

ethanol (4 ml). The reaction was heated gently for 15 minutes. Upon cooling to the ambient temperature, a green solid was obtained. The product was recrystallized from acetone. Anal. Calcd. for $C_{14}H_{25}ClCuN_4O_6$: C, 37.84; H, 5.67; N, 12.61; Cu, 14.30. Found: C, 38.1; H, 5.6; N, 12.5; Cu, 14.4.

In dioxane (10 ml), the complex above (0.31 g) was stirred with $BF_3 \cdot Et_2O$ (1.5 ml). The mixture was then heated to reflux for 30 minutes. The reaction was cooled to the ambient temperature. The product was isolated by filtration and washed with dioxane and ether. Recrystallization was performed in acetone-ethanol to give a blue microcrystalline solid, which was dried in vacuo. Anal. Calcd. for $C_{14}H_{24}BClCuF_2N_4O_6$: C, 34.16; H, 4.91; N, 11.38; Cu, 12.91. Found: C, 34.4; H, 4.9; N, 11.4; Cu, 13.4.

Electrochemistry. A Princeton Applied Research Model 174 polarographic analyzer was used for sampled dc polarography and for cyclic voltammetry. Data were recorded on a Hewlett-Packard Model 7004B X-Y recorder. A simple H-type electrochemical cell was used. The two compartments of the cell were separated by a medium porosity sintered glass frit. The main working compartment had a three-way stopcock arrangement on a gas inlet tube, permitting gas to be bubbled up through the solution or to simply flow above the working solution. A second stopcock at the base of the working com-

partment allowed the working solution to be easily changed. A dropping mercury electrode (PAR Model 9346) served as the working electrode and a platinum wire coiled around the mercury capillary served as the counter electrode. A Ag/Ag^+ reference electrode was placed in the second compartment of the cell. The reference electrode consisted of a silver wire immersed in an acetonitrile solution of $AgNO_3$ (0.01 M) and TBAP (0.1 M), all contained in an 8 mm glass tube fitted on the bottom with a fine porosity sintered glass frit. The silver wire was threaded through a serum cap fitted snugly over the top of the 8 mm tube.

Polarographic analyses were performed with acetone or DMF solutions containing TBAP (0.1 M) as supporting electrolyte. The working compartment also contained a copper(II) sample (0.5 mM), ferrocene (1.0 mM) and some monodentate ligand, L (zero to several mM). In practice, working solutions were prepared in an inert atmosphere chamber (Vacuum Atmospheres, Inc.; filled with helium) from stock solutions of copper(II) and ferrocene. Volumetric additions of ligand were then made.

The procedure for obtaining sampled dc polarograms began and ended with a mercury flow rate measurement. Mercury flowing from the capillary into a solvent was collected with the drop knocker set at drop time of 5 s. (All polarograms were run with t = 5 s.) The

time over which mercury was collected was recorded. The flow rate, m, was calculated in mg s^{-1}. The copper(II) sample was then purged with argon for twenty minutes. The cyclic voltammogram of ferrocene was measured with a platinum disc electrode with the platinum counter electrode coiled around it. The sampled dc polarogram was run at 0.5 mV s^{-1} and the ambient temperature recorded (22° ± 1° C).

The half-wave potential of the sample, $E_{\frac{1}{2}}$, was determined from an E vs. $\ln[i/(i_d-i)]$ plot. The linear regression of the plot was calculated by use of a program written for a Hewlett-Packard Model 25 programmable calculator. The intercept of the plots gave $E_{\frac{1}{2}}$ vs. Ag/Ag^+, with the slope being theoretically equal to -RT/nF.

Instead of attempting to correct potentials measured against the Ag/Ag^+ reference electrode, ferrocene served as an internal reference redox couple. It has been proposed that the oxidation of ferrocene to ferrocenium ion occurs naer the same potential in most solvents.[25] In water the process occurs at +0.400 V vs. nhe.[26] Measuring both $E^f_{ferrocene}$ and $E_{\frac{1}{2}}$[Cu(II/I)] under the same conditions permitted a better estimate of potentials vs. nhe because unknown junction potentials associated with the Ag/Ag^+ could be ignored. Half-wave potentials for samples, $E_{\frac{1}{2}}$, were determined vs. Ag/Ag^+ as described above then corrected using the measured

$E^{f}_{ferrocene}$ and a value of 0.400 V vs. nhe for ferrocene, i.e., $E_{\frac{1}{2}}(nhe) = E_{\frac{1}{2}}(Ag/Ag^{+}) - [E^{f}_{ferrocene} + 0.400\ V]$. All potentials are reported vs. the nhe, using this correction.

Measurements of carbon monoxide binding were performed with DMF solutions saturated with CO at one atmosphere pressure. At this pressure the concentration of CO in solution was taken to be 4.64 mM.[27]

Acknowledgments: We appreciate the assistance of and helpful discussions with Carl A. Koval. Financial support for this research was provided by the National Institutes of Health Grant No. PHS 4 AM18319B-04.

References and Notes

(1) Gagné, R. R; Allison, J. L.; Lisensky, G. C. Inorg. Chem. 1978, 12, 3563.

(2) Gagné, R. R. J. Am. Chem. Soc. 1976, 98, 6709.

(3) Gagné, R. R.; Allison, J. L.; Gall, R. S.; Koval, C. A. J. Am. Chem. Soc. 1977, 99, 7170.

(4) Addison, A. W.; Carpenter, M.; Lau, L. K.-M.; Wicholas, M. Inorg. Chem. 1978, 17, 1545.

(5) Allison, J. L. Ph.D. Thesis, California Institute of Technology, 1979.

(6) Laitinen, H. A. "Chemical Analysis;" McGraw-Hill: New York; 1960, p. 286

(7) Heyrovsky, J.; Kuta, J. "Principles of Polarography," Academic Press: New York; 1966.

(8) The use of shifts in $E_{\frac{1}{2}}$ to calculate equilibrium constants relies on the assumption of chemical and electrochemical reversibility. Since all of the copper complex data in this paper were obtained using dc polarography the only criterion for reversibility was that plots of E vs. $\ln[i/(i_d-i)]$ have slopes of -RT/nF, i.e., 58.6 mV at 22° C for Cu(II/I). It should be noted that previous cyclic voltammetric studies also indicated chemical reversibility for the reaction of 1 and 4 with CO and with 1-methylimidazole.[3] Complex 4 shows

both reduction and oxidation cyclic voltammetric waves whether measured under argon or under CO. Under CO the oxidation peak is distorted, however, which has been interpreted as possibly indicating a slow rate of CO dissociation.[3] The slower technique of sampled dc polarography was utilized to overcome the limitation of cyclic voltammetry.

(9) Schiavon, G.; Zecchin, S.; Cogoni, G.; Bontempelli, G. J. Electroanal. Chem. Interfacial Electrochem. 1973, 48, 425.

(10) Gagné, R. R.; Koval, C. A.; Kober, E. unpublished results. See also Ref. 11.

(11) Koval, C. A. Ph. D. Thesis, California Institute of Technology, 1979.

(12) Gagné, R. R.; Koval, C. A.; Smith, T. J. J. Am. Chem. Soc. 1977, 99, 8367.

(13) Gagné, R. R.; Koval, C. A.; Smith, T. J,; Cimolino, M. J. Am. Chem. Soc. 1979, 101, 0000.

(14) Tolman has defined both a steric factor, the "ligand cone angle," and an electronic factor, the donor-acceptor parameter, for many of these phosphines and phosphites.[15] Ligands with large ($\geq$165°) cone angles, i.e., bulky ligands, exhibit a marked suppression of their binding constants. Ligands with small cone angles, where steric forces are small, show a direct correlation, within

experimental error, between donor-acceptor parameters and the equilibrium constants, K^I, for binding these ligands to complex 1.

(15) (a) Tolman, C. A. J. Am. Chem. Soc. 1970, 92, 2953.

(b) Tolman, C. A. J. Am. Chem. Soc. 1970, 92, 2956.

(16) Gordon, A. J.; Ford, R. A. "The Chemist's Companion"; John Wiley: New York; pp. 144-155.

(17) Patterson, G. S.; Holm, R. H. Bioinorg. Chem. 1975, 4, 257.

(18) Busch, D. H., Pillsbury, D. G.; Lovecchio, F. V.; Tait, A. M.; Hung, Y.; Jackels, S.; Rakowski, M. C.; Schammel, W. P.; Martin, L. Y. "American Chemical Society Symposium Series"; American Chemical Society: Washington, D. C.; Vol. 38, 1976, p. 32.

(19) Pfeiffer, P.; Breith, E.; Lübble, E.; Tsumaki, T. Ann. Chim. 1933, 503, 84.

(20) O'Connor, M. J.; Ernst, R. E.; Holm, R. H. J. Am. Chem. Soc. 1968, 90, 4561.

(21) Lions, F.; Martin, K. V. ibid., 1957, 79, 1273.

(22) Olson, D. C.; Vasilevskis, J. Inorg. Chem. 1971, 10, 463.

(23) Prepared as for 4; Gagné, R. R.; Ingle, D. M.; Kreh, R. P.; McCool, M.; Marsh, R. E., manuscript submitted for publication.

(24) Melson, G. A.; Busch, D. H. J. Am. Chem. Soc. 1964, 86, 4834.

(25) Bauer, D.; Breant, M. "Electroanalytical Chemistry", Bard, A. J., Ed.; Marcel Dekker, Inc.: New York, 1975; Vol. 8, pp. 282-344.

(26) Koepp, H. M.; Wendt, H.; Strehlow, H. Zeit. Electrochem. 1960, 64, 483.

(27) "Properties and Uses of Dimethylformamide"; du Pont, Industrial Chemicals Dept.: Wilmington, 1976.

Appendix II

An Approach to the Synthesis of Binuclear Metal Complexes

Appendix II

An Approach to the Synthesis of Binuclear Metal Complexes

Interest in binuclear metal complexes and metal clusters has led to the synthesis of "face-to-face" metalloporphyrins.[1-4] Collman and co-workers have recently reported an apparent example of four-electron reduction of dioxygen to water catalyzed by a cobalt "face-to-face" porphyrin. Studies of other "face-to-face" complexes containing transition metals built around macrocyclic ligands are a viable path for future research. The synthetic routes to "face-to-face" porphyrins are long, tedious, and low in overall yields—inviting alternatives which are synthetically simpler, but with similar structures and reactivities. Our interest in macrocyclic Schiff-base complexes containing bridging difluoroborate groups suggested such an alternative. The reactivity similarities between these Schiff-base complexes and metalloporphyrins are well established.[6-9] Here we present a general scheme for the synthesis and use of a moiety to bridge two macrocyclic complexes together.

The ultimate goal here is to form "face-to-face" complexes

analogous to those porphyrin complexes made by Collman.[1] To test the feasibility of the method, binuclear complexes of the type shown in Figure I were made. While complexes of this type are expected to exhibit a variety of conformations, they will serve to demonstrate the effectiveness of the bridging moiety. Any reactivity substantially different in these dimer complexes than the reactivity of their mononuclear analogues is expected to arise from the entropic "high concentration" effect of having two metal centers always in close proximity.

The bridging moiety used here is 1,4-bis(difluoroboryl)butane; this was chosen because models of the "face-to-face" complexes indicated a "substrate cavity" between the two metals should accomodate diatomic molecules, whose chemical activation is sought. Bridging moieties containing from one to six carbons may be synthesized by analogous methods.[10-12] The route by which 1,4-bis(difluoroboryl)butane was synthesized is shown in Figure II.

Experimentally, these reactions are routine with the exception that all are air sensitive and pyrophoric. However, 1,4-bis(difluoroboryl)butane is quite volatile, allowing for convenient manipulation by conventional high vacuum techniques.

Complex $\underset{\frown}{1}$ was synthesized by a method analogous to the synthesis of its monomeric counterpart, complex $\underset{\frown}{2}$ (see Figure III).

Figure I

Synthesis of Singly-bridged Dimer Complexes

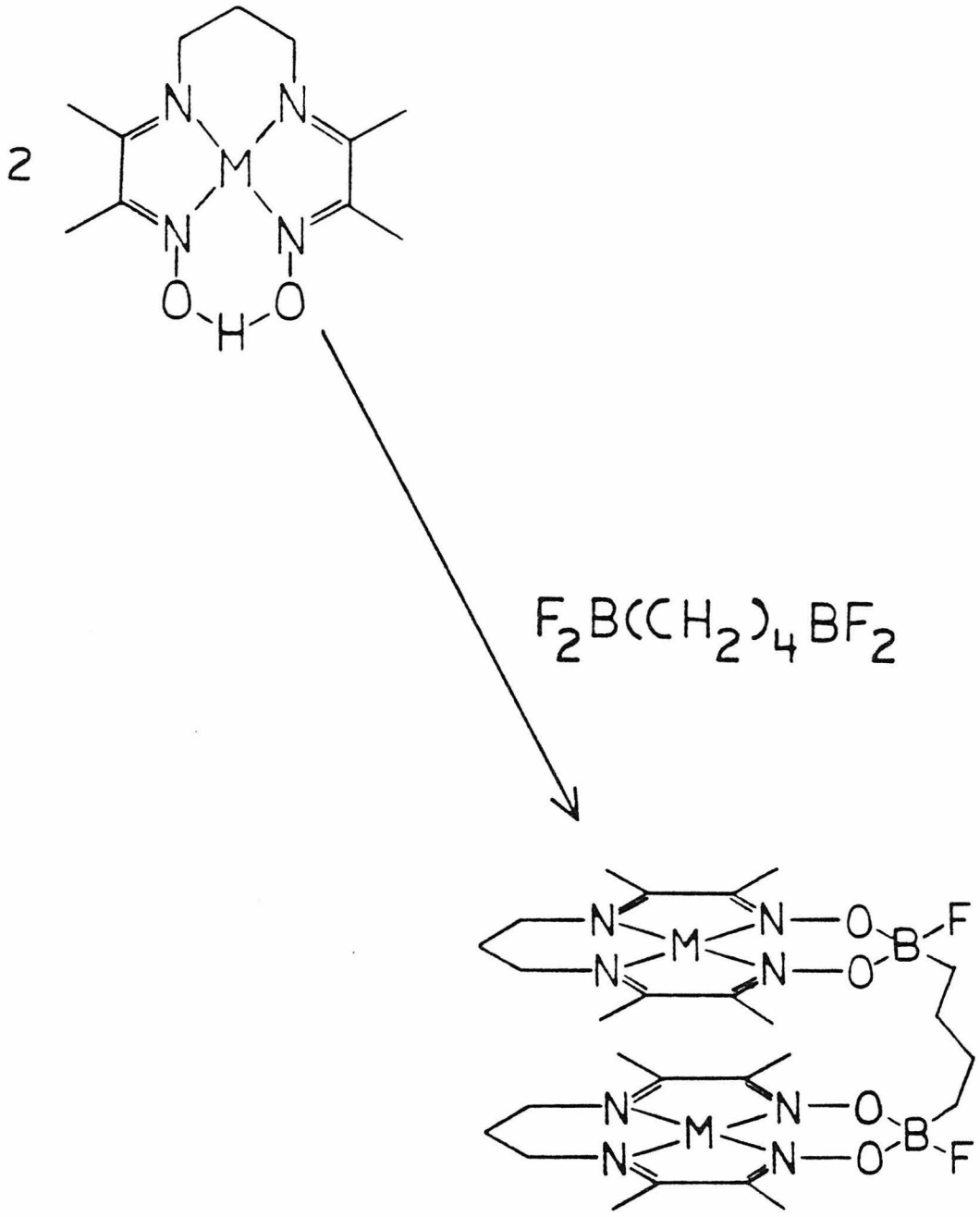

Figure I

Figure II

Synthetic Route to 1,4-Bis(difluoroboryl)butane

a) Synthesis of 1,4-Di-1-borolanylbutane

b) Synthesis of Tetrabutyldiborane

c) Synthesis of 1,4-Bis(dichloroboryl)butane

d) Synthesis of 1,4-Bis(difluoroboryl)butane

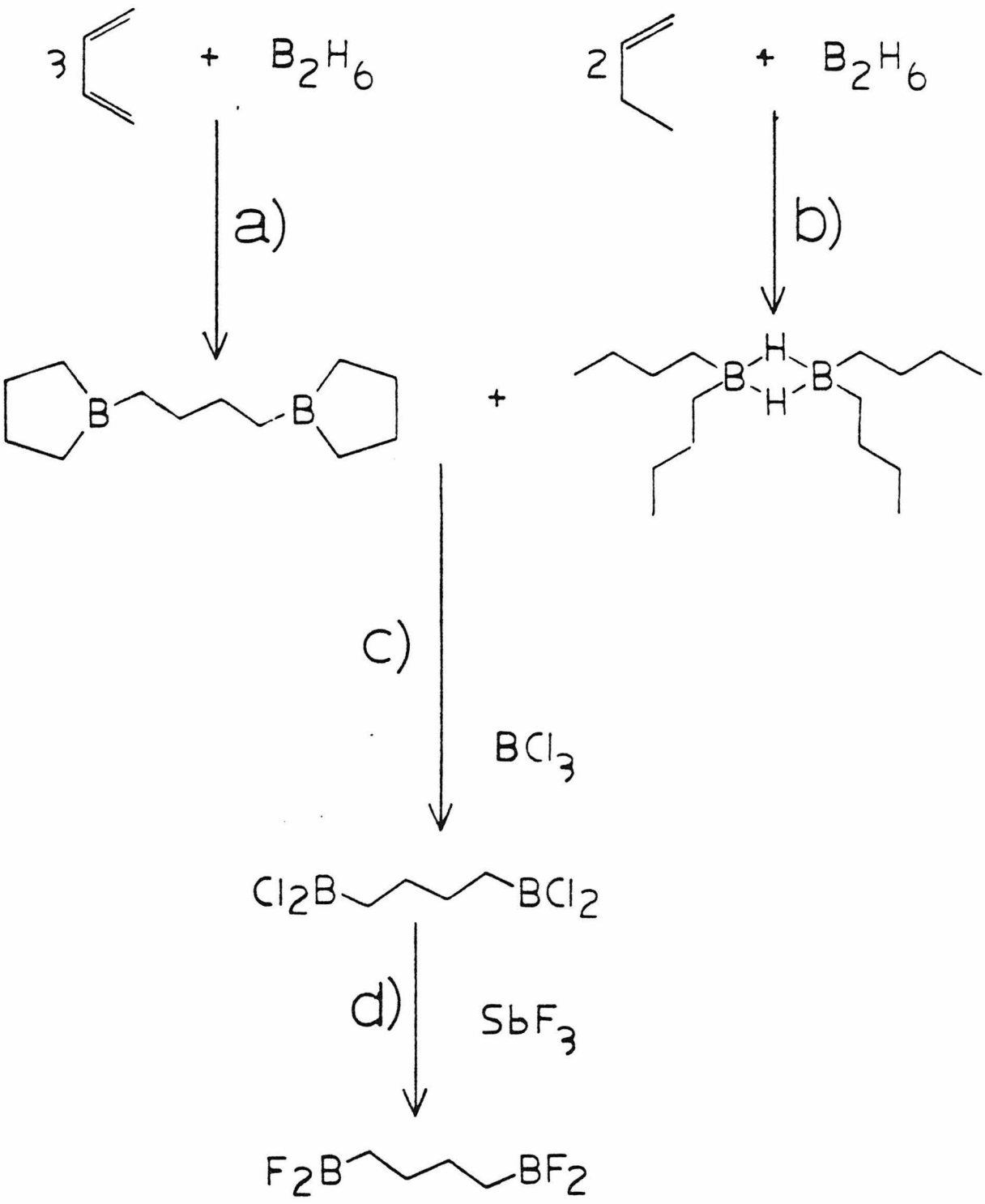

Figure II

Figure III

Skeletal Representation for Dimer Complex 1

and Monomer Complex 2

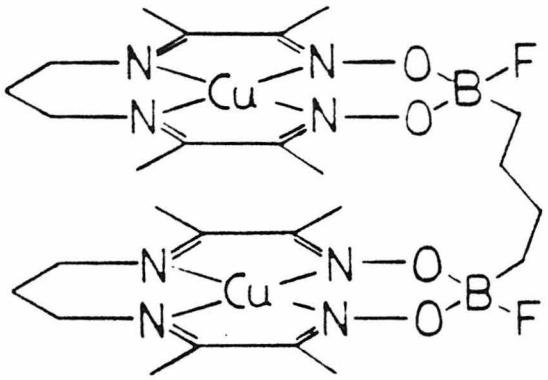

1

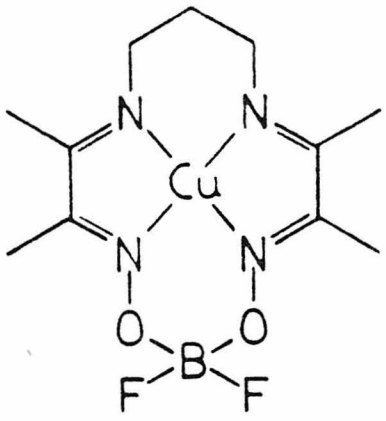

2

Figure III

As to the synthetic ease, complex $\underset{\sim}{1}$ was formed in near-quantitative yield. It is interesting to compare complexes $\underset{\sim}{1}$ and $\underset{\sim}{2}$ in the solid state. The magnetic susceptibility for $\underset{\sim}{1}$ is 1.50 B.M. per copper and 1.85 B.M. per copper for $\underset{\sim}{2}$ at 295 K. The EPR spectrum of $\underset{\sim}{1}$ at 20 K exhibits a triplet Cu(II) dimer spectrum with a weak "half-field" transition (Figure IV). On the basis of a dipolar mechanism, a Cu-Cu distance of near 6 Å is estimated.[13,14] Complex $\underset{\sim}{2}$ shows a normal Cu(II) monomer EPR spectrum. It is, of course, not known whether this interaction in $\underset{\sim}{1}$ is intermolecular or intramolecular, but 6.5 Å is the distance measured for the metal-metal separation from CPK Molecular Models for the "face-to-face" conformation shown in Figure III.

In solution, however, $\underset{\sim}{1}$ and $\underset{\sim}{2}$ are nearly indistinguishable as to their EPR spectra and electrochemical properties (as is expected for the highly non-rigid complex $\underset{\sim}{1}$).

Another complex, $\underset{\sim}{3}$ (shown in Figure V), was synthesized to confirm the identity of the 1,4-bis(difluoroboryl)butane, which eluded analysis due to its extreme reactivity and pyrophoric nature. The NMR spectrum was used to confirm the integrity of the bridging tetramethylene group (in addition to elemental analysis). Complex $\underset{\sim}{3}$ exhibited the expected NMR spectrum(see Experimental). All other physical and chemical properties were also as expected.

Figure IV

Powder EPR Spectrum of 1 at 20 K

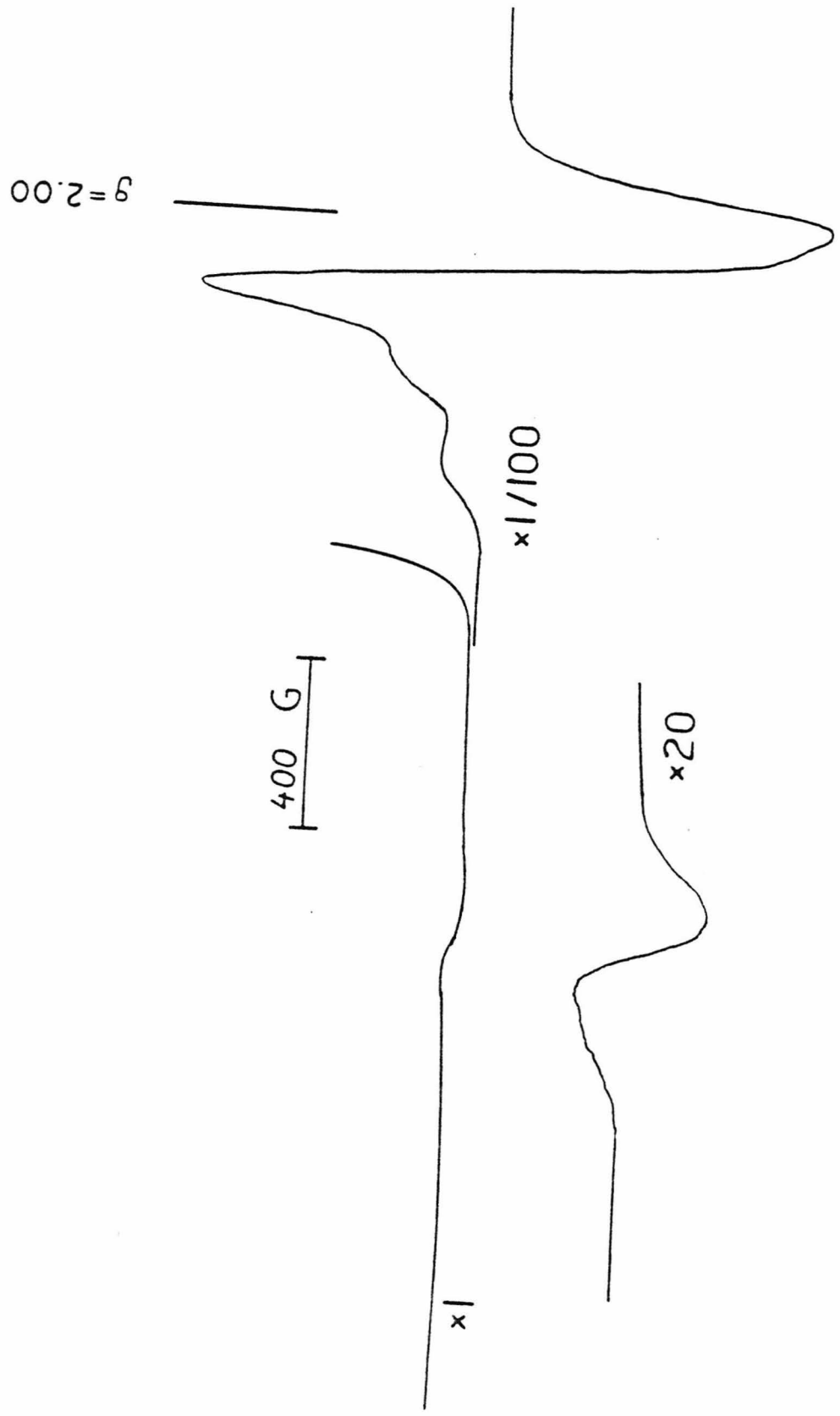

Figure IV

Figure V

Skeletal Representation for Complex 3

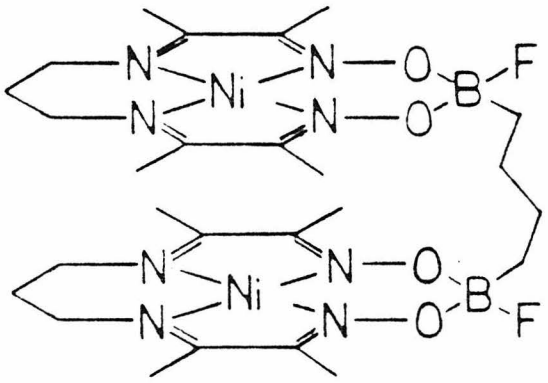

Figure V

The goal of synthesizing "face-to-face" complexes relies on the ability to bring all of the reagents together with the appropriate relative orientations (Figure VI). One short-coming of this approach is the low yield of "face-to-face" product expected on a statistical basis. However, since the reagents are easily made in a small number of steps, low yields are offset by the potentially large scale on which these reactions may be done. The rigidity of these "face-to-face" complexes affords an attractive space between metal centers for "substrate binding."

Attempts to synthesize a "face-to-face" complex were made under high dilution conditions (see Experimental). A small fraction of a dark brown solid, whose IR was consistent with the proposed structure, $\underset{\sim}{4}$ (Figure VII), was isolated. The EPR spectrum in frozen acetonitrile solution at 20 K (Figures VII and VIII) exhibited a very small splitting of the $g_{\perp}$-line, indicative of a long-range dipole-dipole interaction; no "half-field" transition was observed.[15]

This method may afford new binuclear complexes of interest to catalysis that could be complementary to those of the porphyrin system.

Figure VI

Synthesis of "Face-to-face" Dimer Complex

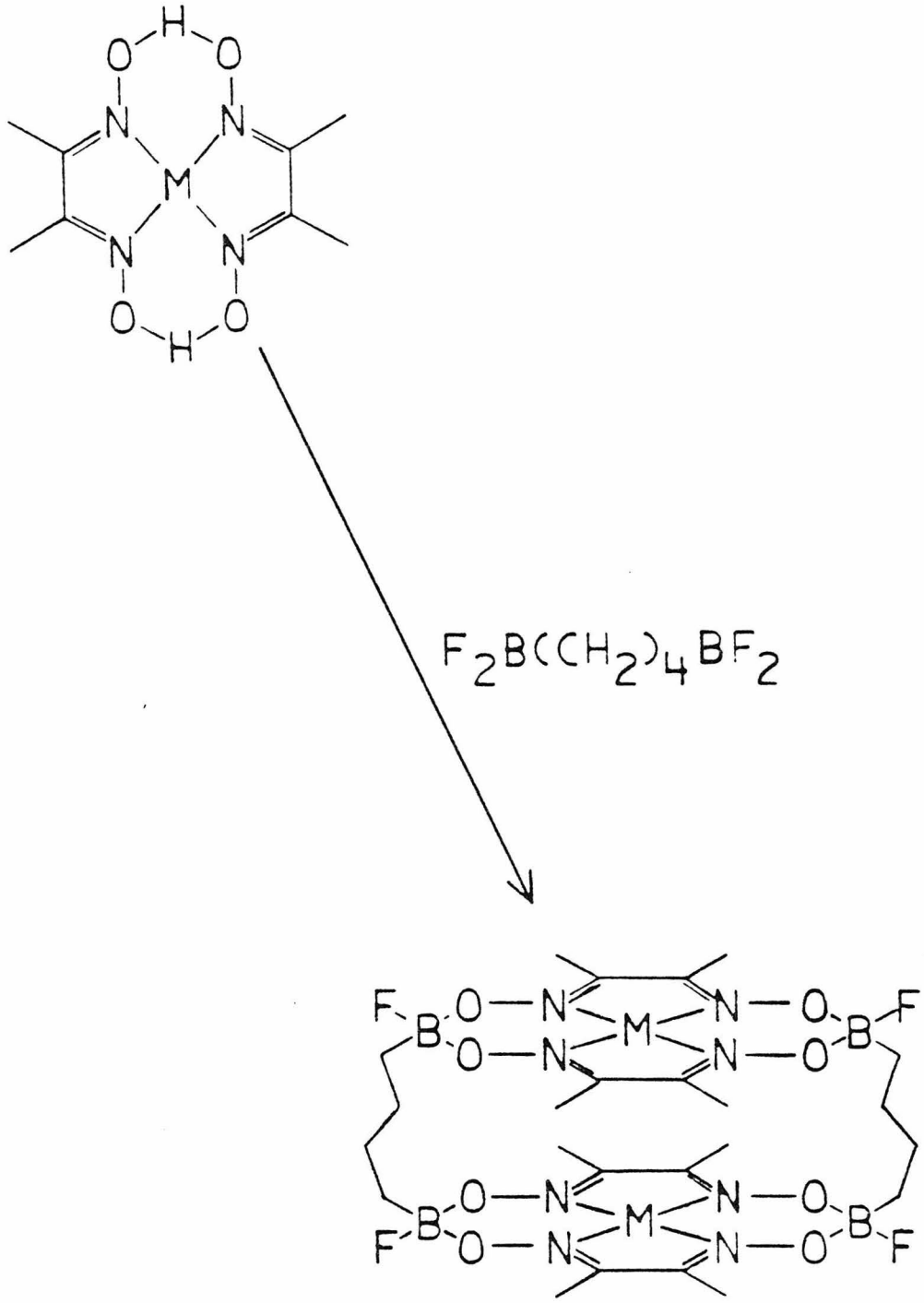

Figure VI

Figures VII and VII

EPR Spectrum of Frozen Acetonitrile

Solution of the High Dilution Reaction Product

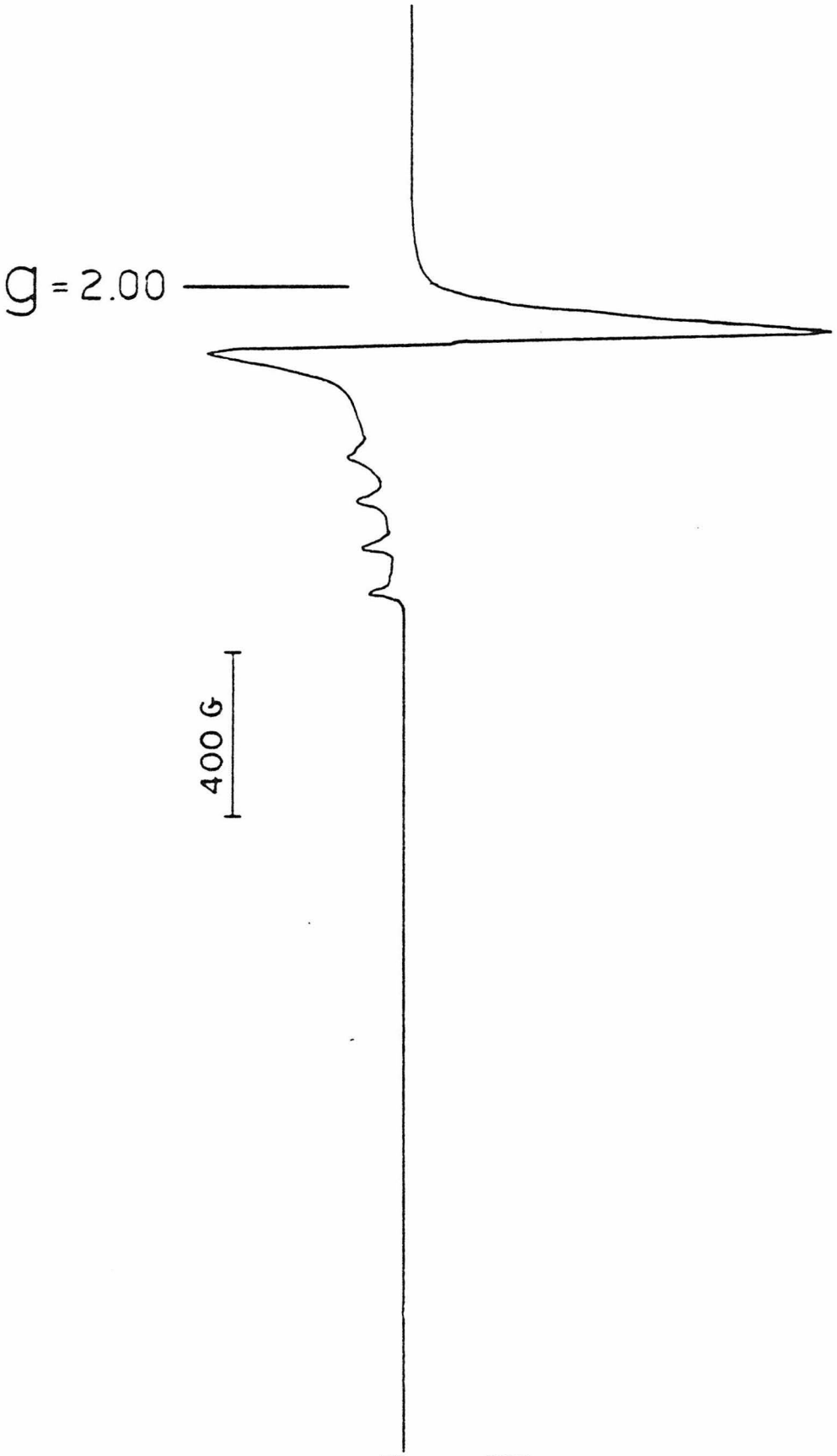

Figure VII

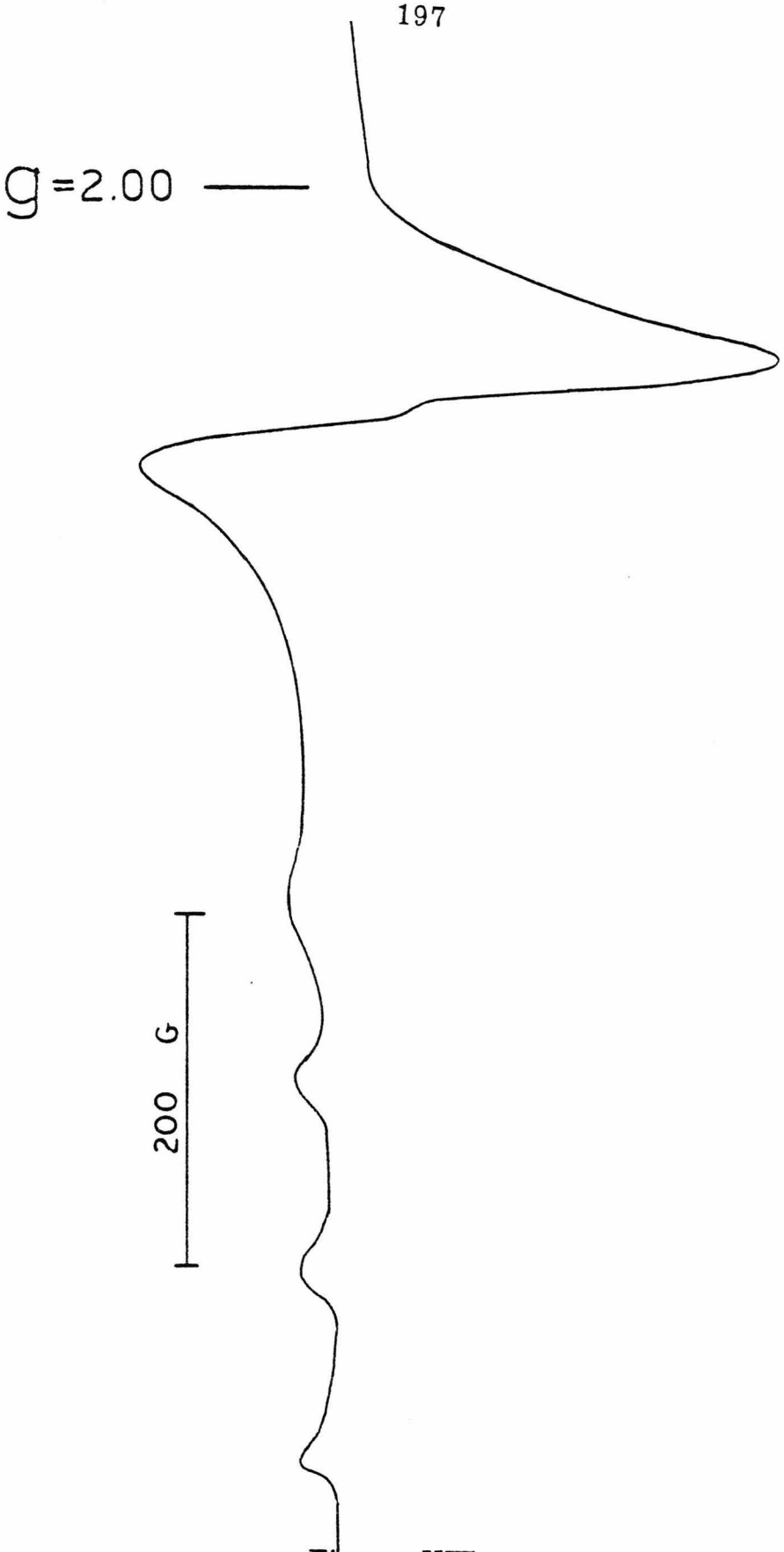

Figure VIII

Experimental

All chemicals used were reagent grade. Reactions involving boranes were all done under an inert atmosphere. The boranes are extremely pyrophoric and are to be handled with respect. Magnetic susceptibilities were determined by the Faraday method. EPR spectra were obtained on an E-line (X-band) Varian spectrometer. Electrochemical measurements were done using a Princeton Applied Research 174A Polarographic Analyzer as described elsewhere.[16] NMR spectra were obtained on a Varion EM-390 spectrometer.

Synthesis of Tetrabutyldiborane. The synthesis was carried out as described by Mikhailov, Akhnazaryan, and Vasil'ev.[17] Through a solution of 1-butene (21 g) in dry diethyl ether (100 ml) at -30° C under a nitrogen atmosphere, was passed over a 4 h period diborane (0.075 mole; made by adding boron trifluoride etherate (36 g) in diglyme (50 ml) to a slurry of sodium borohydride (8.0 g) in diglyme (75 ml)) in a stream of nitrogen. After warming to the ambient temperature overnight, the ether was carefully removed under vacuum. The product was collected by distillation (b.p. 53-58 °C; 0.3 torr). The pyrophoric product was stored under nitrogen.

Synthesis of 1,4-Di-1-borolanylbutane. The synthesis was carried out as described by Zakharkin and Kovredov.[12] A 250 ml three-necked round-bottomed flask was equipped with a stir bar, two gas inlet bubblers, and a dry ice condenser fitted with a mercury and acetone exit bubbler. Diethyl ether (100 ml) was placed in the flask. Simultaneously, 1,3-butadiene and diborane (method described above) in a nitrogen stream were bubbled through the ether. The mixture was stirred under nitrogen overnight. The ether was removed under vacuum. The product was isolated by distillation (b.p. 74-78 °C; 0.3 torr). The pyrophoric product was stored under nitrogen.

Synthesis of 1,4-Bis(dichloroboryl)butane. The synthesis was carried out as described by Kovredov and Zakharkin.[12] Under nitrogen, to 1,4-di-1-borolanylbutane (12 g) was added tetrabutyldiborane (0.75 ml) in a 50 ml three-necked round-bottomed flask equipped with a gas inlet bubbler and dry ice condenser fitted with a mineral oil exit bubbler. Note: at this point the reaction mixture was extremely pyrophoric. The mixture was heated to 100 °C. Excess boron trichloride (36 g) was passed through the bubbler submerged in the liquid over a 2 h period. The mixture was then heated to 140 °C for 3 h. The reaction was cooled to the ambient temperature. The product was carefully distilled (b.p. 48-53 °C; 0.3 torr).

The extremely pyrophoric product was stored under nitrogen.

Synthesis of 1,4-Bis(difluoroboryl)butane. This synthesis was carried out using a vacuum line. Under a static vacuum, 1,4-bis-(dichloroboryl)butane (10 g) was carefully added to an excess of antimony trifluoride (10.6 g).[18] Cautiously, the mixture was heated while stirring. A vigorous exothermic reaction ensued. The volatile product was collected by trap-to-trap distillation. The 1,4-bis(difluoroboryl)butane was stored in vacuo until use. The vapor pressure measured at 25°C was 28 torr.

Synthesis of 1 · 4 Dioxane. [3,3'-(Trimethylenedinitrilo) bis(2-butanone oximato)] copper(II) perchlorate monohydrate[19] (1.0 g) was dried in vacuo at the ambient temperature for 5 h. Dioxane (15 ml; distilled in vacuo from sodium-benzophenone) was distilled trap-to-trap onto the complex. 1,4-Bis(difluoroboryl)butane (0.16 ml) was then distilled trap-to-trap into the reaction vessel at 80 K. The mixture was warmed to the ambient temperature and stirred overnight. The reaction was filtered in air. The precipitate was recrystallized from an acetone-dioxane mixture to give a blue-purple microcrystalline solid. Anal. Calcd. for $C_{42}H_{76}Cl_2Cu_2F_2N_8O_{20}$: C, 39.60; H, 6.04; N, 8.81; Cu, 10.02. Found: C, 39.7; H, 6.0; N, 8.8; Cu, 10.4.

Synthesis of 3. [3,3'-(Trimethylenedinitrilo)bis(2-butanone oximato)] nickel (II) perchlorate[20] (1.0 g) was dried in vacuo 2 h at the ambient temperature. Dioxane (15 ml; distilled in vacuo from sodium-benzophenone) was distilled trap-to-trap onto the complex. 1,4-Bis(difluoroboryl)butane (0.16 ml) was then distilled trap-to-trap into the reaction flask at 80 K. The mixture was warmed to the ambient temperature and stirred overnight. The product was collected in air by filtration. Recrystallization from an acetone-ethanol mixture gave a yellow solid. NMR (d_6-DMSO) δ 0.36 (m,1), 1.13 (m,1), 2.12 (s,3), 2.26 (s,3), 2.52 (m,1), 3.28 (m,2). Anal. Calcd. for $C_{26}H_{44}B_2Cl_2F_2N_8Ni_2O_{12}$: C, 34.37; H, 4.88; N, 12.33; Ni, 12.92. Found: C, 34.5; H, 4.8; N, 12.2; Ni, 12.5.

High dilution reaction between bis(dimethylglyoxime) copper(II) and 1,4-bis(difluoroboryl)butane: Attempted synthesis of 4. Under an inert atmosphere, using carefully degassed solvents, a solution of 1,4-bis(difluoroboryl)butane (0.17 ml) in acetonitrile (700 ml) and a suspension of bis(dimethylglyoxime) copper (II)[21] (0.40 g) in acetonitrile (700 ml) were added simultaneously over a 4 h period, with stirring, to a flask of acetonitrile (1200 ml). The reaction was stirred overnight. The solvent was distilled off of the reaction mixture in the air. The dark product was triturated with hot acetonitrile. The soluble portion was twice recrystallized from aceto-

nitrile. The dark brown solid gave an infrared consistent with the structure, but not inconsistent with an oligomer. The EPR spectrum in acetonitrile is illustrated in Figures VII and VIII.[15]

References and Notes

(1) Collman, J. P.; Elliott, C. M.; Halbert, T. R.; Tovrog, B. S. Proc. Natl. Acad. Sci. USA 1977, 74, 18.

(2) Chang, C. K.; Kuo, M. S.; Wang, C. B. J. Heterocyclic Chem. 1977, 14, 943.

(3) Chang, C. K. J. Heterocyclic Chem. 1977, 14, 1285.

(4) Wasielewski, M. R.; Svec, W. A.; Cope, B. T. J. Am. Chem. Soc. 1978, 100, 1961.

(5) Morroco, M.; Denisovich, P.; Koval, C.; Collman, J. P.; Anson, F. C. submitted for publication.

(6) (a) Morpurgo, G. O.; Mosini, V. J. Chem. Soc. Dalton 1974, 2333.

(b) Brown, G. M.; Hopf, F. R.; Meyer, T. J.; Whitten, D. G. J. Am. Chem. Soc. 1975, 97, 5385.

(7) (a) Green, M.; Tauzher, G. Transition Met. Chem. 1975, 1, 1.

(b) Walker, F. A. J. Am. Chem. Soc. 1970, 92, 4235.

(8) (a) Costa, G.; Mestroni, G.; de Savorgnani, E. Inorg. Chim. Acta 1969, 3, 323.

(b) Walker, F. A.; Bezioz, D.; Kadish, K. M. J. Am. Chem. Soc. 1976, 98, 3484.

(9) (a) Lovecchio, F. V.; Gore, E. S.; Busch, D. H. J. Am. Chem. Soc. 1974, 96, 3109.

(b) Felton, R. H.; Linschitz, H. J. Am. Chem. Soc. 1966, 88, 1113.

(10) Zakharkin, L. I.; Kovredov,A. I. Izv. Akad. Nauk SSSR, Ser. Khim. 1964, 2, 393.

(11) Zakharkin, L. I.; Kovredov, A. I. Izv. Akad. Nauk SSSR, Otd. Khim. Nauk 1962, 9, 1564.

(12) Kovredov, A. I.; Zakharkin, L. I. Izv. Akad. Nauk SSSR, Ser. Khim. 1964, 1, 50.

(13) Chasteen, N. D.; Belford, R. L. Inorg. Chem. 1970, 9, 169.

(14) Boas, J. F.; Dunhill, R. H.; Pillbrow, J. R.; Srivastava, R. C.; Smith, T. D. J. Chem. Soc. (A) 1969, 94.

(15) Anal. Calcd. for $C_{24}H_{40}B_4Cu_2F_4N_8O_8$: C, 35.37; H, 4.95; N, 13.75. Found: C, 35.6; H, 4.8; N, 5.3.

(16) Gagné, R. R.; Allison, J. L.; Ingle, D. M. Inorg. Chem. 1979, 18, 0000.

(17) Mikhailov, B. M.; Aknazarayan, A. A.; Vasil'ev, L. S. Dokl. Akad. Nauk SSSR 1961, 136, 828.

(18) Finch, A.; Schlessinger, H. I. J. Am. Chem. Soc. 1958, 80, 3573.

(19) Gagné, R. R.; Allison, J. L.; Gall, P. S.; Koval, C. A. J. Am. Chem. Soc. 1977, 99, 7170.

(20) Uhlig, V. E.; Friederich, M. Z. anorg. allg. Chem. 1966, 343, 299.

(21) Frasson, E.; Bardi, R.; Bezzi, S. Acta Cryst. 1959, 12, 201.

Propositions

Proposition 1

Within the past few years, several reports of "face-to-face" or "cofacial" diporphyrins have appeared in the chemical literature.[1-4] Recently, Collman, Anson, and coworkers[5] have reported the electrochemical reduction of dioxygen to water without the production of hydrogen peroxide catalyzed by "face-to-face" dicobalt diporphyrins. Cofacial dimetallodiporphyrins whose rings are "polarized" by appropriate substituents might have some very interesting properties. Cram and coworkers[6] have studied a somewhat analogous organic system, [2.2]-paracyclophanes, that demonstrates this point. In [2.2]-para-

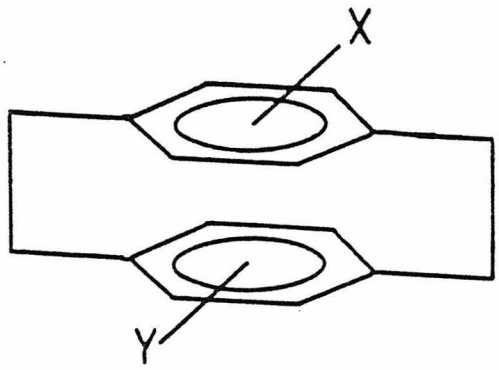

[2.2]-PARACYCLOPHANE

cyclophane, two benzenes are held in close proximity in a cofacial sense by side chains much like in cofacial diporphyrins; if the rings are appropriately substituted with electronegative and electropositive groups (for example, X = NO_2 and Y = NH_2) moderate intensity intramolecular charge transfer visible bands are observed that are not seen in the spectrum of a mixture of monomers (nitrobenzene and aniline). Chang[3] has reported an effect in cofacial (non-polarized) diporphyrins of having the two parallel rings in close proximity; the Soret band is blue shifted, while the visible bands are red shifted. These two porphyrin rings are obviously interacting. Can this interaction be increased by polarizing the complex?

One can envision interligand intramolecular charge transfer in cofacial diporphyrin complexes that decay into transient mixed valence complexes that might have unusual properties. These transient

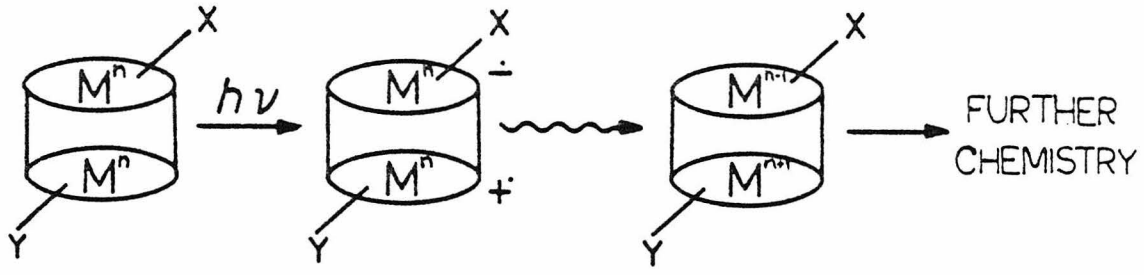

mixed valence species may have significant lifetimes, if the ratio of metal-to-metal charge transfer is low. In some cases, the reduced metal or the oxidized metal form cannot be formed (i.e., reduction of Ni(II)TPP gives ligand reduction,[7] oxidation of Co(III)TPP gives ligand oxidation[8]), while the oxidized metal or the reduced metal, respectively, is stable; in cases such as these, a species with one metal reduced and the other ligand oxidized (or the reverse) may be formed. These species might have reasonable lifetimes. EPR studies of frozen irradiated samples might provide insight into these species.

Furthermore, Umezawa and Yamamura[9,10] have observed visible light-assisted electrochemical reduction of oxygen at a platinum electrode coated with surface active cobalt(II) or manganese(III) complexes of tetrakis-(N-stearylpyridinium)porphyrin tetraiodide. In basic aqueous media, oxidation of water to oxygen or hydrogen peroxide has been proposed. Charge separation upon irradiation with visible light is proposed to occur, in the case of manganese, for example, forming Mn(IV) and Mn(II) porphyrins, which in turn give rise to a photocurrent accompanied by the reduction of oxygen to hydrogen peroxide. The polarized cofacial porphyrins might undergo this same phenomenon, but with higher efficiency due to the enhancement of the charge transfer. This could lead to the development of

a practical photochemical oxygen electrode.

Several syntheses of cofacial porphyrins have been reported.[1-4] The approach of Collman[1] could be modified easily to give cofacial bis(tetraphenylporphyrins) with appropriate electron-donating and electron-withdrawing groups. Condensation of 4-methoxy-2-nitrobenzaldehyde with an equivalent amount of 4-methoxybenzaldehyde with two equivalents of pyrrole in acetic acid should give a mixture from which the desired dinitroporphyrin may be isolated by column chromatography. Subsequent reduction (LAH , THF) of the nitro groups would give porphyrin A. Condensation of 4-chlorobenzaldehyde with

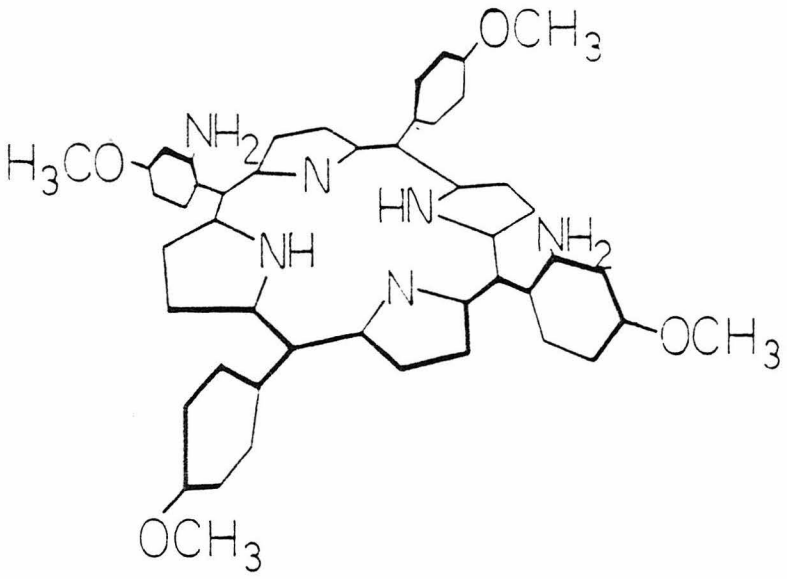

PORPHYRIN A

an equivalent amount of 4-chloro-2-nitrobenzaldehyde with two equivalents of pyrrole should lead, after separation of the isomers and reduction of the nitro groups, to porphyrin B. Addition of excess

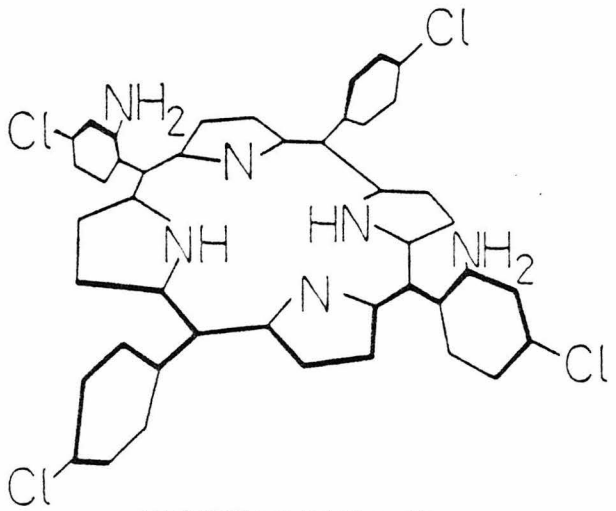

PORPHYRIN B

phosgene to porphyrin A (in benzene containing 1% pyridine), followed by removal of the excess phosgene in vacuo and finally addition of porphyrin B, should lead to a cofacial porphyrin, "Coface-I". Coface-I has both electron-withdrawing chloride and electron-donating methoxy groups needed for the proposed properties. Earlier work[11] has shown that cobalt tetraphenylporphyrins with these para-substituents on the phenyl rings show a pronounced influence on the redox properties of both the metal and the ligand; the anticipated charge-

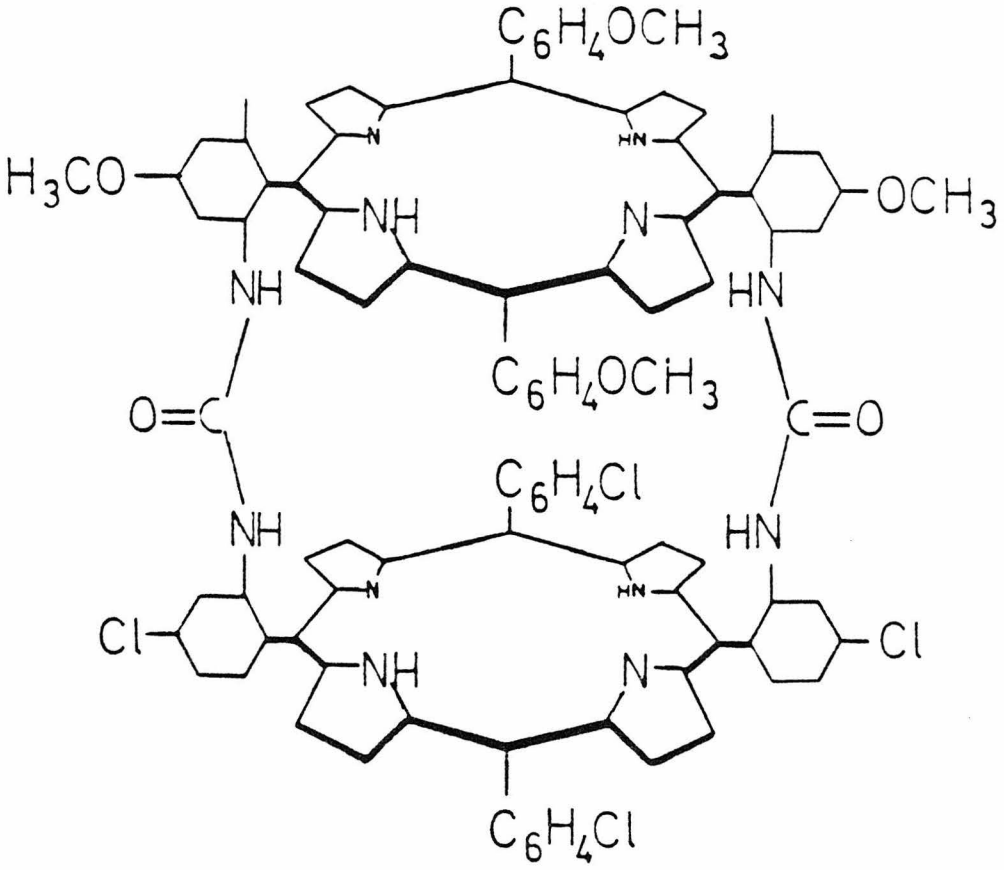

COFACE-I

transfer electronic properties of Coface-I are, therefore, highly probable, as the porphyrin does feel the inductive effect of the phenyl groups.

Another series of cofacial diporphyrins reported by Chang,[3] in which the interplanar separation can be varied from 6.4 to 4.2Å, also lends itself to the synthesis of "polarized" cofacial diporphyrins. Since porphyrins can be easily nitrated,[12] porphyrin C can be made. Reduction of porphyrin C (LAH, THF), treatment with p-toluene-sulfonylchloride, and refluxing with n-butylamine should give por-

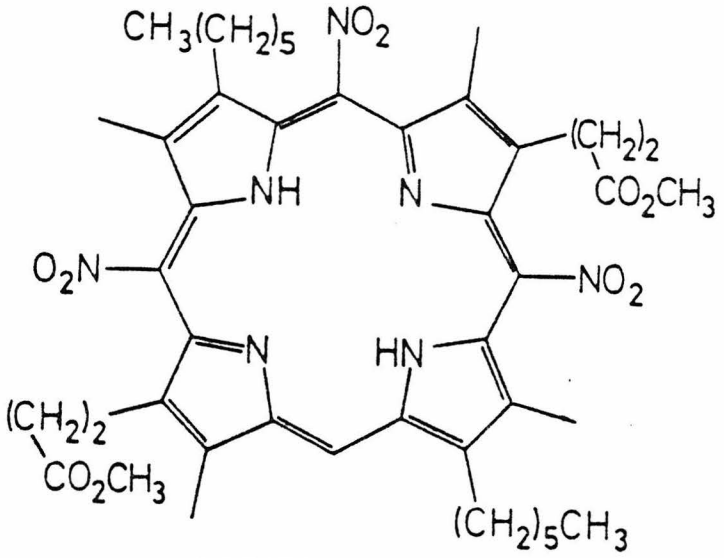

PORPHYRIN C

phyrin D. Porphyrin C can also be converted to the diacid chloride. High dilution condensation of the diacid chloride of porphyrin C with

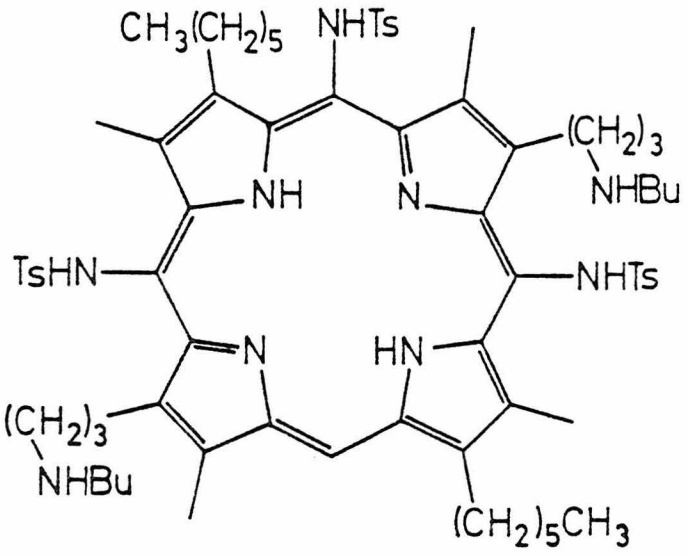

PORPHYRIN D

porphyrin D should give a cofacial diporphyrin. Reduction (B_2H_6, THF) of this cofacial diporphyrin should reduce the amide linkages; finally, removal of the protecting tosylate groups from the porphyrin ring amines to give "Coface-II" may be done by acid treatment.

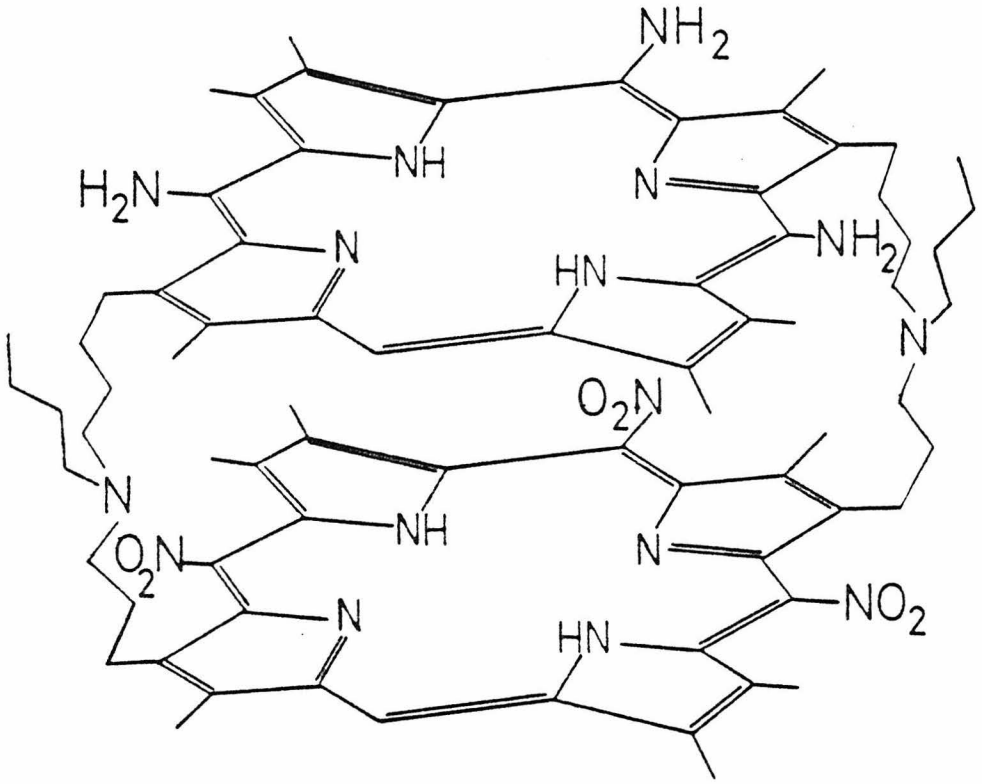

COFACE - II

Coface-II should exhibit very strong charge-transfer between the two porphyrins due to the direct attachment of the substituents to the porphyrin ring.

Investigations of the manganese(III) and cobalt(II) complexes of Coface-I or Coface-II would be an obvious starting point for these

studies. Other metals, and even mixed metal systems,[2] could eventually be studied. Spectroscopic comparisons between the free cofacial diporphyrins, their metal complexes, and their monomeric counterparts would be an easy way to establish the extent of intramolecular charge transfer. Sophisticated spectroscopic techniques might be able to detect transient states. Attempts to build oxygen electrodes, combining the observations of Collman, Anson, and coworkers[5] with those of Umezawa and Yamamura,[10] could lead to some exciting results with implications for practical applications.

References and Notes

(1) Collman, J. P.; Elliott, C. M.; Halbert, T. R.; Tovrog, B. S. Proc. Natl. Acad. Sci. U.S.A. 1977, 74, 18.

(2) Chang, C. K.; Kuo, M.-S.; Wang, C.-B. J. Heterocyclic Chem. 1977, 14, 943.

(3) Chang, C. K. J. Heterocyclic Chem. 1977, 14, 1285.

(4) Wasielewski, M. R.; Svec, W. A.; Cope, B. T. J. Am. Chem. Soc. 1978, 100, 1961.

(5) Collman, J. P.; Anson, F.; Morocco, M.; Koval, C. A. accepted for publication.

(6) Allgeier, H.; Siegel, M. G.; Helgeson, R. C.; Schmidt, E.; Cram, D. J. J. Am. Chem. Soc. 1975, 97, 3782.

(7) Felton, R. H.; Owen, G. S.; Dolphin, D.; Forman, A.; Borg, D. C.; Fajer, J. Am. N.Y. Acad. Sci. U.S.A. 1973, 206, 504.

(8) Felton, R. J.; Linschitz, H. J. Am. Chem. Soc. 1966, 88, 1113.

(9) Umezawa, Y.; Yamamura, T. J. Chem. Soc. Chem. Comm. 1978, 1106.

(10) Umezawa, Y.; Yamamura, T. J. Electrochem. Soc. 1979, 126, 705.

(11) Walker, F. A.; Berioz, D.; Kadish, K. M. J. Am. Chem. Soc. 1976, 98, 3484.

(12) Bonnett, R.; Stephenson, G. F. J. Org. Chem. 1965, 30, 2791.

(13) Chang, C. K. J. Am. Chem. Soc. 1977, 99, 2819.

Proposition 2

The gas phase formation of singlet methylene for studying its reaction with 2-butenes to form chemically activated dimethylcyclopropanes has been extensively studied.[1-3] Highly energized dimethylcyclopropanes were formed, which, in a near-collisionless environment, resulted in geometrically isomerized products. For example, the reaction of cis-2-butene with singlet methylene gives both cis- and trans-dimethylcyclopropane. Increasing the inert gas pressures up to 2000 torr, in order to collisionally deactivate the vibrationally excited cyclopropane, still leads to a large portion of non-stereospecific product.[1] This non-stereospecific result at high pressures has been shown by Bader and Generosa[4] to have been probably due to the formation of collisionally-formed triplet methylene. The problem of the contamination by triplet methylene can be avoided by adding small amounts of dioxygen to the reaction mixture as a triplet (radical) scavenger. Thus, high stereospecificity at high pressures was observed in the presence of dioxygen.[2] The oxygen serves to greatly reduce the reactions of triplet methylene with 2-butene to give dimethylcyclopropanes.

At this time, however, there still does not appear to be any method whereby triplet methylene can be generated in the gas phase free from singlet methylene. Typically, triplet methylene is gen-

erated by mercury-sensitized photolysis of a gaseous mixture of 2-butene, ketene, and mercury vapor. Decomposition of ketene using Hg ($^3P_1$), 2537Å, leads to a considerable amount of singlet methylene.[6] Estimates of thirteen per cent in singlet methylene have been suggested.[5] The decomposition of ketene here is presumably a competition between the direct photolysis of ketene and its mercury-sensitized photochemical decomposition. Furthermore, it appears to be a difficult and uncertain task to calculate the fraction of products that are due to the singlet methylene in order to extract from the total distribution of reaction products exactly what extent of non-stereospecificity there is in the reaction of triplet methylene with 2-butenes.[7] "It is by no means clear," Kirmse[7] suggests, "that the addition of triplet methylene to 2-butenes is entirely non-stereospecific." If triplet methylene adds to 2-butene with some retention of stereochemistry, there may be some implications having bearing on the behavior of vibrationally hot diradicals[8-15] in a triplet manifold. In the absence of any singlet methylene-specific scavenger, an efficient method of generating triplet methylene in the gas phase without the formation of singlet methylene is needed.

In solution chemistry, it is well-documented[16-18] that the thermal decomposition of tetramethyldioxetane leads to singlet and triplet acetone in high yield. Furthermore, triplet acetone so generated can

efficiently induce "photochemical" reactions.[19-23] The acetone triplet has an emission band around 420 to 440 nm.[17] Although this is not sufficiently high an energy to cause the decomposition of ketene, the photosensitized diazomethane photolysis at 435 nm has been shown to give singlet and triplet methylene.[7] One might expect the reaction cross-section for the reaction of triplet acetone with diazomethane to give triplet methylene to be quite large in the gas phase.[24]

Tetramethyldioxetane, being volatile, might just serve as a reagent by which gas phase triplet methylene might be generated. A gaseous mixture of diazomethane, cis-2-butene, tetramethyldioxetane at 50°C might lead to products formed exclusively from triplet methylene.[25-27] Controls to be run would include the reaction below

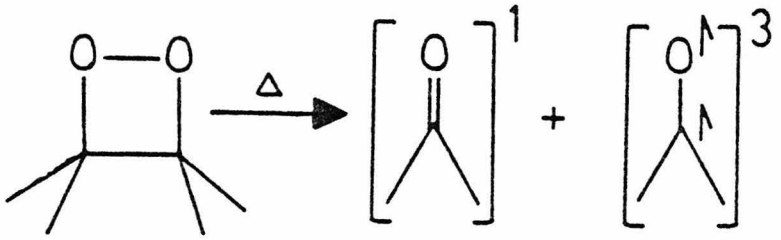

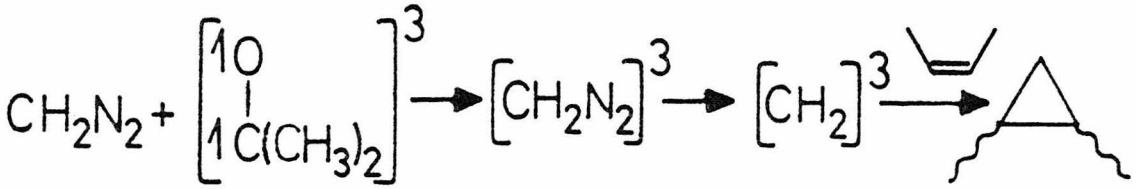

in the presence of triplet methylene scavengers. Tetramethyldioxetane or acetone could react with the triplet methylene, but sufficient amounts of the dimethylcyclopropanes should be formed to permit analysis of the reaction mixture by vapor phase chromatography.

This would be a non-photochemical triplet-induced generation of methylene used to probe the properties of vibrationally excited 1,3-diradicals, which might show non-stereorandom behavior. Such non-random behavior for vibrationally excited singlet diradicals has been proposed, but not conclusively shown.

References and Notes

(1) Frey, H. M. J. Am. Chem. Soc. 1960, 82, 5947.

(2) McKnight, C.; Lee, P. S. T.; Rowland, F. S. J. Am. Chem. Soc. 1967, 89, 6802.

(3) Eder, T. W.; Carr, R. W. J. Phys. Chem. 1969, 73, 2074.

(4) Bader, R. F. W.; Generosa, R. I. Can. J. Chem. 1965, 43, 1631.

(5) Montague, D. C.; Rowland, F. S. J. Phys. Chem. 1968, 72, 3705.

(6) Frey, H. M.; Walsh, R. J. Chem. Soc. Chem. Comm. 1969, 158.

(7) Kirmse, W. "Carbene Chemistry"; Academic Press: New York, 1971.

(8) Stephenson, L. M.; Brauman, J. I. J. Am. Chem. Soc. 1971, 93, 1988.

(9) Bartlett, P. D.; Porter, N. A. J. Am. Chem. Soc. 1968, 90, 5317.

(10) Gerberich, H. R.; Walters, W. D. J. Am. Chem. Soc. 1961, 83, 3935.

(11) Gerberich, H. R.; Walters, W. D. J. A. Chem. Soc.

1961, 83, 4884.

(12) Dervan, P. B.; Uyehara, T. J. Am. Chem. Soc. 1976, 98, 1262.

(13) Dervan, P. B.; Uyehara, T.; Santilii, D. S. J. Am. Chem. Soc. 1979, 101, 2069.

(14) Dervan, P. B.; Uyehara, T. J. Am. Chem. Soc. 1979, 101, 2076.

(15) Santilli, D. S.; Dervan, P. B. J. Am. Chem. Soc. 1979, 101, 3663.

(16) Kopecky, K. R.; Mumford, C. Can. J. Chem. 1969, 47, 709.

(17) Schore, N. E.; Turro, N. J. J. Am. Chem. Soc. 1975, 97, 2482.

(18) Richardson, W. H.; Lovett, M. B.; Price, M. E.; Anderegg, J. H. J. Am. Chem. Soc. 1979, 101, 4683.

(19) White, E. H.; Wiecko, J.; Roswell, D. R. J. Am. Chem. Soc. 1969, 91, 5194.

(20) White, E. J.; Wiecko, J.; Wei, C. C. J. Am. Chem. Soc. 1970, 92, 2167.

(21) White, E. J.; Wei, C. C. Biochem. Biophys. Res. Comm. 1970, 39, 1219.

(22) White, E. J.; Wildes, P. D.; Wiecko, J.; Doshan, H.;

Wei, C. C. J. Am. Chem. Soc. 1973, 95, 7050.

(23) Adam, W.; Cheng, C.-C.; Cueto, O.; Sakanishi, K.; Zinner, K. J. Am. Chem. Soc. 1979, 101, 1324.

(24) Levine, R. D.; Bernstein, R. B. "Molecular Reaction Dynamics"; Oxford University Press: New York, 1974.

(25) The thermal decomposition of diazomethane at these temperatures is slow: $k\,(50\,^{\circ}C) = 1 \times 10^{-11}\ s^{-1}$.[7]

(26) Gas phase pyrolysis of tetramethyldioxetane has been shown to chemiluminesce.[22]

(27) The estimated vapor pressure of tetramethyldioxetane at 50°C is 5-15 torr.[22] Other more volatile dioxetanes are available.[18]

Proposition 3

Models for metalloenzymes that activate dioxygen for catalytic oxygenations are continually being sought. One of the most fascinating of the monoxygenases is cytochrome P_{450}. This iron heme glycoprotein is important in the detoxification of drugs and also serves to perform certain important hydroxylations of hydrocarbons. A recent report[1] has given support to the contention[2] that Fe(IV) = O, ferryl ion, acts as an oxene transfer agent. In this experiment iodosobenzene served as the source of active oxygen; liver microsomal cytochrome P_{450}, thus, in the absence of O_2 and NADH, catalyzed the O-dealkylation of 7-ethoxycoumarin utilizing iodosobenzene. Chang and Kuo[3] have reported the reaction of iodosoxylene with an iron-μ-oxo "strapped" heme complex. A heme product was isolated in which the alkyl "strap" had been hydroxylated — a reaction that apparently

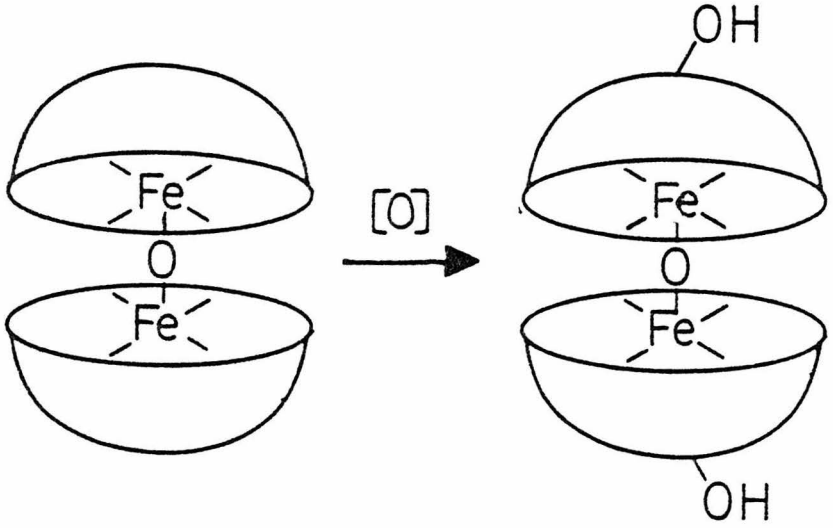

involved an active ferryl complex. Electronic absorption spectra and magnetic susceptibility measurements provided further support that an iron-bound oxene species was formed.

Another communication,[4] in which the reaction of bis(dimethylglyoximato)rhodium(III)hydride is proposed to react with dioxygen to give bis(dimethylglyoximato)rhodium(III) and hydroxide, poses an interesting possibility. A plausable mechanism[4,5] (below) for this reaction involves the formation of a rhodium(IV) oxene intermediate:

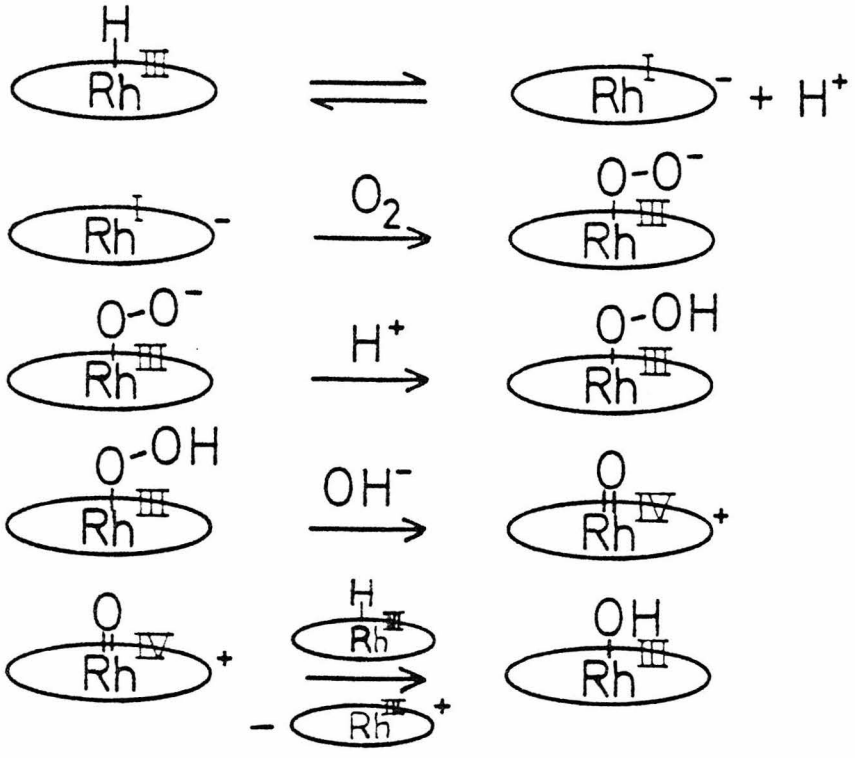

The similarities between porphyrins and bis(dimethylglyoximato) ligand environments being apparent, suggest the possibility that rhodium(IV) oxene complexes might be studied as a model for the

active site of cytochrome P_{450} and that they might possibly have catalytic oxygenating activity of their own.[6]

An obvious starting point for these studies is low temperature reactions of iodosoxylene with bis(dimethylglyoximate)rhodium(III) or a rhodium(III) porphyrin complex. Spectral indications[3] of ferryl ion were obtained by the treatment of octaethylporphyrin ferric chloride in CH_2Cl_2 at -45°C with iodosoxylene. Perhaps a transient or quasi-stable rhodium species could be similarly observed. In addition, a rhodium(IV) species, unlike the diamagnetic rhodium(III) starting material, might be expected to show an EPR spectrum; if a signal was observed, ^{17}O-labelling (I = 5/2) might show direct interaction of the metal and the oxene.

The catalytic oxidation of organic substrates should also be explored. Primary alcohols are only slowly oxidized to the corresponding aldehydes by iodosobenzene at elevated temperatures.[7] A more facile oxidation might be seen to occur in the presence of bis(dimethylglyoximate)rhodium(III). Other, more difficult, rhodium-assisted oxidations of various organic substrates could also be investigated:

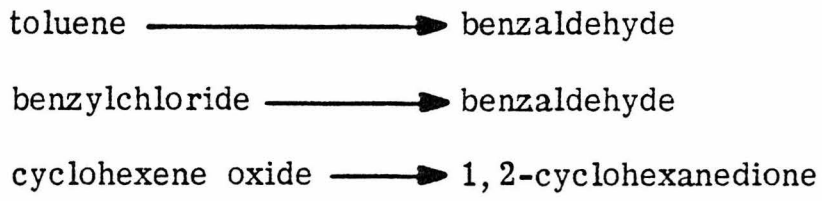

cyclohexene ⟶ cyclohexene oxide

Another avenue of investigation is the cytochrome P_{450} itself. The heme group, ferriprotoporphyrin IX, can be removed from the cytochrome P_{450} of Pseudomonas putida; the holoenzyme can subsequently be reconstituted in the presence of glycerol and large amounts of cysteine.[8] Since rhodium porphyrins are well-known,[9-10] the possiblity exists for creating a rhodium cytochrome P_{450} from rhodium protoporphyrin IX and the apoprotein. While spectral and especially EPR results may reveal a considerable amount of information about the enzyme, changes in the chemical reactivity of the new cytochrome are very promising. Intermediates not long-lived enough in the native enzyme may now be observable; since several of the unobserved steps in the mechanism of the action of cytochrome P_{450} are thought to occur after the first electron is added to the substrate complex,[11] substitution of the metal ions may alter the kinetics of the reaction sufficiently to follow the reaction path by physical techniques.

The lessons to be learned from these investigations are: (1) the properties and reactivity of rhodium(IV) oxene complexes, and (2) further details concerning the mechanism of cytochrome P_{450} by rhodium substitution.

References and Notes

(1) Lichtenberger, F.; Nastainczyck, W.; Ullrich, V. Biochem Biophys. Res. Comm. 1976, 70, 939.

(2) Loew, G. H.; Hjelmeland, L. M.; Kirchner, R. F. Int. J. Quantum Chem.: Quantum Biol. Symp. 1977, 4, 225.

(3) Chang, C.-K.; Kuo, M.-S. J. Am. Chem. Soc. 1979, 101, 3413.

(4) Kljnev, M. V.; Khidekel', M. L.; Strelets, V. V. Transition Met. Chem. 1978, 3, 380.

(5) James, B. R. "Homogeneous Hydrogenation" Wiley: New York, 1973.

(6) Cobalt oxene complexes also present a possible model for cytochrome P_{450}; however, formation of μ-oxo species is apparently more probable for cobalt than rhodium.

(7) Takaya, T.; Enyo, H.; Imoto, E. Bull. Chem. Soc. Jap. 1968, 41, 1032.

(8) Yu, C.-A.; Gunsalus, I. C. J. Biol. Chem. 1974, 249, 107.

(9) Grigg, R.; Shelton, G.; Sweeney, A.; Johnson, A. W. J. Chem. Soc. Perkin I 1972, 1789.

(10) Sadasivan, N.; Fleischer, E. B. J. Inorg. Nucl. Chem. 1968, 30, 591.

(11) Griffin, B. W.; Peterson, J. A.; Estabrook, R. W. in "The Porphyrins" vol. 7, Ed. Dolphin, D.; Academic Press: New York, 1979.

Proposition 4

That life exists is an issue that only a few might try to refute. What life is and how it has come to be is a puzzle that only few claim to understand. Life on our planet revolves about compounds that have the unusual property of optical activity. The source of optical activity in organic molecules is a mystery. Even now chemists try to devise efficient methods by which optically active products may be formed. Typically, optically active solvents or asymmetric catalysts have been employed. More often the scientist has "cheated" and resolved his compound at some point using an available biochemical having optical activity. Yet everywhere around us are inorganic compounds having optical activity. Minerals are by and large optically active; more than one hundred common minerals have optically active forms.[1] If optically active compounds were first made in a primordial world, perhaps some of these minerals may have served as assymmetric templates.

Phase transfer catalysis has in recent years become very popular.[2] More recently a philosophically similar technique has been gaining some attention. Researchers[3-12] have noticed that, when certain reagents are absorbed onto a solid support, such as alumina, facile reactions with organic substrates often occur where the reagent itself in the bulk form does not. For example,[9] potassium permanganate, deposited on

Linde 13X Molecular Sieves by the evaporation of an aqueous potassium permanganate solution, gave a reagent which oxidized secondary alcohols to ketones under mild conditions in a non-polar solvent, benzene; no reaction occurred with a mixture of crushed $KMnO_4$ and the alcohols in benzene. Similarly, oxidations,[5,8,9] reductions,[3,4,6] and substitution reactions[7,10,11,12] have been carried out using reagent-coated solid phases, giving results far different from the native solid reagent. Using optically active minerals for the solid support might serve to induce optical activity in the products.

Many kinds of minerals occur in optically active forms.[1] Orthorhombic elemental sulfur is optically active. Oxides, carbonates, nitrates, borates, sulfates, tungstate, phosphates, and silicates of many metals occur naturally as optically active crystals. While each mineral may have several faces and each face may pose a different microenvironment, the simplest approach to using minerals to induce optical activity would be to adsorb the desired reagent onto powdered or microcrystalline samples of certain chiral minerals. Reagents for nucleophilic substitution reactions such as NaCN and NaBr might be adsorbed onto metal oxides (rutile (TiO_2) or diaspore ($HAlO_2$)), carbonates (magnesite ($MgCO_3$), dolomite ($CaMg(CO_3)_2$), or malachite ($Cu_2CO_3(OH)_2$)), borates like borax ($Na_2B_4O_7 \cdot H_2O$), sulfates (anglesite ($PbSO_4$) or antlerite ($Cu_3(OH)_4SO_4$)), phosphates (wavellite

($Al_3(OH)_3(PO_4)_2 \cdot 5H_2O$) or vivianite ($Fe_3(PO_4)_2 \cdot 8H_2O$)), or silicates (zircon ($ZrSiO_4$), wollastonite ($Ca(SiO_3)$), pectolite ($CaNaH(SiO_3)_3$), or talc ($Mg_3(Si_4O_{10})(OH)_2$). The reagents would desirably be quite dilute so that the assymmetric surface of the mineral could have as much influence over the reaction stereochemistry as possible. Since racemic mixtures of prochiral starting materials would be most reasonable, i.e., 2-chlorobutane, total conversion should also be low. (Quantitative conversion to products would not be very informative about the kinetic stereoselectivity of the reagent.) Not all mineral-supported reagents would be expected to induce reactions, not to mention optical activity. Various non-polar solvents and prochiral substrates could be used. Product isolation would be done simply by filtration. Reactions could be identified by vapor phase gas chromatography; if a reaction was seen to have taken place, the product and starting materials could be checked (after isolation) for optical induction by polarimetry.

Another reaction that might be of interest is epoxidations. Olefin epoxidations can be performed easily using the peroxo molybdenum complex $Mo(VI)O(O_2)_2L$, where L is a base such as N,N-dimethylformide.[13,14] This species, where $L = H_2O$, could also be adsorbed onto minerals. In reactions where L is an optically active amide, i.e., (S)-N,N-dimethyllactamide, simple olefins (propene, 1-butene,

etc.) can be epoxidized with up to 35% enantiomeric excess of the product oxirane.[16] In this case, a surface oxygen of the mineral might act as the base for the molybdenum complex; the environment, being chiral, might consequently induce optical activity in the product oxiranes. Methods for analysis of these products by gas chromatography are known.[16] Furthermore, the action of aqueous hydrogen peroxide on the surfaces of the optically active mineral scheelite ($CaWO_4$) might produce an active oxidizing reagent that could produce optically active oxiranes from olefins.

This approach to solid-supported reagents for organic synthesis could lead to some useful and enlightening chemistry.[17]

References and Notes

(1) Hurlbut, C.S. "Dana's Manual of Mineralogy"; John Wiley and Sons, Inc.: New York, 1971.

(2) Dockx, J. Synthesis 1973, 441.

(3) Lalancette, J.-M.; Rollin, G.; Cumas, P. Can. J. Chem. 1972, 50, 3058.

(4) Andersen, N. H.; Uh, H. Synth. Commun. 1973, 3, 115.

(5) Fetizon, M.; Mourgues, P. Tetrahedron 1974, 30, 327.

(6) Posner, G. H.; Rogers, D. G.; Kuizig, C. M.; Gurria, G. M. Tetrahedron Lett. 1975, 3597.

(7) Posner, G. H.; Runquist, A. W. Tetrahedron Lett. 1975, 3601.

(8) Taylor, E. C.; Chiang, C. S.; McKillup, A.; White, J. F. J. Am. Chem. Soc. 1976, 98, 6750.

(9) Regen, S. L.; Koteel, C. J. Am. Chem. Soc. 1977, 99, 3837.

(10) Leach, B. E. J. Org. Chem. 1978, 43, 1794.

(11) Regen, S. L.; Quici, S.; Liaw, S.-J. J. Org. Chem. 1979, 44, 2029.

(12) Tunido, P. J. Org. Chem. 1979, 44, 2048.

(13) Mimoun, H.; DeRoch, I.S.; Sajus, L. Tetrahedron 1970, 26, 37.

(14) Sharpless, K. B.; Townsend, J. M.; Williams, D. R. J. Am. Chem. Soc. 1972, 94, 295.

(15) Arawaka, H.; Moro-aka, Y.; Ozaki, A. Bull. Chem. Soc. Jpn. 1974, 47, 2958.

(16) Kagan, H. B.; Mimoun, H.; Mark, C.; Schurig, V. Angew. Chem. Int. Ed. Eng. 1979, 18, 485.

(17) The source of optical activity in minerals will not be considered here.

Proposition 5

One of the largest families of all of the flowering plants is the Orchidaceae family, comprised of more than 25,000 species. Many scientists, collectors, hybridists and hobbyists have long displayed an almost fanatic interest in these plants. Collectors have risked life and limb in primitive and hostile lands seeking to discover new species. Of commercial interest as cut flowers are relatively few genera: Cattleya and its close relatives (the most common of the "corsage orchids"), Vanda, Cymbidium, Paphiopedelum, Oncidium and their related genera, and Phalaenopsis. Over the past century, hybridization has led to more hybrids than there are known species. For the most part, hybridization has been accomplished by a relatively few number of growers. In fact, hybridists are often regarded as a special group, possessing a mysterious "insight" into his art. The successful hybridist is judged as such by their ability to produce new crosses, which manifest vivid new colors and forms. The achievement of good color is often that criterion which separates the serious hybridizer from the "dabbler." Perhaps after a century of artful hybridization, it is now time for a more systematic and logical approach.

The colors exhibited in orchid flowers belong to three basic

chemical groups: anthocyanins, carotenes, and chlorophylls.[1] Only one report[2] of a systematic study of orchid anthocyanins appears to have been done. No in depth investigation into the pigments of Phalaenopsis has apparently ever been done — despite the hundreds of hybrids in this important genus. That much hybridization has been done because a particular grower had two plants in bloom simultaneously seems of little doubt. Those other artificial crosses that have been made were done on the basis of intuition and experience. In the breeding of pink Phalaenopsis, color is the primary, but not unique, objective. It is obvious from observing the species from which the pink, purple, and reddish hybrids have come that there are many hues. Thus it is highly probable that there are several different pigments from which to draw to make just those shades that the hybridist seeks. Luckily, shades of red are easily distinguished by the human eye.

In contrast, variations in the tint of yellow are most difficult, as such colors largely arise from electronic transitions in the ultraviolet region, rather than the visible region. Perhaps as a result, there has been relatively little progress in this area.[3] Phalaenopsis is a large genus of some forty or more species ranging from Tibet and China through Indonesia to the Philippines, Australia and the islands of the Malayan Archipelago.[4] Hybridists have recently[5] noticed that sometimes crossing two yellow species yields a hybrid with more

intense coloring than either parent. One possible interpretation is that there exist more than one kind of yellow pigment among Phalaenopsis species. Although color inheritance in orchids is often complex,[1] genetic distribution of color in the progeny may be overcome by raising a representative number of a given cross.

De Leon[6] noted, and to a large extent it is still true, that the main sources of yellow pigmentation in hybridization of Phalaenopsis come from two species: Phal. mannii and Phal. Lueddemanniana. Sweet[7-13] has noted at least eighteen species and varieties of this genus that have predominantly yellow pigmentation. Possibly different yellow pigments are present in different species that are not closely related. If several yellow pigments can be shown to exist and be somewhat species specific, hybridization of yellow Phalaenopsis might be aided by knowing which species may be combined to have the most (numerically) yellow pigments, i.e., a flower having two or three different yellow pigments might show more intense coloration than one having only one source of yellow color.

Simply, the flowers of several sections of the genus would need to be studied. For example, Phal. sumatrana, Phal. Lueddemanniana, Phal. fasciata, Phal. violacea var. Murtoniana, Phal. javanica, Phal. fuscata, Phal. cochlearis, Phal. mannii, Phal. micholitzii, and Phal. mariae var. alba, representative of most of the yellow species of

the genus, would be studied. Pigments could be separated by standard chromatographic techniques.[1] Electronic absorption spectra could be used to distinguish the isolated flower pigments. Thus it could be established whether there are several yellow pigments, if they are predominantly contained in certain species, and finally which species they are contained in. Such information could be used to aid hybridists in their search for better yellow color in Phalaenopsis.

Finally, of course, such an approach might well be applied to other orchids and non-orchid breeding problems by establishing indirectly the presence of different pigment gene pools.

References and Notes

(1) Arditti, J. "Orchid Biology: Reviews and Perspective, I"; Cornell University Press: Ithaca, 1977.

(2) Stanford, W. W.; Krallis, A. X.; Fourakis, E.; Kapri, K. Orchid Digest, 1964, 28, 362.

(3) Noble, M. " You Can Grow Phalaenopsis Orchids"; Mary Noble: Jacksonville, 1971.

(4) " Handbook on Orchid Culture" American Orchid Society: Cambridge, 1976.

(5) Ewing, J. " The Role of Species in Novelty Phalaenopsis Breeding" John Ewing: Aptos, 1978.

(6) De Leon, C. M. Am. Orchid Soc. Bull. 1967, 36, 387.

(7) Sweet, H. R. Am. Orchid Soc. Bull. 1968, 37, 867.

(8) Sweet, H. R. Am. Orchid Soc. Bull. 1968, 37, 1089.

(9) Sweet, H. R. Am. Orchid Soc. Bull. 1969, 38, 225.

(10) Sweet, H. R. Am. Orchid Soc. Bull. 1969, 38, 321.

(11) Sweet. H. R. Am. Orchid Soc. Bull. 1969, 38, 505.

(12) Sweet, H. R. Am. Orchid Soc. Bull. 1969, 38, 681.

(13) Sweet, H.R. Am. Orchid Soc. Bull. 1969, 38, 889.